Genetic interactions of *dksA*: a transcription global regulator in quality control of central dogma processes.

By

Lucas M Onder

A dissertation submitted in partial fulfillment of

the requirements for the degree of

Doctor of Philosophy

(Genetics)

at the

UNIVERSITY OF WISCONSIN-MADISON

2021

Date of final oral examination: 07/22/2021

The dissertation is approved by the following members of the Final Oral Committee:

Jade (Jue) D. Wang, Professor, Bacteriology (Genetics Trainer)

Allen Laughon, Professor, Genetics

Robert Landick, Professor, Biochemistry

Richard Gourse, Professor, Bacteriology

Jacob O. Brunkard, Assistant Professor, Genetics

Dissertation Abstract

By
Lucas Onder
Under the supervision of Professor Jade Wang
at the University of Wisconsin-Madison

The ability of bacteria to regulate gene expression to adapt to stressful environments is critical for their survival and pathogenesis. The stringent response is the bacterial stress response mediated by the rapid accumulation of (p)ppGpp. A key co-factor of (p)ppGpp is the transcription factor DksA in *E. coli*. While the mechanism of gene regulation by DksA at promoters has been well characterized, the role DksA plays during transcription elongation remains unknown. In this work, we combine high throughput functional genomics with in *vivo* transcription and translation kinetics assays to identify the role DksA plays in promoting robust protein synthesis in different nutrient conditions. In terms of transcription elongation, we found that *dksA* mutants display a slower transcription elongation rate. However, Term-seq analyses of wild-type and *dksA* mutants indicate that a *dksA* mutant does not experience premature transcription termination genome-wide, suggesting that DksA plays a role in preventing transcriptional pausing or allowing faster transcription elongation rates, but does not promote transcription termination. In terms of translation, we found that *dksA* mutants display a slower translation elongation than wild-type cells. Strikingly, *dksA* mutant also experiences strongly increased tmRNA tagging, ssrA-mediated proteolysis, and strong activation of the alternative ribosome rescue pathway, suggesting that DksA promotes ribosome processivity and complete translation. We observe that nutrient rich media is able to mask severe phenotypes in Δ*dksA* cells and that *dksA* is essential in the

absence of supplemented amino acids. However, our Transposon-sequencing experiments reveal that, even in the rich media, *dksA* mutant displays synthetic interactions with multiple transcription elongation and protein quality control genes. These include *clpX* and *clpP*, which are critical to the removal of incompletely translated polypeptides generated by ribosomes stalled at non-stop codon. Finally, our Transposon-sequencing experiments also reveal multiple factors involved in DNA repair and chromosome organization, cell division and cell envelop integrity. This work documents a more extensive role of DksA as an essential regulator of the central dogma processes.

Table of Contents

Chapter 1: Global Regulation of Transcription by Nucleotides and (p)ppGpp

Lucas M. Onder, Jue D. Wang*, Jonathan Jagodnik, Wilma Ross, and Richard L. Gourse*

University of Wisconsin-Madison, Department of Bacteriology, 1550 linden Drive, Madison, WI 53706, USA

* Co-corresponding authors

In Press. (2021). RNA Polymerases as Molecular Motors. *Chemical Biology*. Royal Society of Chemistry.

Author contributions: L.M.O, J.D.W, J.J, W.R. and R.L.G. wrote the paper. L.M.O and R.L.G made the figures.

1.1 Abstract

The activity of the RNA polymerase (RNAP) molecular machine is highly regulated in response to the external environment. In this chapter, we focus on regulation of transcription by ribonucleotides- the substrates of RNAP, and by nucleotide derivatives that act as signaling molecules to control transcription. We explain how the concentration of the ribonucleotides directly regulate RNAP activity during transcription initiation by affecting the rate limiting step of nucleotide addition, which depends on both the identity of the initiating nucleotide and by the promoter sequence. We describe recent breakthroughs about how the stress signaling nucleotide alarmones ppGpp and pppGpp [(p)ppGpp] regulate the synthesis or degradation of the substrates of the transcription machinery regulated transcription

in an organism-specific manner, or they directly modify the activity of the core transcription machinery itself in conjunction with the transcription factor DksA. Finally, we describe emerging work characterizing how (p)ppGpp and DksA act beyond transcription initiation by coordinating transcription with other macromolecular machines involved in DNA-replication and repair to promote genome stability.

1.2 Introduction

The activity of the RNA polymerase (RNAP) molecular machine is highly regulated in organisms from humans to bacteria. Gene expression is regulated in response to the external environment and to internal cues in order to mediate feedback and homeostatic controls, to mount stress responses, and to initiate developmental pathways. Most attention surrounding gene expression control has focused on protein-based transcription factors, receptor-mediated protein modifications, and ligands that allosterically regulate repressors, activators, riboswitches, or alternative sigma factors. In this chapter, we focus on less appreciated regulators of transcription, notably ribonucleotides themselves and ribonucleotide derivatives that act as signaling molecules to control the synthesis or degradation of the substrates of the transcription machinery or the activity of the core transcription machinery itself. We focus on more recent aspects of the voluminous literature on these subjects.

Nucleotide derivatives can serve as signals of the nutritional status of the cell and/or of the external environment, and therefore they are sometimes referred to as alarmones [1]. Perhaps the most well-characterized of these alarmones are guanosine tetraphosphate and guanosine pentaphosphate, collectively called (p)ppGpp. Although these alarmones are produced throughout the bacterial domain of life, as well as in chloroplasts [2], there is significant evolutionary diversity in how they are utilized. Here we will focus primarily on the action of these alarmones in the model Gram-negative bacterium *E. coli* and in the model Gram-positive bacterium *Bacillus subtilis*, but we emphasize that there are additional mechanisms for (p)ppGpp utilization that are not represented by the mechanisms observed in these two species.

2. Changing NTP concentrations can regulate transcription initiation and elongation

ATP, GTP, CTP, and UTP concentrations range from low micromolar to millimolar in *E. coli* and *B. subtilis*. Fluctuations in the environment, including nutrient starvation and entrance into stationary phase, result in changes in nucleotide levels. The efficiency of transcription initiation is sensitive to the concentrations of the NTP substrates, as the K_m for the first NTP is much higher than for the elongating NTPs [3]. In both *E. coli* and *B. subtilis*, the K_m for the initiating NTP for rRNA promoters is unusually high (weaker affinity) compared to standard promoters [4–8]. As a result, fluctuations in NTP concentrations have stronger effects on rRNA promoters than on most other promoters. The effects of NTP concentration on rRNA promoters results primarily from the instability of the open complex which therefore has a tendency to fall back to earlier transcription initiation intermediates in the absence of NTP substrates. When NTP pools

are high, however, they drive transcription initiation forward by mass action. Although the promoter sequences that determine open complex lifetime are complex, there is an almost perfect correlation between regulation of rRNA promoters by NTP concentration and open complex lifetime [9]. A decline in NTP levels during nutrient depletion and as cells enter stationary phase thereby contributes to the decrease in rRNA transcription at that time, and when cells go deeper into stationary phase, further NTP depletion may be the major contributor to reduction in rRNA synthesis[4,8].

Specific DNA sequences also differentially affect transcription elongation. Although the affinity of the transcription complex for the elongating substrates is generally much higher and more uniform than for the initial substrate, each succeeding NTP has its own characteristic K_m depending on the identity of the template base and the surrounding sequences [10]. RNAP pauses at positions where the affinities are weak, depending on the availability of the substrate NTP (see also [11]). An evolutionarily conserved “universal pause sequence” has been identified that increases the propensity for pausing [12–14]. Low cellular NTP concentrations increase the magnitude of the effects of DNA sequences and elongation and termination factors. Thus, changes in NTP concentration can change the transcription start site or cause backtracking, transcription slippage, reiterative transcription, and even transcription attenuation, and thereby alter transcription elongation, pausing, and termination (reviewed by[15]). Such effects of NTP concentrations were documented long ago in several pyrimidine biosynthetic operons, where high UTP concentrations feedback regulate gene expression by a variety of different mechanisms. For example, in the *codBA* operon, high intracellular levels of UTP favor transcriptional initiation at a position that results in non-productive, reiterative

transcription, whereas low UTP concentration leads to initiation at the adjacent position and productive elongation [16]. In the *pyrBI* operon, high UTP concentrations lead to transcriptional attenuation, whereas low concentrations of UTP lead to productive elongation [17]. A long A+T track in the initial transcribed region of the *upp* operon leads to reiterative transcription, sensitizing the operon to the effects of high UTP concentration [18].

More generally, recent studies have shown that NTP concentrations can affect the rate of promoter clearance. Specifically, high NTP concentrations promote the transition from the initiation to elongation complex by helping RNAP escape from a scrunched, backtracked, paused intermediate in which σ region 3.2 competes with the growing RNA chain for the RNA exit channel ([19]; see also[20]).

3. The nucleotide derivatives pppGpp and ppGpp control transcription by multiple mechanisms

a. Historical background. (p)ppGpp production consumes GTP. Therefore, (p)ppGpp synthesis reduces purine nucleotide pools in both proteobacteria like *E. coli* and in firmicutes like *B. subtilis*. This depletion is most apparent in gram positives, as reported in early work from Freese and colleagues [32,33] showing that (p)ppGpp promotes sporulation in *B. subtilis*, largely as a result of the reduction of the GTP concentration. (p)ppGpp also inhibits GTP synthesis in *B. subtilis* by binding directly to, and inhibiting, enzymes needed for GTP synthesis (Figure 1). This includes guanylate kinase, the enzyme that produces GDP from GMP [34,35] and HprT and XpT[35–37], purine salvage enzymes that convert guanine, hypoxanthine and xanthine to GMP, IMP and XMP, respectively. While (p)ppGpp does not inhibit guanylate kinase in proteobacteria like *E.*

coli, it was shown recently that (p)ppGpp also reduces GTP synthesis directly by binding to PurF, HprT and Gsk enzymes in *E. coli* needed for *de novo* and salvage purine biosynthesis [38–40].

b. Regulation of transcription by (p)ppGpp binding to enzymes responsible for the synthesis of NTPs. (p)ppGpp production consumes GTP. Therefore, (p)ppGpp synthesis reduces purine nucleotide pools in both proteobacteria like *E. coli* and in firmicutes like *B. subtilis*. This depletion is most apparent in gram positives, as reported in early work from Freese and colleagues [32,33] showing that (p)ppGpp promotes sporulation in *B. subtilis*, largely as a result of the reduction of the GTP concentration. (p)ppGpp also inhibits GTP synthesis in *B. subtilis* by binding directly to, and inhibiting, enzymes needed for GTP synthesis (Figure 1). This includes guanylate kinase, the enzyme that produces GDP from GMP [34,35] and HprT and XpT[35–37], purine salvage enzymes that convert guanine, hypoxanthine and xanthine to GMP, IMP and XMP, respectively. While (p)ppGpp does not inhibit guanylate kinase in proteobacteria like *E. coli*, it was shown recently that (p)ppGpp also reduces GTP synthesis directly by binding to PurF, HprT and Gsk enzymes in *E. coli* needed for *de novo* and salvage purine biosynthesis [38–40].

Figure 1.1 ppGpp, *de novo* and salvage purine synthesis pathways, and effect of NTP concentrations on rRNA transcription initiation

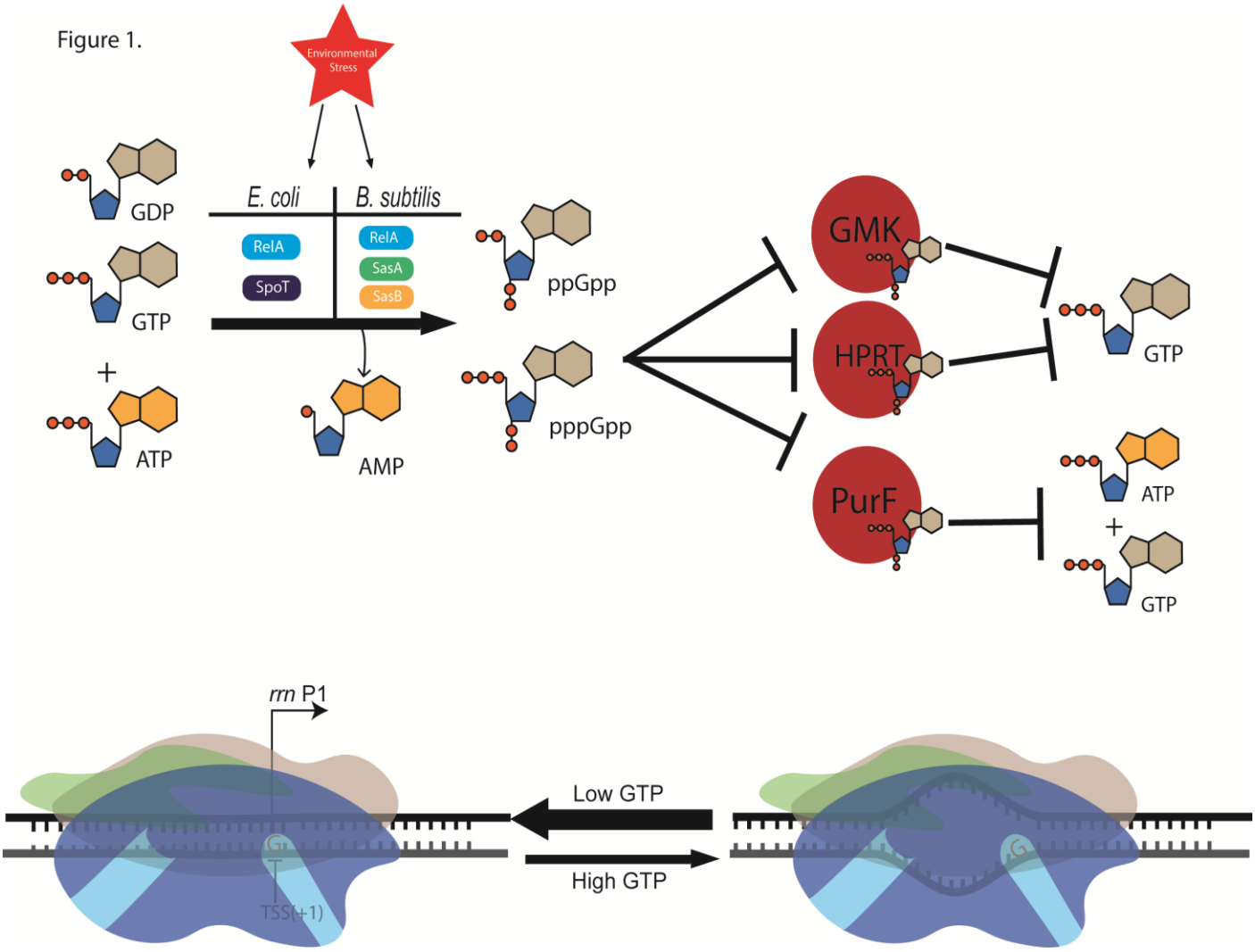

Top. After an environmental stressor such as nutrient limitation (p)ppGpp is synthesized from GDP or GTP by the addition of a pyrophosphate from ATP to the 3′-hydroxyl group resulting in ppGpp or pppGpp, respectively. In *E.coli*, production of ppGpp is by only RelA and SpoT, whereas production of ppGpp in gram positives is by RelA, SAS1, and SAS2. Direct inhibition of Gmk, HprT and PurF by ppGpp results in a negatively feedback loop, resulting in repression of GTP and ATP levels. PurF is inhibited by ppGpp only in *E. coli*, whereas Gmk is inhibited by ppGpp only in *B. subtilis*. HprT is inhibited by ppGpp in both

organisms. **Bottom**. Reduction of iNTP levels results in inhibition of promoters that require high iNTP concentrations in order to initiate transcription. For example, all 10 rRNA operons in *B. subtilis* initiate with GTP, and low levels of GTP result in inhibition of rRNA in *B. subtilis* due to the instability of the open complex formed by rRNA promoters with RNAP. In *E. coli*, 6 of the 7 *rrn* P1 promoters initiate with ATP and are inhibited by low ATP concentrations, the other *rrn* P1 promoter starts with GTP and is inhibited by low GTP concentrations, and the 7 *rrn* P2 promoters start with CTP and are inhibited by low CTP concentrations.

The reduction of GTP concentration by (p)ppGpp has promoter-specific effects on transcription initiation. Transcription initiates with GTP from both the *rrn* P1 and P2 promoters in all 10 rRNA operons in *B. subtilis*. Because these promoters form short-lived open complexes (as they do in *E. coli*), rRNA transcription initiation is strongly dependent on high GTP concentrations[8]. Since (p)ppGpp induction reduces the GTP concentration by 60%-90% in *B. subtilis*, rRNA synthesis is reduced accordingly. This appears to be the major mechanism for control of rRNA synthesis in firmicutes, as the rRNA response to (p)ppGpp after amino acid starvation is defective in *relA* mutants[8]. In contrast, the primary mechanism by which (p)ppGpp regulates rRNA transcription in proteobacteria is by binding directly to RNAP [41,42] (see below).

Whereas (p)ppGpp negatively regulates rRNA promoters by decreasing GTP pools in *B. subtilis*, (p)ppGpp positively regulates transcription from promoters for branched chain amino acids (BCAA). The best characterized is the *ilv* operon encoding enzymes for synthesis of leucine and isoleucine. During amino acid starvation, *ilv* operon expression

is up-regulated more than 30 fold [43]. This results in large part from an increase in transcription from promoters controlled by CodY, a repressor whose binding to DNA is dependent on GTP as a cofactor, i.e. when (p)ppGpp reduces the GTP concentration, this derepresses promoters inhibited by CodY-GTP [4445]. Consistent with this model, deletion of the genes encoding the three (p)ppGpp synthetases, RelA, YwaC and YjbM, results in a loss of *ilv* transcription [43].

It has also been reported that changes in ATP concentrations have a CodY-independent effect on some promoters [4647]. In this case, it was shown that (p)ppGpp accumulation results in a decrease in the intracellular GTP concentration and a reciprocal increase in the ATP concentration, stimulating transcription initiation from genes whose initiating nucleotide is ATP, including the *ilvB* operon. In support of this model, maximum transcription initiation from these promoters requires a much higher concentration of the initiating nucleotide (ATP), and switching the initiating nucleotide from A to G disrupts this regulation.

To examine the effects of (p)ppGpp on the transcriptome of *B. subtilis* comprehensively, microarray gene expression profiling was performed using wild type and (p)ppGpp^0 strains. To delineate the downstream effects of (p)ppGpp, these gene expression profiles were compared with that of a (p)ppGpp^0 Δ*codY* strain and a (p)ppGpp^0 *guaB*^{down} strain in which GTP synthesis is reduced by lowering expression of *guaB* which encodes IMP dehydrogenase, an enzyme involved in GTP biosynthesis [48]. Their transcriptomes were characterized after guanosine addition (to increase GTP levels) or by addition of arginine hydroxamate (to induce amino acid starvation), allowing for a comprehensive snapshot of the transcriptome in various backgrounds. Analysis of

expression profiles of the *ilvB* operon, including the *ilvBHC* and *leuABCD* genes, confirmed that they are indeed induced in wild type cells upon (p)ppGpp induction. In (p)ppGpp^0 cells, expression is strongly inhibited even during amino acid starvation, indicating that amino acid biosynthesis in (p)ppGpp^0 cells is extremely misregulated. This misregulation is responsible for the branched-chain amino acid auxotrophy observed in (p)ppGpp^0 cells. Genes in the *ilv* operon are highly expressed in a (p)ppGpp^0 Δ*codY* strain, revealing that CodY-dependent regulation is mostly responsible for the repression of *ilv* under normal growth conditions and its activation by (p)ppGpp.

The genome-wide transcription profiling also revealed profound (p)ppGpp-dependent up-regulation of other components of the CodY regulon [43,48]. These include other BCAA genes including *ilvD* and *ybgE*, the *app* and *opp* oligopeptide ABC transporter operons, and the *dpp* dipeptide ABC transporter operon. CodY functions as a transcription repressor by binding to these promoters when GTP levels are high. Production of (p)ppGpp reduces GTP levels, thus derepressing CodY and inducing gene expression.

Some of the genes whose transcription is strongly activated upon (p)ppGpp accumulation, such as *metE* and the *hom* operon including the *thrBC* genes, are not identified as members of the CodY regulon. Their upregulation can be explained, at least in part, by the changes in GTP and/or ATP levels that affect transcription independently of CodY[43].

Finally, in addition to the GTP and ATP mediated transcriptional effects, there is a strong general decrease in expression of the *de novo* purine biosynthesis genes (the *purEKBCSQLFMNHD* operon) upon (p)ppGpp induction. This is due to direct binding of

(p)ppGpp to the transcription regulator PurR. Thus (p)ppGpp, in addition to regulating gene expression indirectly via its effects on NTP levels, also directly regulates gene expression of the PurR regulon [49].

d. The nucleotide derivatives pppGpp and ppGpp control transcription directly by multiple mechanisms

i. Effects on transcription initiation In *B. subtilis*, characterization of specific promoters provided strong evidence for both positive and negative stringent regulation through changes in GTP concentrations [8,43,49]. However, in proteobacteria, (p)ppGpp exerts its effects on transcription primarily by binding directly to RNAP. We focus first on the effect of (p)ppGpp on transcription initiation in *E. coli*, followed by briefly mentioning its reported effects on transcription elongation.

Full regulation of transcription by (p)ppGpp in *E. coli* requires the small protein DksA [50]. It was initially assumed that DksA prevented a protein folding defect since it was identified originally as a multicopy suppressor of a *dnaK* mutant [51]. However, it was later shown that DksA is a transcription factor that binds directly to the RNAP secondary channel [50,52] and that the suppression of a *dnaK* mutant was dependent on non-physiologically high levels of expression of DksA [53]. The β’ rim helices, the binding site for DksA, are also the binding site for the transcription factors GreA and GreB [54–56]. However, DksA shares little sequence homology with the Gre factors and primarily affects transcription initiation whereas the Gre factors primarily affect elongation [26,50,57–59].

The discovery that DksA is a transcription factor that works synergistically with (p)ppGpp was critical for understanding the stringent response. Together, DksA and (p)ppGpp reduce transcription from rRNA promoters in vitro ~20-fold compared to the ~3-fold reduction observed by (p)ppGpp alone [41,50,60]. (p)ppGpp and DksA also activate transcription of many amino acid biosynthesis genes [42,58]. Consistent with the effects of DksA *in vitro*, deletion of the *dksA* gene results in defects that share similarities with cells incapable of producing (p)ppGpp, including polyauxotrophy [50,58,61,62].

ii. (p)ppGpp binding sites on RNAP. In *E. coli*, (p(ppGpp) interacts directly with RNAP to regulate transcription initiation at specific promoters. Since (p)ppGpp lacks the appropriate 3'OH groups for attack by the incoming NTP, (p)ppGpp should not be able to be utilized as a potential substrate for RNAP chain elongation. Therefore, identification of the (p)ppGpp binding site(s) on RNAP was a crucial step in understanding its mechanism of action. Although an early cocrystal of ppGpp with *T. thermophilus* RNAP suggested that (p)ppGpp might bind near the catalytic site [63], further investigation indicated that potential binding of (p)ppGpp to this site in *E. coli* RNAP was not responsible for effects of (p)ppGpp on transcription by *E. coli* RNAP [64], and in fact, (p)ppGpp binding to that site on *T. thermophilus* RNAP was not likely to be responsible for effects of (p)ppGpp on *T. thermophilus* transcription either [65]. In retrospect, it appears that binding of ppGpp in the *T. thermophilus* co-crystal might have derived from artifactual binding of the alarmone to the so-called E-site of RNAP, a binding site favored by NTPs on their approach to the active site [66]. Consistent with this

hypothesis, when the (p)ppGpp binding site(s) were finally determined and confirmed genetically, it was found that it bound to two distinct sites (which were then dubbed Sites 1 and 2), neither of which corresponded to the site identified in the *T. thermophilus* co-crystal.

Site 1 was discovered by using ^{32}P-6-thio-ppGpp to produce a UV-dependent crosslink within RNAP. After finding that 6-thio-ppGpp crosslinked to one of the two large subunits of RNAP, the subunit harboring the crosslink was identified by fusing *β*' to GFP to distinguish its migration from that of *β on polyacrylamide gels. Single t*hrombin sites were engineered at a series of positions in *β*', and then a crosslink was mapped to an interval of 36 amino acids within the *β*' subunits using cleavage with thrombin. Substitutions were created in RNAP near the site of the crosslink, and RNAPs containing these substitutions were then tested for their responses to (p)ppGpp by *in vitro* transcription [67]. RNAPs containing a deletion of the N-terminal amino acids in ω (ωΔ2–5) or multiple substitutions in *β*' were insensitive to inhibition by (p)ppGpp *in vitro*, suggesting that a pocket was formed by two sections of *β*' and the N-terminal residues in the ω subunit. X-ray structures of co-crystals of *E. coli* RNAP holoenzyme containing ppGpp confirmed the position of the binding site and extended the identification of the liganding residues responsible for forming the binding pocket [68,69] (see Figure 2 and legend for positions of substitutions that reduced or eliminated (p)ppGpp function). However, major conformational change(s) that could account for the effect on transcription were not observed by comparison of the crystal structures ± ppGpp.

Mutations in the *rpoB* or *rpoZ* genes that resulted in RNAPs that failed to respond to ppGpp *in vitro* were introduced into the bacterial chromosome, and the resulting strains

were tested *in vivo* [67]. Surprisingly, the mutant strains lacking Site 1 exhibited only mild defects in responding to amino acid starvation. Furthermore, RNAPs lacking the ppGpp binding site partially recovered a response to ppGpp when DksA was included in the *in vitro* transcription reaction. These results led to the hypothesis that there might be another ppGpp binding site on RNAP (now called Site 2). To identify the putative binding site, RNAP lacking Site 1 was incubated with DksA and ^{32}P-6-thio-ppGpp, and crosslinks were identified to DksA itself. The crosslink to DksA was completely dependent on inclusion of RNAP [41].

ppGpp binding to RNAP was tested using direct binding assays (DRaCALA; differential radial capillary action of ligand assay) [41,70]. These data supported a model in which RNAP contains a ppGpp binding site at an interface of the rim-helices of *β*' and DksA, as well as the one at the interface of *β*' and ω (Site 1). Substitutions for specific DksA residues and for *β*' rim-helix residues reduced effects of ppGpp on inhibition and activation without affecting DksA binding to RNAP, identifying the crucial residues contributing to the ppGpp Site 2 binding pocket (see Figure 2). Whereas Sites 1 and 2 were both required for full inhibition of transcription from an rRNA promoter, only Site 2 was required for full activation of amino acid biosynthetic promoters [41].

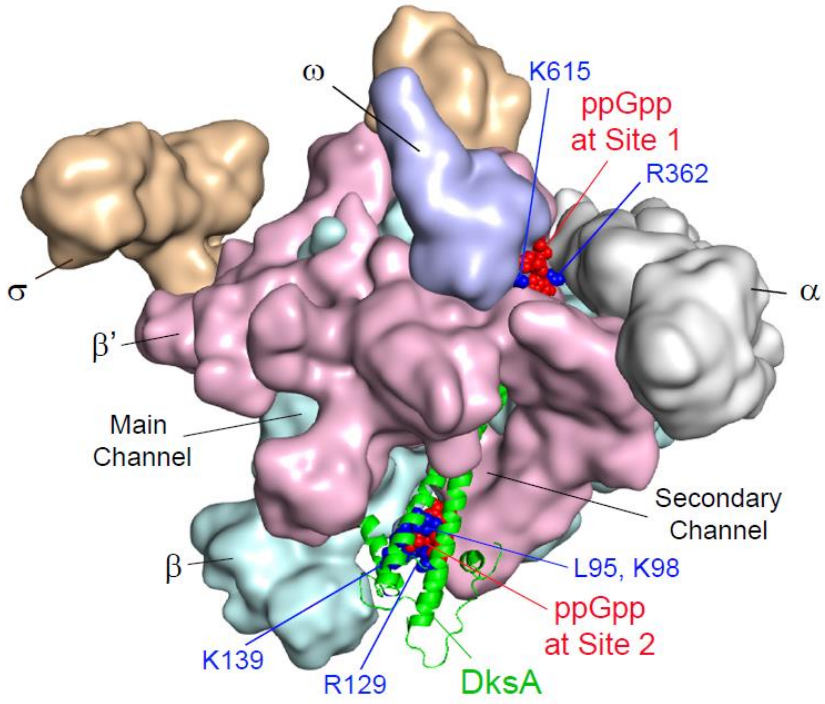

Figure 1.2: Surface view of ppGpp binding Sites 1 and 2 on *E. coli* RNAP

Site 1 is at an interface between the β' and ω subunits, and Site 2 is at an interface between the β' subunit and DksA [41,67-69,71]. DksA binds to the RNAP secondary channel. The RNAP surface representation was created in Pymol using PDB4JKR, with the β' subunit in pink, β in cyan, α in grey, σ in wheat, and ω in light blue. DksA, in green, is shown as a cartoon adapted from PDB 1TJL. ppGpp is shown as red spheres. Residues indicated as blue spheres in Sites 1 and 2 are required for ppGpp binding and function [41,67] including β'R362 and β'K615 in Site 1 and DksA L95, K98, R129, and K139 in Site 2. The locations of the main and secondary channels in RNAP are also indicated.

A crystal structure containing *E. coli* RNAP, DksA, and (p)ppGpp confirmed the positions of the (p)ppGpp binding sites [71] and displayed a small rigid body rotation centered around (p)ppGpp Site 2. However, crystal packing constraints made the significance of this rotation unclear and furthermore prevented identification of major conformational changes resulting from binding of DksA and (p)ppGpp. Recent single particle cryoEM structures, in conjunction with biochemical and mutational studies [72], indicate that DksA and (p)ppGpp exert their effects on transcription by adjusting the conformations of multiple dynamic regions of RNAP, altering the rates of multiple steps in the transcription initiation mechanism (see section below about the mechanism of transcription regulation by TraR).

Although the structural analyses confirmed the positions of the (p)ppGpp binding sites and determined the identities of all of the amino acids contacted by (p)ppGpp, they did not provide information about the relative affinities of the two sites for (p)ppGpp. This question has finally been answered: the two sites on RNAP bind ppGpp with similar affinity [73].

iii. Genome-wide effects of (p)ppGpp binding to RNAP The effects of (p)ppGpp on transcription are global and pervasive. The development of functional genomic tools has facilitated a view of the cellular response at a genomic level, complementing the mechanistic studies. Early studies of the genome-wide effects of (p)ppGpp in *E. coli* utilized expression microarrays on cells treated with serine hydroxamate, an inhibitor of serine tRNA aminoacylation, to induce the stringent response [74]. Additional expression microarray studies compared transcripts produced in

wild-type and Δ*relA* Δ*spoT* strains following isoleucine-exhaustion[75,76]. A fourth study compared steady-state expression in wild-type, Δ*dksA*, and Δ*relA* Δ*spoT* strains [77]. Although each of the studies identified a large number of transcripts that changed with (p)ppGpp levels, there were major differences in the identities of the affected transcripts in the different studies, perhaps not surprising since amino acid limitation itself has profound (p)ppGpp-independent effects on cellular metabolism. Furthermore, the stringent response is a rapid, transient response, dramatically altering transcription within a few minutes of (p)ppGpp induction, and the response has profound consequences on subsequent gene expression. Measurements conducted after the first few minutes of (p)ppGpp induction therefore likely include indirect effects resulting from the initial direct effects of (p)ppGpp on transcription.

Sanchez-Vazquez et al (2019*)* therefore attempted to identify the (p)ppGpp regulon using RNA sequencing (RNA-seq) of transcripts 5 or 10 minutes after ectopic expression of *relA*. (p)ppGpp was induced without concurrent amino acid limitation*.* Expression of 757 genes changed at least two-fold within 5 minutes of induction of (p)ppGpp in the strain containing the wild-type (p)ppGpp binding sites on RNAP, whereas there was little or no response in a strain in which (p)ppGpp was produced but the two binding sites on RNAP were eliminated by mutation. Thus, in *E. coli* at least, (p)ppGpp does not affect transcription directly by binding to transcription factors other than RNAP. In large part because of the increased sensitivity and reliability of RNA-seq versus expression microarrays, more than 75% of the promoter targets reported in this study were not identified in the previous microarray studies [74,76]. *In vitro* transcription analysis of effects of (p)ppGpp/DksA on a large number of the promoters identified in

the RNA-seq experiment confirmed that virtually all the effects on transcription identified in the RNA-seq experiment were direct.

The regulon members identified in the RNA-seq study confirmed previous conclusions that (p)ppGpp inhibits synthesis of multiple components of the translation apparatus, but the number of genes in the translation category was much greater than expected; more than 100 different transcripts related to translation were regulated by (p)ppGpp. Not only were ribosomal RNA and ribosomal protein genes regulated by (p)ppGpp, but so were many of the genes coding for rRNA and tRNA processing enzymes, translation factors, the GTPases that aid in ribosome assembly and maturation, and genes coding for enzymes that modify rRNAs, tRNAs, and r-proteins. Similarly, transcription of genes responsible for biosynthesis of 16 of the 20 amino acids was activated by (p)ppGpp, many more than predicted previously. The regulon also included many unexpected categories of genes, including a large number of genes related to the cell exterior.

iv. Promoter specificity and the mechanism of regulation by ppGpp/DksA and TraR. Unlike canonical factors that regulate transcription initiation by binding to specific DNA sequences adjacent to, or overlapping, the binding site for RNAP, promoter specificity for members of the ppGpp/DksA regulon is not determined by a binding sequence for the factor on DNA. Rather, (p)ppGpp and DksA bind directly to RNAP whether or not the output from the promoter is regulated. Specificity, whether the promoter is activated, inhibited, or unaffected, is determined by the intrinsic kinetic properties of the promoter [78].

Transcription initiation is a multistep process in which there are a series of conformational changes of the complex. Interfaces established in earlier intermediates

trigger subsequent rearrangements to form later intermediates, ultimately leading to DNA opening and alignment of the start site base on the template strand with the catalytic site of the enzyme. The whole process is driven by binding free energy, not by hydrolysis of ATP or other high energy molecules [79].

Studies on the effects of (p)ppGpp and DksA on transcription have recently been supplemented by studies on TraR, a distant DksA homolog that is produced by the proteobacterial F element. TraR is only half the size of DksA, but it binds in the secondary channel of RNAP like DksA, and it activates or inhibits roughly the same set of promoters as (p)ppGpp and DksA [80,81]. Recently, structural studies using single particle cryo electron microscopy on TraR-RNAP complexes and ppGpp-DksA-RNAP complexes have identified multiple conformational changes in RNAP that occur in response to the regulatory factors [72,82,83]. The structures indicate that (p)ppGpp/DksA and TraR cause conformational changes in RNAP that were not apparent from X-ray structures of RNAP containing (p)ppGpp/DksA or TraR because of crystal packing constraints [71]. The results of the cryo EM studies, together with previous mechanistic studies that indicated that (p)ppGpp/DksA and TraR alter “isomerization” steps, i.e. steps in transcription initiation after formation of the closed complex and prior to the NTP incorporation step [50,58,62,81,84], are providing models for how the factor-induced conformational changes affect specific steps in open complex formation.

The prototypic (p)ppGpp-inhibited promoter, the rRNA promoter *rrnB* P1, associates with RNAP very rapidly to form a closed complex, but the open complex is very short-lived [84,85]. As proposed by Travers almost 40 years ago, a G+C-rich region between the -10 hexamer and the transcription start site “discriminates” promoters that are

negatively regulated by (p)ppGpp from those that are activated or unaffected [86]. More recent analyses suggest that the discriminator region is actually a composite of two determinants [42,87]. In general, negatively-regulated promoters are characterized by the absence of a nontemplate strand G two positions downstream of the -10 element (which interacts with σ region 1.2 in unregulated or activated promoters) and by the presence of a G+C-rich region just upstream of the transcription start site (that favors reannealing of the transcription bubble). These two sequence determinants conspire to create a very short-lived open complex. Inhibited promoters also tend to have -10 hexamers that are closer to the consensus at positions between the highly conserved -11A and -7T positions that flip into pockets in the housekeeping sigma factor during open complex formation [42,88].

rRNA promoters are among the strongest in *E. coli*, largely because of the presence of UP elements and near consensus -10 and -35 hexamers that together result in a rapid rate of promoter binding by RNAP. The high activity of rRNA promoters is also attributable to sequences that lead to a rapid rate of promoter escape. rRNA promoters form a “scrunched open complex” that allows for more efficient promoter escape, bypassing the requirement for creating strain to break contacts with promoter DNA during early RNA synthesis [20]. A C residue at position -1 in the nontemplate strand is conserved in >85% of (p)ppGpp/DksA inhibited promoters, including rRNA promoters [42]. This strong preference for the nontemplate strand C at −1 has been proposed to reflect stabilization of the incoming rNTP at +1 (most often a purine) by base stacking with the purine at -1 on the template strand [89]. Thus, the conservation of the C at -1 in negatively

regulated promoters may reflect more the requirement for rapid promoter escape than regulation by ppGpp/DksA.

Positively regulated promoters (such as the promoter for the anti-adapter protein *iraP* and a variety of amino acid biosynthesis promoters, including *argI*) isomerize to the open complex very slowly in the absence of (p)ppGpp/DksA or TraR, but they make very stable open complexes [41,58,72,84]. (p)ppGpp/DksA or TraR activated promoters tend to lack consensus bases in the -10 element at -10, -9, and -8 and have A+T-rich discriminator regions. Consistent with the importance of a non-consensus -10 hexamer for activation, mutations in the -10 element that increase the similarity to the consensus sequence bypass the requirement for (p)ppGpp [90,91].

The conformational changes in RNAP caused by ppGpp/DksA or TraR binding have been identified in single-particle cryoEM studies [72,83,92]. These studies identify a few general principles for positive and negative control of transcription initiation, depending on the kinetic properties of the promoter. As predicted, (p)ppGpp/DksA and TraR affect multiple steps in the mechanism[93,94]. They activate transcription of positively regulated promoters by increasing the rates of formation of specific intermediates subsequent to closed complex formation, including capture of the -10 hexamer and displacement of sigma region 1.1, facilitating entry of promoter DNA into the main DNA channel of the enzyme [72,83,92]. It has also been proposed that (p)ppGpp/DksA could increase transcription from the *uspA* promoter by facilitating promoter clearance [95].

In contrast, the cryo EM studies suggest that (p)ppGpp/DksA and TraR inhibit transcription initiation of negatively regulated promoters by at least three different mechanisms. They stabilize an intermediate subsequent to nucleation of strand

opening, thereby impeding progression to later intermediates [83,92]. They alter interactions between RNAP and the downstream DNA duplex thereby inhibiting productive open complex formation [50,62,72,96]. And on the fraction of the promoter population that escapes the inhibitory effects in earlier intermediates, they sterically interfere with incorporation of the initial NTP [71]. The fraction of the overall effect attributable to each mechanism would depend on which step(s) in the mechanism are rate limiting for the specific promoter.

Recent single molecule imaging studies indicate that secondary channel binding factors (SCFs), including GreB and DksA, do not bind to preformed open complexes but instead associate with promoters only as a complex with RNAP, and they dissociate relatively quickly from the promoter complex [97]. These data are consistent with a previous report indicating that DksA has a 10-fold higher affinity for free RNAP than for RNAP in a preformed open complex [98]. On negatively-regulated promoters like *rrnB* P1 where RNAP dissociates quickly from the DNA, the SCF remains with the complex only as long as RNAP is bound, dissociating from the promoter together with RNAP. Consistent with this model, no SCFs were observed on rRNA promoter complexes that had initiated transcription. Thus, on strongly negatively-regulated promoters like *rrnB* P1, DksA-ppGpp or TraR must exert most of their inhibitory effects before the NTP incorporation step. On weakly inhibited promoters (that form somewhat longer-lived promoter complexes), the SCFs might sterically inhibit NTP incorporation (in agreement with the model proposed by Molodtsov et al. (2018).

In contrast, promoters positively regulated by DksA/ppGpp or TraR form long-lived open complexes. DksA/ppGpp or TraR would be expected to dissociate from RNAP before

RNAP dissociates from the promoter. Dissociation of the factor while RNAP is still bound to the promoter would allow completion of the transcription initiation program and nucleotide incorporation subsequent to the activated steps that occur earlier in the kinetic pathway.

v. Effects of (p)ppGpp and/or DksA on transcription elongation, RNA fidelity, and genome integrity.

Effects of (p)ppGpp and DksA on transcription are not limited to initiation. They also have been reported to affect transcription elongation, which in turn can affect other processes that share the DNA template, most importantly, DNA replication.

Although elongation by RNAP is processive, it is interrupted by pauses whose durations vary widely. RNAP pauses frequently at defined sequences, referred to as elemental pauses, that are relatively short-lived, and from which RNAP generally recovers with high efficiency [12]. Most pauses that mediate gene regulation are thought to originate from elemental paused complexes that interrupt the nucleotide addition cycle [99],but cis- or trans-acting factors can exacerbate the elemental paused state and drive the complex into a backtracked state that requires rescue by Gre factors. Since (p)ppGpp stimulates pausing [100] and promotes backtracking [101], (p)ppGpp could stimulate pausing by stabilizing the backtracked elongation complex.

(p)ppGpp can reduce the chain elongation rate of *E. coli* RNAP *in vitro*[100,102]. Since these early studies were done before the discovery of DksA, the effects must have resulted from (p)ppGpp binding to Site 1. However, there are also reports that DksA amplifies the effects of ppGpp on elongation [103].

Older reports had shown that amino acid limitation induces (p)ppGpp production, decreasing the mRNA chain elongation rate *in vivo*. The effects of (p)ppGpp were only observed on translated genes *in vivo*, and not on rRNA operons [104]. Furthermore, an antitermination sequence determinant in the rRNA precursors, boxA, was required for reducing the inhibitory effects of (p)ppGpp on elongation [105], suggesting that the rRNA antitermination system counteracts the effects of (p)ppGpp on stable RNA genes (which are not translated). In contrast, (p)ppGpp dependent pausing of RNAP on translated genes helps facilitate coupling of transcription and translation and thus it was proposed that it prevents premature termination of mRNA synthesis.

RNAP variants have been identified that partially mimic the effects of (p)ppGpp by selecting for growth of Δ*relA* Δ*spoT* or Δ*dksA* mutant cells on media without amino acids [61,62,106], or by suppression of the loss of viability caused by various mutations needed for DNA repair (e.g. [107,108]). These RNAPs all made open complexes with reduced open complex lifetimes (e.g. [62,84,106]) and/or made shorter arrays of RNAPs on DNA templates, suggesting they made less stable elongation complexes [109]. DNA damage induces (p)ppGpp synthesis, and it was proposed that (p)ppGpp works synergistically with UvrD to facilitate backtracking of RNAP away from the site of DNA lesions or adducts to promote DNA repair[101].

ChIP experiments examining genome-wide RNAP occupancy showed that RNAP processivity is decreased on protein-encoding genes in Δ*dksA* cells compared to wild type cells: RNAP signals are enriched closer to the promoters and fewer signals were found near the 3’ end of the transcribed sequences in in Δ*dksA* cells [110]. Thus, it was proposed that DksA prevents loss of cell viability because it prevents stalling of

transcription elongation complexes on protein-encoding genes [110]. When coupled with a mutation that slows the translation rate, cells lacking *dksA* lost viability, suggesting a genetic interaction between *dksA* and the ribosome.

These *in vivo* studies also supported a role for DksA in facilitating transcription processivity under circumstances where translation was inhibited, such as during amino acid starvation[110]. DksA was found with RNAP both at promoters and throughout transcribed sequences[110]. In a strain lacking *dksA*, RNAP was more prone to pause at promoter proximal sites, and this effect was amplified when cells were starved for amino acids, especially in protein coding genes. How DksA and (p)ppGpp are able to decrease elongation rates and promote transcription termination *in vitro* [103] while DksA is able to increase processivity *in vivo* [110] is a paradox that has not yet been resolved.

In bacteria, transcription errors occur about 10,000-fold more frequently than replication errors [111,112]. There have been conflicting reports on the effect of DksA/(p)ppGpp on transcription fidelity[113]. Using two different kinds of *in vivo* reporter assays, it was reported that Δ*dksA* cells showed a higher level of transcription errors than wild-type cells [113,114], but it was recently reported that only GreA, and not GreB or DksA, acted as a transcription fidelity factor using RNA-seq measurements on a genome wide scale during log phase growth [115]. One possibility is that GreA does not directly increase transcription fidelity *per se*, but instead results in an increase of fidelity *in vivo* because of its ability to restart backtracked RNAP complexes [115]. Measurements of transcription error rates were not measured under (p)ppGpp inducing conditions.

Finally, DksA has been implicated in prevention of replication-transcription conflicts by reducing replication arrest during amino acid starvation [116]. In the presence of DksA, RNAP allowed completion of DNA replication following amino acid starvation,

presumably because DksA reduces RNA synthesis at the levels of initiation and prevents stalling of transcription elongation complex and its subsequent blocking of replication fork progression. In the absence of DksA, however, replication arrest was only rescued by the addition of rifampicin, which blocks RNA chain growth beyond the first two or three nucleotides and thus ultimately reduces elongation complexes from interfering with replication [116].

vi. Regulation of transcription by ppGpp binding to RNA

Riboswitches are transcripts whose expression is regulated by ligands, usually small molecules that bind to the transcript with high-affinity [117,118]. The riboswitch is composed of two RNA domains, a ligand-binding motif, sometimes referred to as the aptamer, and a domain that responds to a conformational change in the aptamer domain upon ligand binding and changes gene expression, sometimes referred to as the expression platform[118]. Riboswitches can alleviate or provoke premature termination of transcription, or they can alter ribosome binding to the mRNA, increasing or decreasing translation. Riboswitches act *in cis*, in contrast to trans-acting small RNAs that regulate gene expression by base-pairing with target transcripts. Thus, riboswitches couple sensing and regulatory functions, providing fast responses to changing ligand concentrations.

Recently, (p)ppGpp-binding riboswitches were described in several related firmicutes [119]. Among these, the (p)ppGpp-binding motif of the *ilvE* mRNA from *Thermosediminibacter oceani*, encoding a branched chain amino acid transferase, has a remarkably high affinity for both ppGpp and pppGpp, with a dissociation constant of about 10 nM. The (p)ppGpp-binding motifs constitute a subclass of a widespread riboswitch family in mRNAs involved in branched chain amino acid metabolism, identified by *in silico* methods [120]. Another subclass of the same riboswitch family was identified as a guanidine-binding motif, and a third subclass was

characterized as having a phosphoribosyl pyrophosphate (PRPP) binding motif [121]. The structures of one of the PRPP binding aptamers and one of the (p)ppGpp aptamers [122] were solved with the bound ligand. Strikingly, point mutations in the PRPP and (p)ppGpp binding motifs switch the specificities of the two aptamers [119,122].

These results highlight the ability of RNA aptamers to acquire new binding specificities for related ligands. Presumably this has happened many times during the course of evolution. In any case, these results suggest that (p)ppGpp-binding riboswitches, along with other base- and nucleotide-derived riboswitches, may have been important regulatory mechanisms in primordial living cells, perhaps even preceding the evolution of protein-binding transcription factors [117].

Acknowledgements

Work in the Gourse lab is supported by R01 GM37048 from the National Institutes of Health. JJ was supported in part by a long-term EMBO fellowship. Work in the Wang lab is supported by R35 GM127088 from the National Institutes of Health and an HHMI Faculty Scholar Program. LO was supported in part by an NIH predoctoral training grant T32 GM007133.

Chapter 2:

DksA is essential for robust transcription elongation and protein synthesis across nutrient limiting conditions.

Lucas M Onder, Bin Wang, Jeremy W Schroeder, Aude E Trinquier, Samantha Du, Lingjun Li, Jue D. Wang

Author contributions: L.M.O performed transcription and translation kinetics, term-seq, Tn-seq, Growth curves, WGS, ssrA-his6 purification, western blot analysis. B.W Performed the LC/MS and analysis of ssrA-his6 Proteins, A.E.T performed the Ribosome quantification, J.W.S performed the Term-seq and TN-seq analysis. S.D performed the spotting assays, growth curves and colony sectoring.: L.M.O, and J.D.W, wrote the paper.

2.1 Abstract

Our understanding how bacteria coordinate gene expression with cell growth to adapt to stressful environments remains unknown. The stringent response is the bacterial stress response often associated with nutrient limitation that requires transcriptional reprograming and the transcription factor dksA and the rapid accumulation of cellular guanosine tetra-phosphate (ppGpp) or penta-phosphate (p)ppGpp, a key secondary metabolite that regulates various biochemical and physiological processes in *E. coli*. Extensive studies to understand the mechanism of gene regulation by DksA during the stringent response have been performed but the role it plays in regulating bacterial steady-state exponential growth remains unknown. Through the use of in *vivo* transcription and translation kinetics assays combined with titrating nutrient availability to cells we identify the role DksA plays in promoting robust protein synthesis across nutrient limiting conditions. Additionally, we systematically identify genetic interactions of DksA through Transposon-sequencing experiments to identify ClpX and ClpP. Two proteins critical to the proteolysis of truncated polypeptides which can be formed either due to mRNA lacking stop codons or premature transcription termination of mRNA transcripts. These truncated proteins must be rescued by the tmRNA ribosome rescue pathway and degraded by clpXP. We show that loss of dksA results in over production

of ribosome synthesis and slower translation elongation in poor nutrient conditions. Term-seq experiments were used to test the role of transcriptional robustness and show that Δ*dksA* cells do not experience premature transcription termination, suggesting DksA plays a role in preventing transcriptional pausing or kinetically allowing faster transcription elongation rates. We observe that nutrient rich media such as LB is able to mask severe phenotypes in Δ*dksA* cells and in the absence of supplemented amino acids DksA is essential.

2.2 Introduction

Growth rate and regulation

Microbial cells must make constant adjustments in order to adapt their growth within various environments. Their survival is dependent on adaptation to environmental and nutrient shifts. Changes must be made to DNA replication, cell division, gene expression, and protein synthesis to ensure cellular survival. However, adjusting gene expression are not the only systemic change that must take place (Imholz et al. 2020). It is also important to adjust the rate at which replication, transcription and translation (the central dogma processes) occur to levels appropriate to the nutrient availability resulting in faster rates in nutrient rich media and slower rates during nutrient poor conditions (Iyer et al. 2018; Dai et al. 2017). However the rate limiting step of bacterial growth and growth rate is protein synthesis (Dai et al. 2017). In nutrient rich medium *E. coli* cells will allocate a major fraction of their proteome for ribosomal proteins and other proteins necessary for translation in order to maintain high protein synthesis rates as well as rapid growth (Scott et al. 2014; Klumpp et al. 2013; Dai et al. 2017). In contrast, when nutrient availability is low, *E. coli* cells will allocate a majority of their proteome to

metabolic proteins needed for nutrient uptake, metabolism, and catabolism, resulting in lower ribosome abundance and slower growth rates (Hui et al. 2015; Scott et al. 2014).

ppGpp and growth rate.

In order to adapt to changes in nutrient availability, such as accessibility to nitrogen sources, *E. coli* cells will produce the alarmone guanosine tetraphophosphate ppGpp to adjust gene expression, metabolic rates, and the rates of central dogma processes**.** During acute starvation of amino acids which resulting in the stringent response, ppGpp is produced to alter gene expression and suppresses central biochemical processes to enable bacteria to survive and adapt to these conditions (Imholz et al. 2020). Additionally, small changes in nutrient availability will cause milder adjustments to basal ppGpp levels.

Both transcription and translation respond to changes in ppGpp levels and make adjustments to central dogma processes necessary for cellular viability. For transcription regulation by ppGpp, RNAP contains two sites that bind ppGpp, Site 1 located sandwiched between the omega subunit and the *β*' subunit and site 2 is between DksA and the *β*' subunit(Ross et al. 2013; Ross, Sanchez-Vazquez, et al. 2016). Nutrient shifts that cause changes to basal levels of ppGpp will cause increased occupation ppGpp within the two binding sites of RNA Polymerase (RNAP) in order to respond to the nutrient shifts and mediate gene expression(Myers et al. 2020; Ross, Sanchez-Vazquez, et al. 2016; Sanchez-vazquez et al., n.d.). DksA is a transcription factor that binds directly to the RNAP secondary channel and works synergistically with ppGpp to regulate the transcription stringent response (Ross et al., 2016b; Paul et al. 2004; Perederina et al. 2004). In contrast to ppGpp, the concentration of the ω-subunit

of RNAP and DksA remains constant under differing growth conditions and nutrient availability (Brian J Paul et al. 2004; Myers et al. 2020).

Artificial changes that either increase or decrease (p)ppGpp levels will cause growth defects in *E. coli*. Increased (p)ppGpp levels result in limited ribosome synthesis to inhibit growth rate, while decreased (p)ppGpp levels will limit the production of metabolic proteins which also results in a slower growth rate(Zhu and Dai 2019). Additionally, artificial induction of ppGpp done with a titratable expression of the relA+ gene (encoding constitutively active relA protein) has been shown result in slowing down of transcriptional elongation following production of ppGpp (Zhu et al. 2019). This may suggest that under nutrient-limiting conditions, cells with higher basal ppGpp levels may be the cause of slower transcription elongation.

Transcription and translation coupling

In bacteria, transcription and translation occurs concurrently with the ribosome being able to control genes transcribed by RNAP while RNAP regulates the number of ribosomes being transcribed in the cell based on nutrient availability. One-way ribosomes can be arrested is by “non-stop” translation or translation that becomes arrested at the 3` ends of mRNA due to the absence of a stop codon. Decoupling of transcription and translation can result in premature transcription which would result in a truncated mRNA likely lacking a stop-codon and requiring rescue by the transfer-messenger (tmRNA) system (Buskirk and Green 2017; Zhu et al. 2019).

clpXP and tm-RNA

Translation of polypeptides by the ribosome is an essential process for cell survival. Cellular stressors can inhibit ribosome processivity resulting in ribosomal arrest during elongation or termination thus limiting the cell's capacity for protein synthesis. This limitation can be harmful to cellular viability. Bacterial cells have developed quality control pathways in order to rescue ribosomes that have been stalled and in need of rescuing(Buskirk and Green 2017). The primary method *E.coli* uses to rescue ribosomes that are stalled or on truncated mRNAs is through transfer-messenger RNA (tmRNA) which work together with the accessory protein SmpB, which interacts with the ribosome and guides tmRNA to the stalled ribosome(Miller and Buskirk 2014). Collectively tmRNA and SmpB rescue stalled ribosomes through the "trans-translation" pathway(Keiler 2008; Miller and Buskirk 2014). As the name indicates, tmRNA functions as both an aminoacylated-tRNA to allow for addition of amino acids to the truncated polypeptide chain while also acting as an mRNA by interacting with the decoding region of the actively translating ribosome. The tmRNA will be "trans-translated" to add a polypeptide sequence (AANDENYALAA) as well as coding for a stop codon to terminate and recycle the stalled ribosome(Keiler 2008). This added polypeptide sequence is recognized by the ClpXP protease system and degraded into small peptide fragments. ClpXP is a serine protease complex that subsists of two distinct proteins: a AAA+ ATPase ClpX and the peptidase ClpP(Bittner, Arends, and Narberhaus 2016). ClpX recognizes polypeptide sequences that have either been tagged by tmRNA or a number of proteins containing specific C-terminal sequence motifs(Fei et al. 2020). From there ClpX will unfold the protein and translocate

the polypeptide chain into the proteolytic active site of ClpP to be degraded(Fei et al. 2020).

Some proteins targeted for proteolysis by ClpP include minD and ZapC which are involved in regulating cell division(Flynn et al. 2003). Additionally, ClpP promotes adaptation into stationary phase in *E.coli* through regulation of *rpoS* (sigmaS) (Flynn et al. 2003). ClpXP plays a critical role in recovery of cells following DNA damage by degrading proteins that would be otherwise toxic to cells during regular exponential growth conditions. ClpXP has also been shown to be important in recovery due to metal stress and protects cells against nitrative stress.(Flynn et al. 2003; Neher et al. 2006; Robinson and Brynildsen 2015).

An alternative pathway for ribosome rescue is through the protein ArfA which is able to rescue stalled ribosomes by binding the empty A-site of the ribosome and recruiting RF2, which will rescue stalled ribosomes but not target the truncated peptide for degradation (Chadani et al., 2012). Additionally, ArfA was found to be synthetically lethal in cells lacking tmRNA. In wild-type *E. coli* cells tmRNA inhibits production of the ArfA protein by tagging it for degradation with ArfA expression increasing only when tmRNA becomes saturated by stalled ribosomes (Chadani et al. 2010).

Various TN-SEQ screens identify dksA

Various studies using transposon-sequencing screens (tn-seq) have identified transposon insertions within *dksA* making it a gene of interest in their studies. These studies vary in scope, organism and range. For example, dksA was identified as a factor essential for squid colonization in the squid symbiont *Vibrio fischeri (Brooks et al.,*

2014). Additionally, dksA is required by *Salmonella enterica* for survival within host macrophages, for virulence in mice and host cell entry (Henard and Vázquez-Torres 2012; Azriel et al. 2016). Salmonella typhimurium requires *dksA* for virulence and colonization of chick alimentary tracts(Turner et al. 1998). Additionally, *dksA* has been identified to be essential for transmission of *Borrelia burgdorferi,* the Lyme disease-causing spirochete, into *I. scapularis* nymphs (deer ticks) and for its subsequent infection of mice (Boyle et al. 2021). Within *Pseudomonas aeruginosa, dksA* is required during carbon and oxygen limitation (Basta, Bergkessel, and Newman 2017). Within *Acinetobacter baumannii*, a gram-negative pathogen lacking the global stress regulator σS, *dksA* was shown to be essential for infection of *Galleria mellonella* larvae (wax moth) and for promoting tolerance of various environmental stresses such as oxidative, osmotic, and copper stress (Maharjan et al. 2021).

One common theme among these screens identifying *dksA* is that they all are selecting for cells that must be able to adapt to a new environment and respond to nutrient shifts whether it is colonizing a squid, infecting mice, or surviving within macrophages. These articles highlight the critical role that dksA plays in promoting cellular adaptation to their ever-changing environments.

Phenotypic overlap between dksA and clpP

There are some phenotypic similarities between dksA and clpP such as both playing a critical role in virulence as well as in cellular survival due to nitric oxide stress and nitric oxide detoxification as well as adjustment for entering stationary phase (Chou and Brynildsen 2019; Brown et al. 2002; Flynn et al. 2003; Robinson and Brynildsen 2015). Specifically worth noting is that *Δ*dksA cells experiencing nitric oxide stress show

2-3-fold lower mRNA levels when tested with qPCR and the protein reporting showing ~10- fold lower levels of protein output indicating that protein synthesis is severely impaired possibly indicating translational limitations occurring in *Δ*dksA cells (Chou and Brynildsen 2019). Additionally*, Δ*dksA cells show a 2-3-fold increased ssrA tagging following production of DNA-protein crosslinks (Krasich et al. 2015a).

Proteomic profiling experiments used to identify clpXP substrates using a non-proteolytic clpXP by using a non-proteolytic $ClpP^{trap}$ mutation identified dksA as a substrate of clpXP indicating a physical interaction between the proteins(Flynn et al. 2003).

Additional experiments using $ClpP^{trap}$ showed 25% of clpXP substrates to be SOS-response proteins following nalidixic acid treatment (a DNA gyrase inhibiter and DNA damage causing agent). These experiments showed that DNA damage-response proteins were rapidly degraded by ClpXP in order to allow for cells to respond to the environmental stress such as DNA damage and then recovery from the acute stress by degradation of proteins that would be otherwise toxic(Neher et al. 2006). DksA also has a role in preventing DNA damage following environmental shifts. Serine hydroxamate treatment of Δ*dksA* cells leads to rapid degradation of lexA indicating DNA damage. LexA degradation then leads to induction of the DNA damage (SOS) response with transcripts increasing by 20-100 fold increases compared to wild-type cells (Tehranchi et al. 2010).

We have identified a critical genetic interaction between the transcription factor dksA and proteolytic machinery clpXP through a tn-seq screen in *E. coli*. Our transposon-sequencing screen identified clpX and clpP as having strong synthetic genetic

interactions with dksA. Together these factors likely work synergistically in responding to stress and recovering from that stressor with dksA playing a role in regulating the transcription response due to stress and clpXP being able to turn over and degrade proteins that would otherwise be toxic to the cells environment as well as degrade proteins resulting from stalling of translation. Previous studies from our lab have shown that dksA promotes replication and transcription elongation during nutrient starvation (Zhang et al. 2014; Tehranchi et al. 2010). The findings of this work expand the role dksA is known to play in coordinating the central dogma processes by demonstrating that dksA promotes translation elongation as well.

2.3 Methods

2.3.1 Strains and growth conditions

All E. coli strains used are derivatives of MG1655. Deletion mutants were constructed by P1 phage transduction from the Keio collection (Baba et al., 2006). Unless indicated, cells were grown at 37 C with vigorous shaking at 220 rpm. Strains were grown in MOPS medium with 0.4% glycerol and either +0.4% or 0.1% Cas Amino acids or LB media as specified in experiments.

2.3.2 Generating Transposon Library

Transposon libraries were made using a protocol adapted from (Wetmore et al. 2015). We generated the Wild-type and dksA transposon mutant libraries by conjugating *strains jdw 401 and JDW618* with WM3064 harboring the pKMW3 *mariner* transposon vector library (APA752). We combined 1:4 ratio of mid log ~0.6 OD donor and acceptor cells and APA752, conjugated them for 12 h at 37°C on 0.45-µm nitrocellulose filters (Millipore) overlaid on LB agar plates containing DAP, and

plated the resuspended cells on LB plates with 50 µg/ml kanamycin to select for mutants. After overnight growth at 37°C, we scraped the kanamycin-resistant colonies into LB, determined the OD_{600} of the mixture, and diluted the mutant library back to a starting OD_{600} of 0.2 in 250 ml of LB with 50 µg/ml kanamycin. We grew the diluted mutant library at 37°C to a final OD_{600} of 1.0, added glycerol to a final volume of 20%, made multiple 1-ml −80°C freezer stocks.

2.3.3 Minimal media downshift

An overnight culture was grown in Mops + 0.4% Cas media and then back diluted 1:200 into Mops + 0.4% Cas media and grown to an OD ~ 0.2 then 100 uL of cells spun down on a cellulose membrane column and washed twice with 400 uL prewarmed Mops minimal media then resuspended in 100 uL Mops minimal media. These cells were then added to 900 uL of mops minimal media in 2mL deep well blocks, serial diluted 10-fold and grown at 37 degrees. Cells were spotted every 8 hours onto LB agar plates.

2.3.4 Western Blot

Cells were grown to an OD ~0.8 and harvested by centrifugation. and loaded onto a 12% SDS/Page gel, transferred to a membrane and blotted with a polyclonal anti-his6 antibody. Membranes were then blotted with anti-rabbit antibody and scanned on an odyssey scanner.

2.3.5 RNA Isolation for term-seq and transcription kinetics

Cells were grown to an OD ~0.4 and added in a 1:1 ratio of chilled RNA stop solution containing 60% ethanol, 2% phenol and 10 mM EDTA. Samples were centrifuged for one minute at 18,000g supernatant was removed and cell pellets were resuspended in 50 uL T.E+ Lysozyme 1mg/mL final and incubated at room temperature for 5 minutes.

350 uL of lysis buffer containing 8M Guanidine hydrochloride, 20mM MES, 20mM EDTA, 1% BME was added and samples were vortexed. 400 uL of 100% Ethanol was added to samples and vortexed briefly. 700 uL of samples were added to an RNA mini spin columns (Enzymax) and centrifuged for one minute at 8,000g. Discarding flow through, spin columns were then washed once with 450 uL of 3 M Na-acetate ph 5.2 and centrifuged for 45 seconds at 8,000 g. Discarding flow-through, columns were then washed with 320 uL 70% ethanol with centrifugation for 45 seconds at 8,000G. Discarding flow-through, columns are then spun dry for 2 minutes at maximum speed. 40 uL of prewarmed DEPC-treated water was then added for 2 minutes before centrifuging for 2 minutes at 8,000G. Isolated RNA was treated with 1 uL DNase 1for 30 minutes at 37 degrees, followed by addition of 5 uL of 50 mM EDTA to and heat inactivation at 75 degrees for 10 minutes. RNA concentrations were then determined via nano-drop.

2.3.6 Reverse transcription and qPCR

RNA was reverse transcribed by incubating 250 ng - 1ug with 1 µl of 10µM random hexamer + 1 uL dNTP 10mM (NETB N0447S), incubating at 65°C for 5 min, and immediately placing on ice for 2 min. Next, 1 ul of MASHUP reverse transcriptase (Pippete Jockey), 4 µl of 5X MU Buffer, and 1 µl of 100 mM DTT were added, and the reaction was incubated at 50°C for 60 min and then terminated by incubation at 80°C for 15 min. RNA was hydrolyzed by adding 10 µl 1 M NaOH to the 20-µl RT reaction heated for 10 minutes at 70 C then neutralized with 10 µl 1 M HCl then brought to a final volume of 200 µl with ddH2O.

qPCR

Reactions were set up on ice using 2 uL of neutralized and diluted cDNA, 11 ul of 2x hotstart Taq, 8 ul ddH2O, 1,1 ul evagreen Dye, and 0.5 uL of forward and reverse primers (25 uM) into a final volume of 22 uL. Reactions were then run on a CFX Connect real-time PCR detection system (Bio-Rad). qRT-PCR reaction protocol is as follows: 95°C for 15 min, followed by 40 cycles of 95°C for 10 s, 60°C for 20 s, and 72°C for 30 s.

2.3.7 Transcription kinetics assays

E. coli cells were exponentially grown to OD600 ~0.4 followed by the induction of lac operon expression through adding 5 mM isopropyl-β-D-thiogalactoside (IPTG). Following the IPTG induction, 750 uL of cell culture was withdrawn at 15-s interval and transferred into a 1.7 mL Eppendorf tubes containing 750 uL stop solution containing 60% ethanol, 2% phenol and 10 mM EDTA (pre-cooled in −20 °C). The total cellular RNA was then extracted as described above.

As adapted from (Zhu et al. 2019) the final concentration of RNA was then measured with a NanoDrop-1000 micro-spectrophotometer. 0.5-1-μg total cellular RNA was used for cDNA synthesis with Mashup reverse transcriptase. The qRT-PCR reaction was set up as described above using the Bio-rad CFX96 Touch real-time PCR system. The lacZ mRNA abundance of a sample taken immediately before IPTG addition (referred to as “t0 sample”), M(0), was set as “1”. The relative lacZ mRNA abundance in each time point, N(t), was equal to 2Cq0–Cqt, where Cq0 means the Cq value of basal sample and Cqt means the Cq value at each time point. The lacZ mRNA abundance was plotted vs. time to obtain the transcriptional kinetics curve from which the transcriptional time of two mRNA sub-regions was estimated (detected by the corresponding **primer**

pairs) (Zhu et al. 2019) **.** For each condition, the average and standard deviation of two qpcr probes from three independent biological samples was performed. For the experiments with bicyclomycin (Bcm), cell was first exponentially growing to OD600~0.3, 20 μg/mL Bcm was added to exponentially growing cells; after 30 seconds, IPTG was added to induce the transcription of lacZ mRNA.

2.3.8 Translation kinetics assay

Measurements of the translational elongation speed of E. coli were based on a lacZ induction assay with a 10 second initiation time, as described in (Zhu et al. 2019). Cells were back diluted to 0.01 OD and grown until they reached an O.D of ~0.4. A pre-induction sample was taken and then IPTG was added to a final concentration of 5 mM. 400 uL of culture was harvested every 15 seconds and added to 5 uL of 34mg/ml Chloramphenicol stop solution, vortexed briefly and placed on ice. Collected cells were centrifuged at 4°C for 2 minutes at 19,000g then frozen and stored at -80 ^{o}C until use. Cells were resuspended in 400 uL Z buffer containing 34mg/ml chloramphenicol and the OD 595 was measured. 100 uL of cells were then lysed by addition of 10 ul of rLysozyme and 10uL Pop culture reagent followed by 30 minutes incubation at room temperature. Then lacZ kinetics activity was measured by adding 30 uL of cells and 150 uL Zbuffer plus ortho-nitrophenyl-β-galactoside (ONPG) and beta galactosidase activity was measured by colorimetric assay measuring OD 420 over time. LacZ elongation rate was then calculated as 1,024 aa/(Tfirst – 10 s), Tfirst being the time that lacZ activity was first detected above t0 levels of lacZ activity.

2.3.9 *Term-seq library preparation (*Protocol adapted from (Dar et al. 2016))

. Cells were grown overnight in Mops + 0.1% Cas then back diluted 1:100 into Mops + 0.1% Cas and grown to an OD of ~0.4 where 3 mL of untreated sample was taken and added to stop solution containing 60% ethanol, 2% phenol and 10 mM EDTA, pre-cooled at −20 °C. The remaining samples were then treated with Bicyclomycin (100 ug/ml [final]) and/or Serine hydroxamate (0.5 mg/ml [final]) for 20 minutes, then 3 mL of culture was added to 3 mL of stop solution. RNA was then extracted as described above using RNA Spin columns. Term-seq libraries were prepared similarly as in Dar et al. (2016) with a few exceptions.

RNA (2 to 5 µg) was ligated to a phosphorylated DNA Ligation adaptor oligo with 10 µl of RNA solution, 2 µl of a 10 µM DNA adapter solution, 2.5 µl of 10X T4 RNA ligase1 buffer, 2.5 µl of 10 mM adenosine triphosphate, 2 µl of dimethyl sulfoxide, 9.5 µl 50% PEG8000, and 1 µl of T4 RNA ligase1 High concentration enzyme (NEB, M0437M). The reaction was incubated for 2.5 hours at 23°C and then cleaned by adding 55 µl) paramagnetic SPRI beads mixing well by pipetting and leaving the reaction-bead solution to rest at room temperature for 2 min. Beads were then washed with 200 µl of 80% ethanol (EtOH), allowing an incubation period of 1 min for each wash. 80% ethanol was then discarded and the sample was washed again with 200 uL 80% EtOH. The beads were air dried for 5 min then the RNA was eluted in 9 µl of H_2O.

The RNA was fragmented with fragmentation buffer (Ambion) in 72°C for 1.5 min. The fragmentation reaction was cleaned with SPRI beads 2.2× as described above and eluted into 15 µl of H_2O. Ribosomal RNA was depleted by MICROBExpress (Life technologies, AM1905) according to the manufacturer's protocol. Depleted RNA was reverse transcribed by incubating 11 µl of RNA with 1 µl of 10µM reverse transcription

primer(oJW4176), incubating at 65°C for 5 min, and immediately placing on ice for 2 min. Next, 1 ul of MASHUP reverse transcriptase (Pippete Jockey), 4 µl of 5X MU Buffer, 1 µl of 100 mM DTT, and 1 µl of 10 mM deoxynucleotide triphosphates (NEB N0447S) were added, and the reaction was incubated at 50°C for 60 min and then terminated by incubation at 80°C for 15 min. RNA template was degraded by adding 1 µl of ribonuclease (RNase) H (NEB, M0297) and the incubating the reaction 30 min at 37°C. The reaction was cleaned with SPRI beads at a 46 µl and eluted in 10 µl of H_2O. 10 microliters of the resulting cDNA was ligated to a cDNA-specific ligation adapter (3' ligation adapteroJW4177). The reaction was incubated at 23°C for 4 hours, then cleaned with SPRI beads at 45 µl, eluting the cDNA in 23 µl of H_2O. Twenty-two microliters of ligated cDNA solution were mixed with 1.5 µl of forward and reverse primers, at 25 µM each 10 uL Q5 Reaction buffer, 1 uL 10mM dNTPs, 0.5 uL Q5 High Fidelity Polymerase in a vinal volume of 50 uL. The library was amplified by using the manufacturer's protocol with 18 amplification cycles then 5 uL of library was run on a 2% agarose gel and the final PCR product was cleaned with SPRI beads at a 0.9× ratio (40.5 µl) and eluted into 22 uL. The final term-seq libraries size was determined with a dsDNA D1000 Tapestation kit (Agilent, 5067-5582), and subjected to paired-end sequencing using the NextSeq 550 system (Illumina) at the MIGS Center.

2.3.10 *Term-seq data analysis*

We performed the term-seq analysis similarly to how RPP values were calculated in (Zhang et al. 2014), with a few modifications. We chose a subset of 1,329 of the longest transcriptional units generated from the Send-seq (Ju, Li, and Liu 2019). The mean transcript length was calculated as the average transcript length (L) = term-seq

signal/ transcriptional unit as defined by Send-seq (Ju, Li, and Liu 2019; Zhang et al. 2014).

2.3.11 *Measuring 70S ribosomal concentrations*

Cells were grown in 100 mL cultures to mid-log phase *i.e.*, OD600 = ~0.6. Aliquots were removed for serial dilutions and viable CFU cell counting. Cultures were centrifuged for 10 mins at °C 6000 rpm resuspended in 20 mL 1x Buffer A + 6 mM BME and combined into one falcon tube. Buffer A was aspirated off and cells were frozen on dry ice and stored at -80°C.

Cells were resuspended in 1.7 mL 1x Buffer A+ 6 mM BME + 4 ul DNase I on Ice then lysed using a pre-chilled French press with a small cell (4 mL max volume) 900psi (medium pressure), 2 passages. Lysed cells were transferred into 2 mL Eppendorf tubes and centrifuged at 13200 rpm at 4°C for 30 mins. Supernatant was transferred to TLA 100.3 tube then spun in an Ultracentrifuge at 80,000 rpm at 4°C for 40 mins. Pellet was resuspended in 500 uL 1x Buffer A (4°C) with 6 mM BME and RNA concentration measured by A260 on nanodrop (diluted 1/10) with buffer A as a blank. 70S ribosome concentrations were calculated with extinction coefficient of 24 pmol/A260 unit: A260 x 24 x (6.02 x 1011) /viable count, where 6.02 x 1011 is Avogadro's number (molecules per pmole)(Condon et al. 1993).

2.3.12 *TmRNA-his6 purification*

Cells were transformed with pKW24 containing tmRNA-his6(Roche and Sauer 2001). 1 liter cultures were grown in Mops 0.4% Cas media, harvested by centrifugation and

resuspended in 5 ml of L8 buffer (100 mM NaH_2PO_4,10 mM Tris·HCl, pH 8.0,150 mM NaCl,1 mM PMSF,20 mM imidazole/8 M urea) per gram of wet weight and lysed by stirring for 1 hour, followed by sonication. The lysate was cleared by centrifugation at 10,000 × *g* for 30 min, and the supernatant was added to 5 ml of Ni-NTA resin (Qiagen, Valencia, CA) equilibrated in L8 buffer. After mixing for 1 h, the resin was washed sequentially with 200 ml of L*X* buffer (L buffer with *X* = 8, 6, 4, 2, and 0 M urea), and bound protein was eluted with 10 ml of L0 buffer containing 500 mM imidazole. Samples were then buffer exchanged using spin columns and L0 buffer to remove imidazole (Hong et al. 2007).

2.4 Results

DksA is required for survival in minimal media and for robust protein synthesis

Following amino acid starvation by either nutrient downshift or serine hydroxamate (SHX) treatment, cells begin producing ppGpp to activate the stringent response, which produces proteins necessary for amino acid biosynthesis and shuts down transcription of rRNA operons (B. J. Paul, Berkmen, and Gourse 2005; Gourse et al. 2018). It has been shown that *ΔdksA* cells have much slower doubling times in poorer nutrient conditions and is a polyauxotroph (Ross, Sanchez-vazquez, et al. 2016; Murphy and Cashel 2003). Our experiments show that wild-type cells have negligible differences in growth rate following changes in Cas amino acids (CAA) concentration. *ΔdksA* cells show declining growth rate as CAA concentrations are reduced. (Fig 2.1A-E). After ~18–24 hours in minimal media, *ΔdksA* cells begin to die, with complete loss of cellular viability by 48 hours; barring the appearance of spontaneous suppressors that allow growth of *ΔdksA* on minimal medium (Murphy and Cashel 2003). We also tested p0 cell

survival in minimal media which previous work has shown is essential for viability in media only containing glucose (Iyer et al. 2018).

Previous work has shown that *ΔdksA* cells lose viability when combined with a *rpsL* mutation that leads to reduced ribosome elongation rates (Zhang et al. 2014). To look at translation elongation rates and protein synthesis, we performed LacZ translation kinetic assays with 15-second time points in wild-type and *ΔdksA* cells. The translation kinetic assays showed that protein synthesis rates decline in *ΔdksA* cells even in LB media and that protein synthesis sharply declines as the nutrient quality (Cas amino acid concentration) decreases. We conclude that DksA promotes protein synthesis and translation elongation and is conditionally essential under amino acid starvation conditions.

In addition to translation kinetics, we looked at transcription kinetics using a qPCR method that measures RNAP progression *in vivo* and tested this across nutrient conditions in wild-type and Δ*dksA* (Zhu et al. 2019). We observe that *ΔdksA* cells have the same transcription rate in LB as wild-type cells and that wild-type cells maintain transcription rates of ~13 codons/second even in MOPS plus 0.1% CAA media. However, as CAA concentration is reduced, *ΔdksA* cells begin showing reduced transcription rates (Fig 2.2A). Translation elongation rates appear to be more sensitive to nutrient quality as even wild-types cells show a slight decline in elongation rates between LB media and MOPS + 0.1% CAA media (Fig. 2.2B). This decrease in translation elongation rate is more severe in *ΔdksA.*

Because we observed slower translation elongation rates in *ΔdksA* cells relative to their transcription elongation rate, we hypothesized that *ΔdksA* cells may be experiencing

transcription-translation uncoupling which could lead to premature transcription termination by Rho. Previous work has shown that uncoupling of transcription-translation by a premature stop codon in the RNA to terminate translation causes incomplete mRNA transcripts due to premature transcription termination (Zhu et al. 2019). Completed uncoupled transcripts could be rescued by the addition of Bicyclomycin (BCM), an antibiotic that inhibits Rho and prevents premature transcription termination (Miyoshi et al. 1972; Zhu et al. 2019). To test this hypothesis, we first performed measured transcription kinetics in wild-type and *ΔdksA* cells following treatment with Bicyclomycin. However, we did not observe an increase in lacZ transcripts in *ΔdksA* cells upon addition of BCM to the media before the addition of IPTG (Fig. 2.2C). To further test the premature transcription termination hypothesis, we looked to measure whether shorter RNA-transcripts could be detected in *ΔdksA* cells. To do so we analyzed previously published data generated by performing RNA-seq in wild-type and *ΔdksA* cells in LB media, then washed cells and resuspended in MOPS minimal media(Gray 2020). With this RNA-seq data set we calculateda value similar to RPP (L/Lo) where L is the average gene length and Lo is the length of the open reading frame, in this case individual genes to generate a weighted center of transcript coverage from the RNA-seq reads to test whether *ΔdksA* cells contained shorter transcripts in response to nutrient downshift. by identifying the median pile up of RNA-seq reads across all genes(Fig. 2.2D) (Zhang et al. 2014). This analysis generated a weighted center of coverage in the samples with 95% confidence intervals and showed a 2.5% lower center of coverage of reads in *ΔdksA* cells following nutrient downshift, a difference that was significantly larger than in wild-type cells.

Term-seq analysis of wild-type and *ΔdksA*

To further test whether *ΔdksA* cells experience premature transcription termination, we performed Term-seq in wild-type and *ΔdksA* cells, treating exponentially-growing cultures with SHX, BCM or both SHX and BCM (Dar et al. 2016). We then generated 1329 transcriptional units from Send-seq experiments to measure whether premature transcription termination events occurred within open reading frames. Finally, we generated histograms of the mean centerof-coverage of term-seq reads similarly to how RNA polymerase progression was calculated in (Zhang et al. 2014) (average length of sequencing reads / length of the open reading frame) to generate a center-of-read coverage from the Term-seq reads. This allowed us to detect truncated 3′ ends oftranscripts terminated prematurely, including upstream of known Rho termination sites (Fig. 2.3A–D). The data suggests that premature transcription termination (PTT) events are not occurring more frequently in *ΔdksA* cells. Following SHX treatment wild-type and *ΔdksA* cells both have a lower mean transcript length. The most striking difference in transcript length occurred between wild-type and *ΔdksA* cells following BCM treatment where the transcript length cluster in a narrower manner in *ΔdksA* cells than in wild-type. This suggests that *ΔdksA* cells are not experiencing PTT more frequently then wild-type cells (Fig 2.3A; B) but rather that DksA increases RNAP's elongation rate directly, perhaps by suppressing transcriptional pausing.

Transposon-sequencing screen identifies synthetic defects in Δ*dksA* cells with transposon insertions in ClpX and ClpP

In order to identify critical genetic interactions of DksA, we performed a transposon-sequencing (Tn-seq) screen in wild-type and *ΔdksA* cells in LB media (Fig. 2.4A). We

identified ~40 genes that we qualified as having a synthetic genetic interaction with DksA by having a more than 2-fold fewer transposon insertions within those genes (Fig. 2.4B). We identified two major pathways with fewer transposon insertions, genes involved in lipid polysaccharide biosynthesis and those encoding the ClpXP proteolytic machinery. Other genes of interest included the cell division regulator SlmA, polyphosphate kinase Ppk, the efflux pump TolC, and the RNA binding stress regulator Hfq (McQuail et al. 2020; Gray 2020). We chose to follow up on ClpXP due to both genes being strong hits in the transposon screen and test if they may be linked to the translation defects, we observed in *ΔdksA*. To investigate the relationship of DksA with ClpXP, we generated double deletion strains *ΔdksAΔclpP* and *ΔdksAΔclpX,* then compared growth rates in double deletion knockouts with and without rescue of wild-type DksA carried on a plasmid (Fig. 2.4C). Both strains exhibited more severe growth defects in MOPS + 0.4% CAA and a ~12-hour lag time and milder growth defects in LB medium. We confirmed synthetic growth defects between DksA and ClpXP and showed that the presence of wild-type DksA rescued cell growth.

ΔdksA cells show increased SsrA-His_6 tagging and higher expression of ArfA

Having shown that *ΔdksA* cells have impaired protein synthesis and slower translation elongation rates as well as a genetic interaction with ClpXP, we tested whether loss of DksA results in increased SsrA tagging. We were unable to generate viable *ΔdksA ΔssrA* colonies that also harbored the SsrA-His_6 plasmid, so we instead used a merodiploid strain containing wild-type *ssrA* on the chromosome and a plasmid containing a SsrA-His_6 variant under the control of the endogenous *ssrA* promoter. SsrA-His_6 tags polypeptides at arrested ribosomes with a His_6 tag instead of the tmRNA

tag that is normally recognized for degradation by clpXP (Flynn et al. 2003; Hong et al. 2007). Exponentially-growing cells were harvest from wild-type and *ΔdksA* which were grown in either LB or MOPS + 0.4% CAA media then used for Western blot analysis. We used an anti-His_6 antibody to detect SsrA-His_6 tagging and observed 4–5-fold higher tagging in *ΔdksA* grown in MOPS + 0.4% CAA than in wild-type cells (Fig. 2.5A–B). Similar levels of SsrA-tagging were observed in LB media. Previously-generated gene expression microarray experiments performed in wild-type and Δ*dksA* cells following 20-minute SHX treatment showed induction of ArfA expression in Δ*dksA* cells following SHX treatment (Tehranchi et al. 2010) (Fig. 2.5C). ArfA is regulated and inhibited by SsrA tagging and degradation; its expression increases only when SsrA is titrated by stalled ribosomes (Buskirk and Green 2017). We purified the SsrA-His_6 proteome and subjected it to a proteomic analysis which showed higher ArfA abundance in *ΔdksA* cells than in wild-type (Fig. 2.5D). This suggests that *ΔdksA* cells experience more ribosomal stalling and stress requiring rescue by the tmRNA ribosome rescue system and ArfA.

ΔdksA cells show higher 70S ribosome concentrations and reduced protein expression in MOPS + 0.1% CAA

After showing defects in translation elongation in *ΔdksA* as well as increased SsrA tagging, we next measured 70S ribosome concentrations in exponentially-growing cells. The role of DksA as an rRNA transcription inhibitor has been thoroughly studied both *in vivo* and *in vitro*. Previous studies have shown changes in RNA/protein ratio relative to the growth rate between wild-type and *ΔdksA* cells, suggesting the presence of more ribosomes in *ΔdksA cells* (B. J. Paul, Berkmen, and Gourse 2005; Brian J. Paul et al. 2004). To test this directly we purified ribosomes with ultracentrifugation to detect

ribosome levels in LB media and MOPS + 0.1% CAA. We observed similar levels of ribosome content between wild-type and *ΔdksA* cells grown in LB (Fig. 2.6A). In wild-type cells ribosome concentration was lower in Mops + 0.1% CAA compared to LB media. However, in *ΔdksA grown* in MOPS + 0.1% CAA, we observed an ~1.5-2 fold increase in ribosome abundance compared to growth in LB media and a ~2–3-fold increase relative to wild-type cells grown in MOPS + 0.1% CAA. As shown earlier, DksA growth rate is titratable by adjusting CAA concentration (Fig. 2.1B), and we observe much slower doubling times in *ΔdksA* cells as CAA concentration decreases (Fig. 2.6B), a striking contrast to the parallel increase in ribosome abundance. To investigate long-term protein synthesis output, we grew cells in different media conditions and transformed cells with plasmid which contains inducible YFP under the control of P_{LtetO} (Butzin and Mather 2018). In LB, DksA expression lagged slightly behind wild-type YFP expression (Fig. 2.6C). However, in MOPS + CAA media, wild-type cells had almost identical YFP expression compared to the severe drop off in YFP production and intensity that was observed in *ΔdksA* cells. These data, taken together with earlier results, demonstrate severe defects in translation in *ΔdksA* cells, despite an increase in ribosome abundance, suggesting that DksA plays a critical role in coordinating ribosome biosynthesis with nutrient availability in order to promote protein synthesis across nutrient conditions.

2.6 Discussion

We report here an essentialrole of the *E. coli* secondary channel binding factor DksA under amino acid starvation conditions (Fig 2.1). We show that DksA is necessary for

robust protein synthesis and this phenotype is masked by rich nutrient conditions such as LB (Figs 2.1- 2.3).

In this study, we used *in vivo* assays to measure transcription and translation kinetics across nutrient conditions to show that DksA promotes translation elongation in addition to its known role in promoting transcription elongation (Fig 2.2). DksA works synergistically with ppGpp to regulate the transcriptional stringent response through its interactions with RNAP(Sanchez-Vazquez et al.; Ross et al., 2016b). For this reason, we also tested the transcription and translational rates of RNAP Site 1 Site 2 mutations and *E. coli* cells unable to produce ppGpp (p0 cells) with p0 cells showing the most severe loss in elongation rate (Fig S2.1). This fits with our finding (Fig 2.1) that p0 (*ΔrelA251::kan ΔspoT207::cat*) cells die more quickly than *ΔdksA* cells following amino acid starvation.

One alternative to the model proposed by Zhang et al. (2014) is that *ΔdksA* cells may be experiencing premature transcription termination (PTT) following SHX treatment instead of increased pausing of RNAP. To test this model we used term-seq to see if premature termination events were occurring in *ΔdksA* cells (Dar et al. 2016). We compared termination sites of transcription units between wild-type and *ΔdksA* cells, the results indicating that *ΔdksA* cells do not experience a obvious increase in PTT (Fig 2.3A; B).

This suggests a model that DksA increases RNAP's elongation rate either directly, perhaps by suppressing transcriptional pausing, or indirectly through its role as a transcriptional regulator driving higher NTP concentrations and lower ppGpp levels. This latter model is based on Thin layer chromatography (TLC) experiments that showed *ΔdksA* cells to have lower ATP (61.5%) , GTP (90%) and ppGpp levels (345%)

relative to wild-type cells grown in the same media (Brian J. Paul et al. 2004). One hypothesis is that these NTP and ppGpp levels continue to diverge from wild-type levels as nutrient conditions become more depleted. Testing of this model would require further experiments to look at NTP and ppGpp concentrations *in vivo* together with comparison oftranscription and translational elongation rates.

To identify critical genetic interactions of DksA we performed a transposon-sequencing screen find genes that would be synthetically lethal or synthetically sick in a *ΔdksA* background (Fig 2.4). We chose to focus on the clpX and clpP hits identified from the Tn-seq screen as both these genes are involved in the tmRNA-ribosome rescue pathway; our previous experiments suggested that protein synthesis is strongly diminished in *ΔdksA* cells (Fig 2.1). Additionally, analysis of previously published microarray expression analysis performed in *ΔdksA* cells reveals a 10-fold increase in ArfA transcript following SHX treatment compared to SHX-treated wild-type cells. ArfA is synthetically lethal with ssrA and is post-transcriptionally regulated by ssrA. When ssrA is titrated by stalled ribosomes ArfA is able to promote its own expression through a feedback loop resulting in increased ArfA levels (Garza-Sánchez et al. 2011). We confirmed from previous observations that cells lacking dksA showed higher ssrA-tagging (Fig 2.5) and that the increase in tagging occurring in *ΔdksA* was dependent on nutrient conditions (Krasich et al. 2015b). To our surprise the genetic interaction between dksA and ClpX (or ClpP) was not fully synthetic lethal (FigS3). We tested this with plasmid rescue of dksA introduced into the double deletion strains *ΔdksAΔclpX and ΔdksAΔclpP*. The double deletions strains were able to lose the plasmid containing dksA. One explanation for the lack of synthetic lethality between these genes could be

increased ppGpp levels in *ΔdksA* cells serving to buffer a genetic interaction that would otherwise be lethal(Brian J. Paul et al. 2004).

To look at protein output over a longer timescale we used plasmids containing tetracycline inducible YFP to look at protein expression over time and across differing nutrient conditions. We observed a sharp decline in protein output in *ΔdksA* as nutrient conditions worsened, paralleling sharply increased doubling times (Fig 2.6 B-C). This correlation suggests that inhibited translation elongation may be an important factor in limiting growth in *ΔdksA* cells but only under limited nutrient conditions(Iyer et al. 2018; Scott et al. 2014). Further experiments will need to be done to see if this is due to slow growth rate of dksA cells or directly due to loss of *dksA*.

Previous studies showed that RNA:protein ratios were strikingly increased at low growth rates in *ΔdksA* cells, and rRNA growth rate dependence was abolished in the ΔdksA strain (Brian J. Paul et al. 2004). Such imbalances of RNA/Protein ratios would be detrimental to growth rate control under nutrient limiting conditions.

Those results suggested that DksA controls the activities of rRNA promoters, potentially leading to an overabundance of ribosomes in *ΔdksA* cells. We directly looked at ribosome concentration by purifying ribosomes with ultracentrifugation to see if dksA controls ribosome biosynthesis across nutrient limiting conditions (Fig 2.6A). We observed an almost 3-fold increase in ribosome concentration within *ΔdksA* cells compared to wild-type in Mops 0.1% CAA media. This observation that dksA mediates ribosome biosynthesis across nutrient conditions leads us to our current model explaining the pleotropic effects of dksA and its vital role under conditions of amino acid starvation (Fig2.6A).

I propose a model to explain that the observed growth defects in *ΔdksA* are due to an issue of “too many mouths to feed” where cells have excess abundance of ribosomes but lack the amino acid pool necessary to keep pace with charging of tRNA’s, the result being in an overall measurably slower translation elongation rate that inhibits cell growth. In contrast, wild-type cells are able to maintain higher protein synthesis output with fewer ribosomes (Fig2.6A). In this model “less is more”, in that the fewer ribosomes in wild-type cells are capable of more efficient translation, yielding more dynamic protein production that enables more productive cell growth (Fig 2.7A-D). Rich nutrient conditions such as LB media mask the translation defects in *ΔdksA* cells since the protein output is similar to that in wild-type cells when the environment is rich in amino acids (Fig2.6C). The observed translational defects and misregulation of ribosome synthesis could account for the essential role of DksA under amino acid starvation conditions. Depletion of amino acids would be one of many physiological or environmental stress factors that cells such as *Salmonella*, *Vibrio* and *Borrelia burgdorferi* would experience during the harsh changes in environments during infection or colonization of hosts. Inability to adapt to those stressful environments could explain the loss of virulence in *ΔdksA* cells across bacterial species (Ii et al. 2014; Turner et al. 1998; Boyle et al. 2021).

2.7 Figures

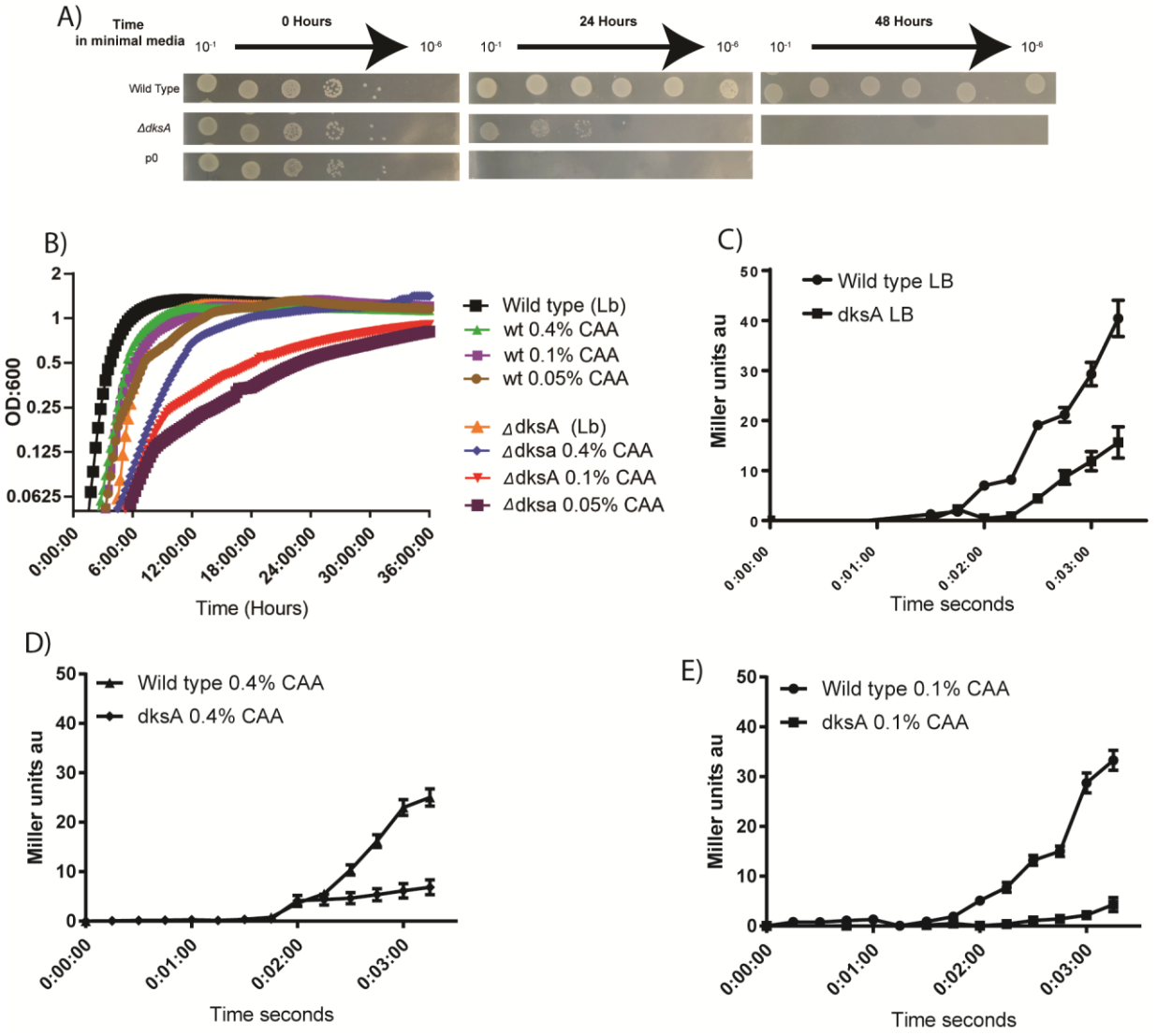

Figure 2.1: DksA is essential for survival in minimal media. A) Deletion of dksA results in cell death in MOPS Minimal Media. We also test a P0 strain (*ΔrelA251::kan ΔspoT207::cat)* that is unable to produce ppGpp and previously been shown to be essential for growth in minimal media B) Wild-type cells show negligible differences in growth rate following changes in CAA concentration. Δ*dksA* cells show declining growth rate as CAA concentrations are reduced. C–E) *ΔdksA* show less robust translation elongation and protein synthesis rates compared to wild-type cells. Protein synthesis rate diminishes in Δ*dksA* cells as CAA concentrations decrease.

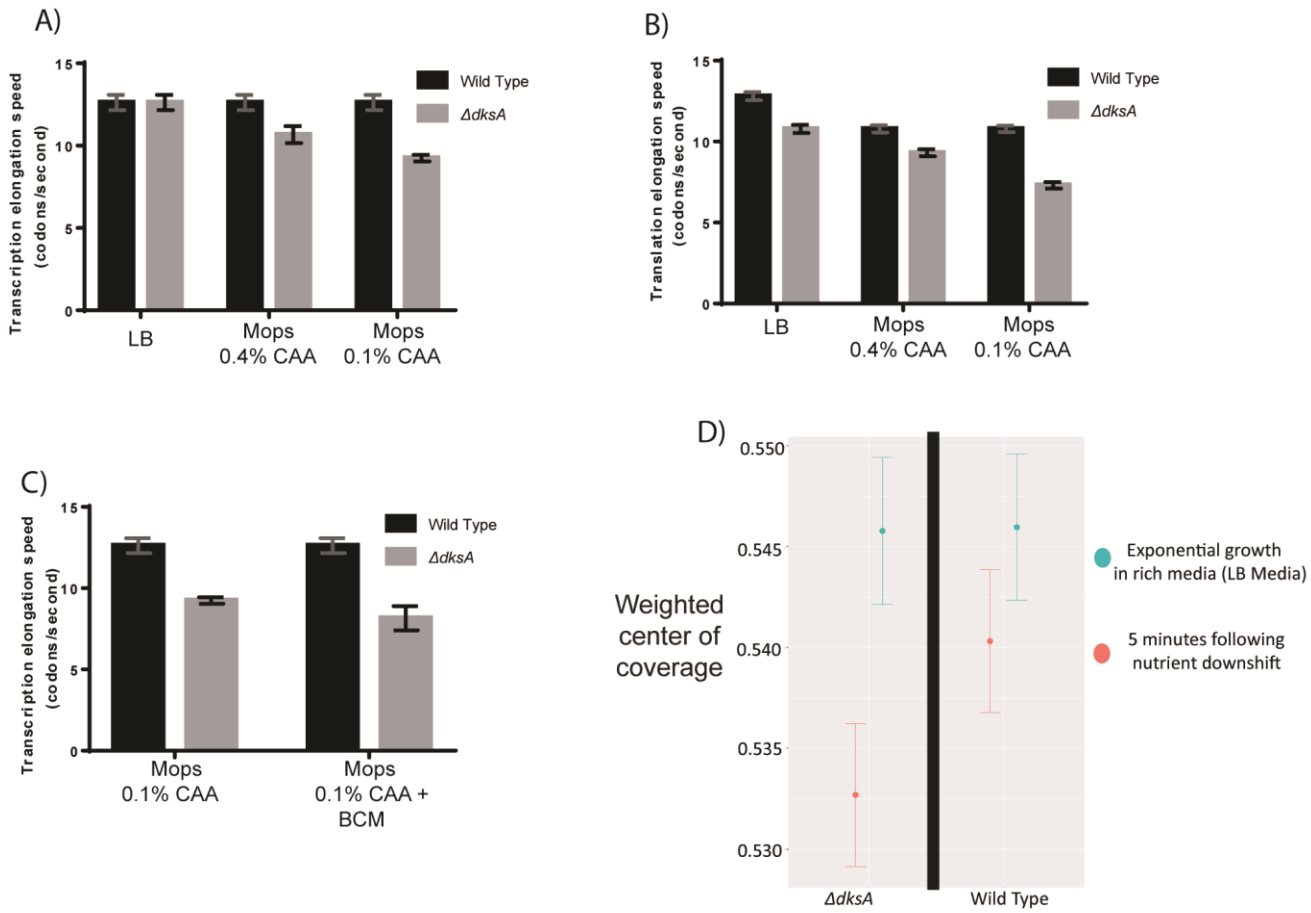

Figure 2.2: DksA buffers transcription and translation rates across nutrient limiting conditions. **A)** Wild-type cells maintain transcription rates between LB and MOPS + 0.1% CAA. Transcription elongation rates decrease in Δ*dksA* cells as nutrient availability declines. **B)** Wild-type cells show a mild reduction in translation rate following reduction in nutrient quality compared to Δ*dksA* cells which show a more drastic drop-in translation rate. **C)** Addition of bicyclomycin does not rescue slower transcription rates in Δ*dksA.* **D)** Following nutrient downshift RNA-seq analysis of Δ*dksA* cells show a reduced center of sequencing reads within genes, suggesting slightly shorter RNA transcripts.

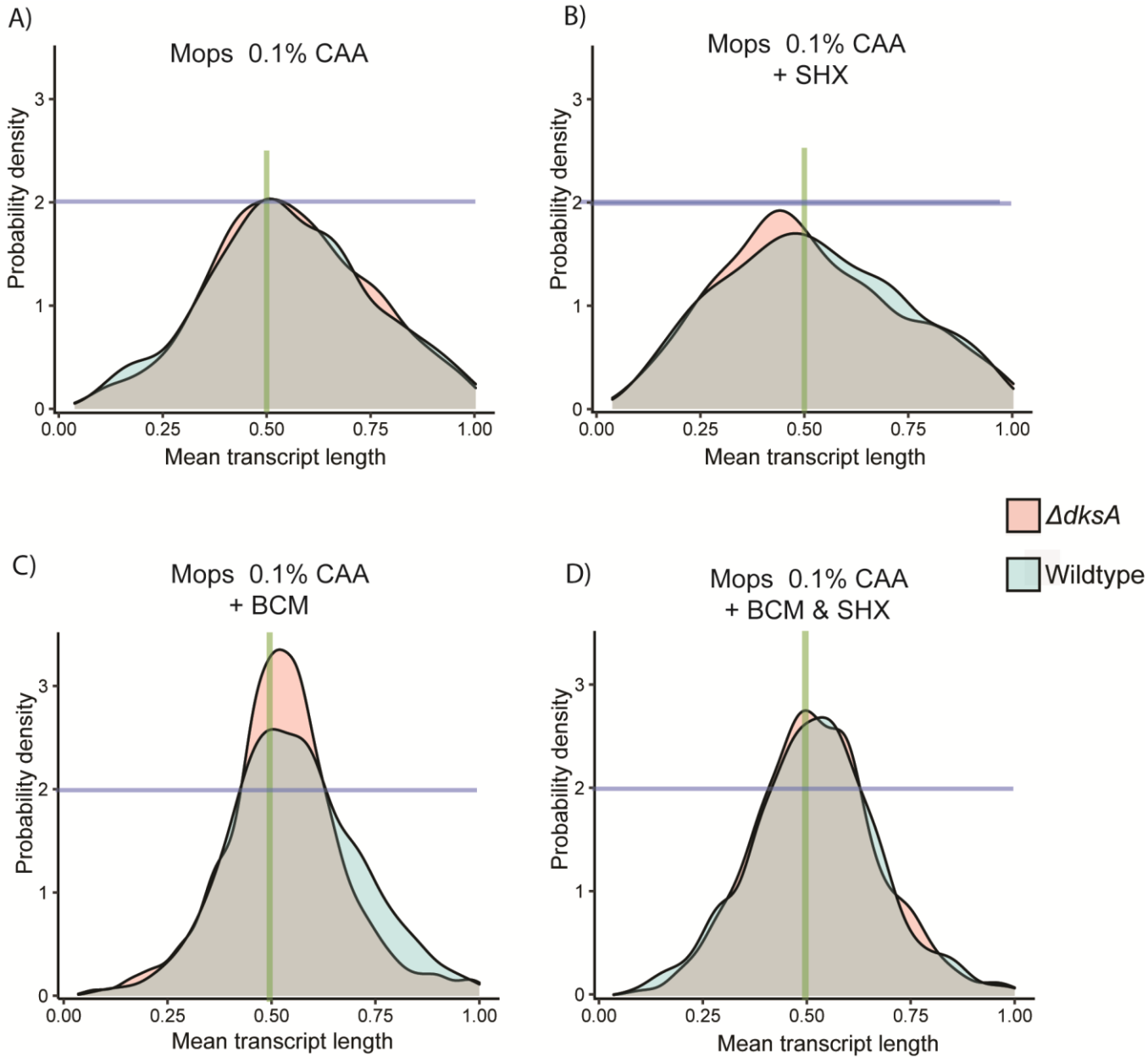

Figure 2.3: Term-seq analysis of wild-type and Δ*dksA*. **A)** Wild-type and dksA cells show similar center of coverages across transcriptional units. **B)** Δ*dksA* cells show a slightly lower mean transcript lengths value following SHX treatment. **C)** Δ*dksA* cells show less deviation in mean transcript lengths following BCM treatment **D)** Wild-type and Δ*dksA* cells show similar mean transcript lengths following SHX and BCM treatment.

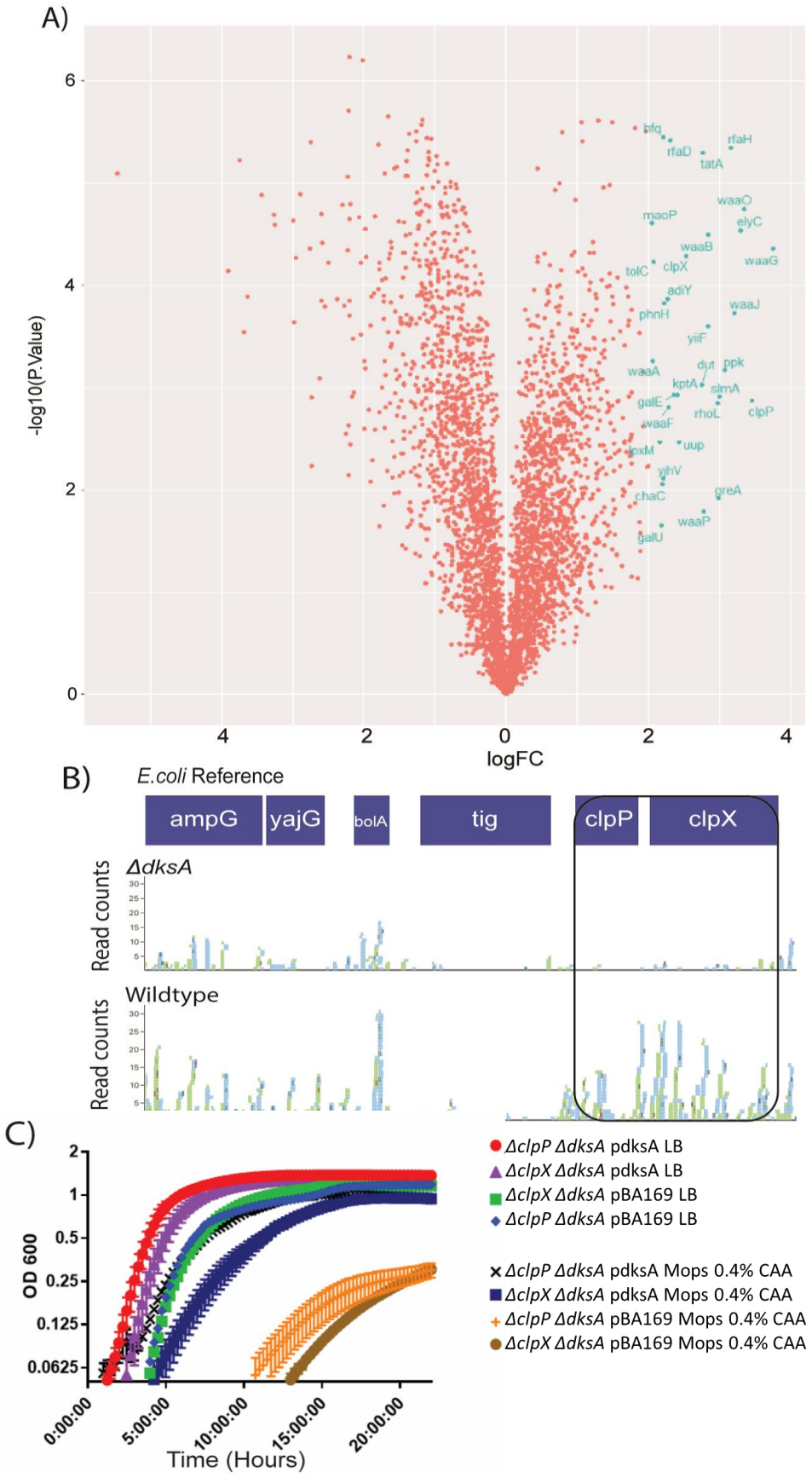
A)
-log10(P.Value)
logFC
infq
rfaD
rfaH
tatA
waaO
maoP
elyC
waaB
waaG
tolC
clpX
adiY
waaJ
phnH
yiiF
waaA
dut
ppk
kptA
slmA
galE
rhoL
clpP
waaF
lpxM
uup
yihV
chaC
greA
waaP
galU
B)
E.coli Reference
ampG
yajG
bolA
tig
clpP
clpX
ΔdksA
Read counts
Wildtype
Read counts
C)
OD 600
Time (Hours)
ΔclpP ΔdksA pdksA LB
ΔclpX ΔdksA pdksA LB
ΔclpX ΔdksA pBA169 LB
ΔclpP ΔdksA pBA169 LB
ΔclpP ΔdksA pdksA Mops 0.4% CAA
ΔclpX ΔdksA pdksA Mops 0.4% CAA
ΔclpP ΔdksA pBA169 Mops 0.4% CAA
ΔclpX ΔdksA pBA169 Mops 0.4% CAA

Figure 2.4: Transposon-sequencing screen identifies synthetic defects in Δ*dksA* cells with transposon insertions in ClpX and ClpP. **A)** A tn-seq screen performed in wild-type and Δ*dksA* cells identified both ClpX and ClpP, as well as genes involved in lipopolysaccharide biosynthesis, stress factor Hfq, efflux pump TolC, and cell division factor SlmA. **B)** Wild-type cells see a uniform distribution of transposon insertions throughout ClpX and ClpP compared to Δ*dksA*, which shows very few transposon insertions. **C)** Complementation of *dksA* on a plasmid rescues the severe growth defects seen in double deletion strains Δ*dksA*Δ*clpP* and Δ*dksA*Δ*clpX.* Cells showed more severe growth defects including a 12-hour lag time when grown in MOPS + 0.4% CAA media compared to LB media.

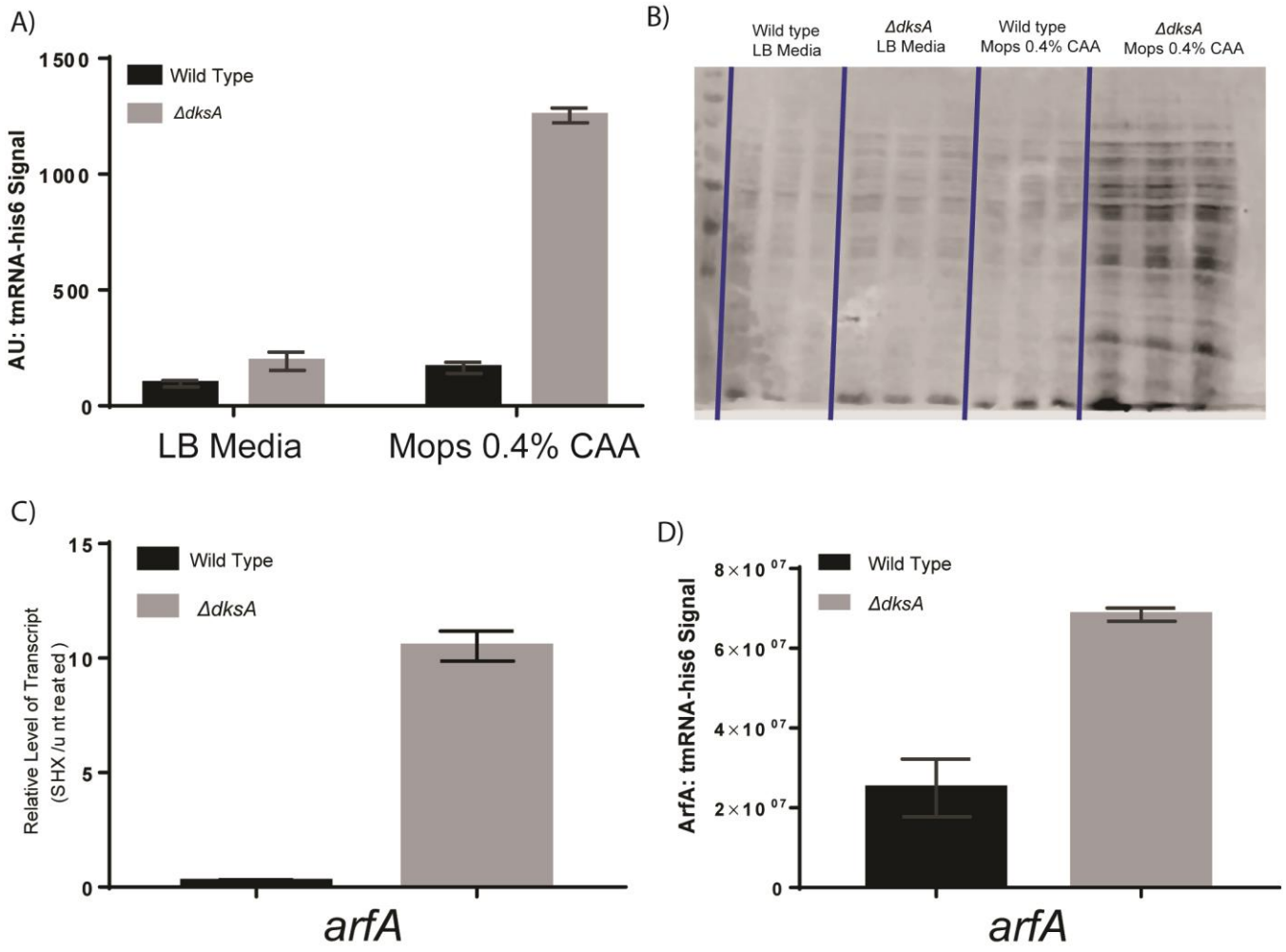

Figure 2.5: Δ*dksA* cells show increased SsrA-His$_6$ tagging and increased expression of ArfA. **A)** Quantification of Western blot analysis against SsrA-His$_6$ using an anti-His$_6$ antibody to measure SsrA tagging shows 4–5 fold higher tagging compared to wild-type cells in MOPS + 0.4% CAA media. **B)** Western blot of SsrA-His$_6$ tagging in wild-type and *ΔdksA* in LB or MOPS + 0.4% CAA media. **C)** Δ*dksA* cells show higher ArfA expression following SHX treatment. **D)** Purified SsrA-His$_6$ proteins purified by Ni-NTA column and subject to LC/MS proteomic analysis shows higher abundance of ArfA in Δ*dksA* cells relative to wild-type.

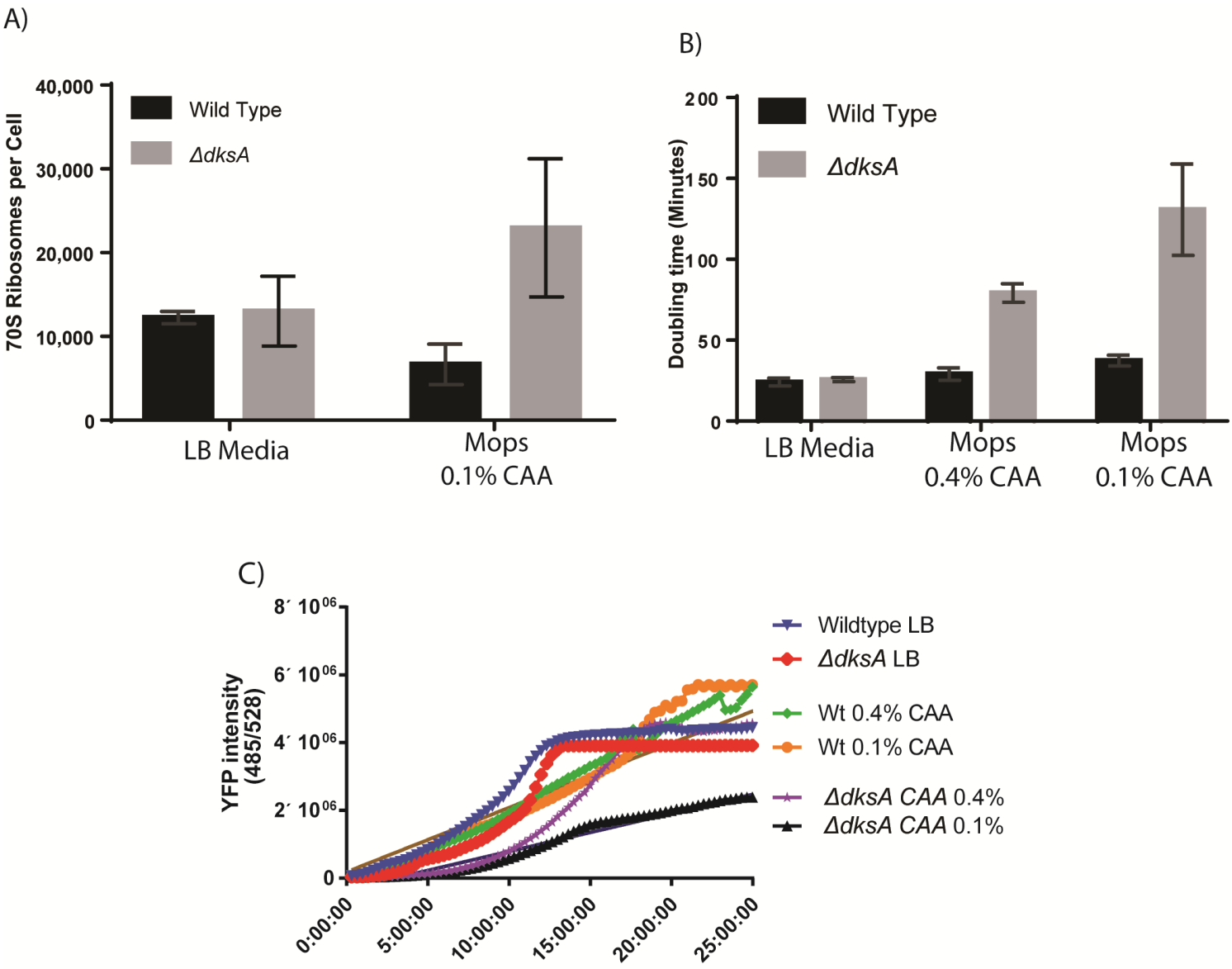

Figure 2.6: Δ*dksA* cells show higher 70S ribosome concentrations and weaker expression of YFP in MOPS + 0.1% CAA. **A)** Ribosomal profiling shows similar concentration of 70S ribosomes in wild-type and Δ*dksA* cells in LB whereas Δ*dksA* cells show higher amounts of ribosomes in MOPS + 0.1% CAA media**. B)** Cells lacking DksA show much slower doubling times when CAA concentrations are decreased. **C)** The ability of Δ*dksA* cells to express YFP following induction with IPTG is severely impaired in nutrient-titrating conditions with lower CAA concentration.

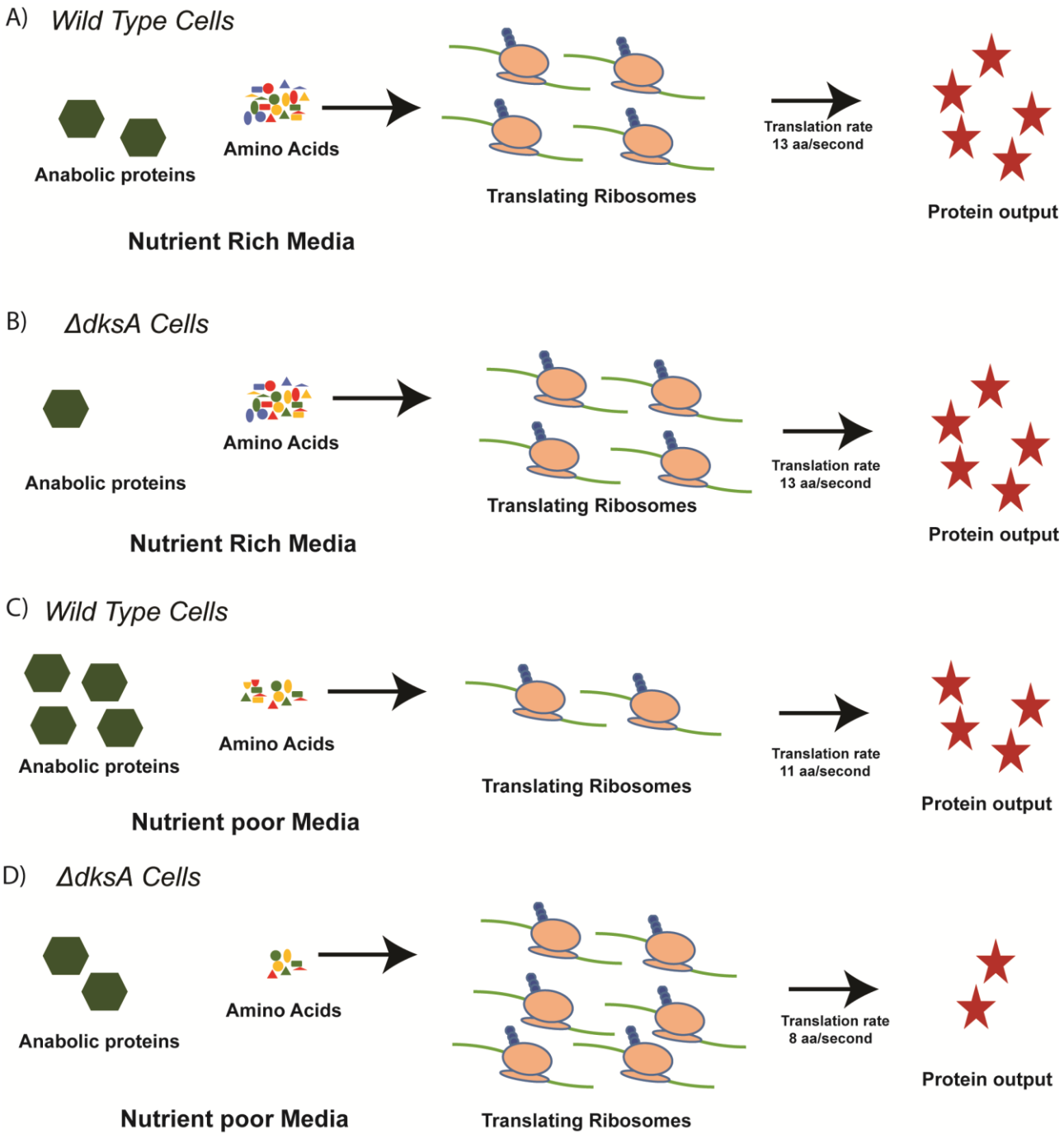
A) Wild Type Cells
Anabolic proteins
Amino Acids
Translating Ribosomes
Translation rate
13 aa/second
Protein output
Nutrient Rich Media
B) ΔdksA Cells
Anabolic proteins
Amino Acids
Translating Ribosomes
Translation rate
13 aa/second
Protein output
Nutrient Rich Media
C) Wild Type Cells
Anabolic proteins
Amino Acids
Translating Ribosomes
Translation rate
11 aa/second
Protein output
Nutrient poor Media
D) ΔdksA Cells
Anabolic proteins
Amino Acids
Translating Ribosomes
Translation rate
8 aa/second
Protein output
Nutrient poor Media

Figure 2.7: The “too many mouths to feed” model explains how mis-regulation of rRNA transcription can lead to translational defects in Δ*dksA* cells. A) Wild-type cells in rich media can focus on production of ribosomes to maintain rapid translation elongation and growth rates B) Cells lacking DksA can maintain rapid growth rate and translation elongation rates due to the nutrient rich media. C) When cells are grown in poorer nutrient conditions, wild-type cells will produce fewer ribosomes in order to maintain growth rate and switch to the production of anabolic proteins to synthesize the amino acids essential for maintaining protein synthesis through high translation rates. D) When Δ*dksA* cells are grown in nutrient-poor media, they are unable to robustly activate amino acid biosynthesis genes or stop production of ribosomes. This leads to an overabundance of ribosomes starved of amino acids, resulting in slower translation rates and compromised protein synthesis.

Chapter 3: Conclusion, Discussion and Future Directions

Ultimately, the goal of this work is to attempt to explain some of the many pleotropic effects observed in Δ*dksA* cells and explain the necessity of dksA across diverse bacteria to infect and colonize hosts. As described in the introduction, DksA is essential for virulence or colonization across a wide spectrum of bacterial including *Salmonella enterica, Vibrio fischeri, Acinetobacter baumannii, Borrelia burgdorferi and E. coli*(Maharjan et al., 2021; Henard and Vázquez-Torres, 2012; Brooks et al., 2014; Chou and Brynildsen, 2019 Kim et al.,2021).

These results suggest that many defects observed in *ΔdksA* strains are due to multiply factors such as misregulation of ribosome synthesis leading to an overproduction of ribosomes and a lack of transcriptional activation at amino acid biosynthesis operons. Together these defects impair the ability of *ΔdksA* cells to synthesize proteins and could explain the essential role of DksA under amino acid starvation conditions.

The work in chapter 2 endevored to expand our knowledge of how bacteria coordinate gene expression and cell growth as a means of surviving stressful environments. Extensive studies on the mechanism of gene regulation by DksA have focused on how it functions in facilitating RNAP transcriptional initiation at promoters. However, the role DksA plays in regulating bacterial steady-state exponential growth has many open-ended questions. Through the use of in *vivo* transcription and translation kinetics assays and nutrient titration we have identified asignificant impact DksA has on protein synthesis across nutrient limiting conditions. Additionally, we systematically identified genetic interactions of DksA through Transposon-sequencing experiments to identify ClpX and ClpP, suggestive of an increase in non-stop arrested translation in the absence of DksA.

ClpX and ClpP are critical to the proteolysis of polypeptides generated by non-stop translation proteins that must be rescued by the tmRNA ribosome rescue pathway. Consistent with this hypothesis, we find that loss of dksA results in over production of 70S ribosomes and slower translation elongation rates. Term-seq experiments were used to test the role of transcriptional robustness, revealing that Δ*dksA* cells do not experience premature transcription termination. These results suggest that DksA may instead contribute to preventing transcriptional pausing or kinetically allowing faster transcription elongation rates. We observe that nutrient rich media such as LB is able to mask severe phenotypic defects in Δ*dksA* cells that arise in the media lacking amino acids. Whole genome sequencing experiments under nutrient limiting conditions suggest that DksA either promotes replication through rRNA operons or is able to prevent DNA damage from occurring at rRNA operons (Fig S6). Together, these new findings broaden our view of DksA as an essential regulator at multiple levels of central dogma processes.

Growth rate control is dependent on dksA

Growth rate control in *E. coli* has long been established as a positive relationship between nutrient conditions, ribosome content and growth rate, wherein poor nutrient conditions are correlated with lower ribosome content and a slowed growth (Klumpp et al. 2013; Brian J. Paul et al. 2004; Dai et al. 2017; Hui et al. 2015). Previous studies found that dksA was critical in regulating RNA/protein ratios in connection with growth rate (Brian J. Paul et al. 2004). Our results suggest growth rate control is dependent on DksA in *E. coli* based on the increased ribosomal content we observe under nutrient-poor conditions with slower growth rates. DksA is necessary for *E. coli* to adapt to environmental and physiological changes to maintain cell growth and viability.

This work also identified genetic interactions between ClpXP and DksA. Our results suggest that this interaction may be due to the role DksA plays in promoting protein synthesis and regulating the transcriptional stress response. We predict that in the absence of DksA, ClpXP machinery is critical to cellular viability by promoting protein quality control through proteolysis of truncated and toxic polypeptides.

I hypothesize that DksA and ClpXP compensate for one another through (1) the ability ofDksA to mediate the transcriptional response necessary for adapting to environmental and physiological stressors in the absence of the ClpXP ribosome rescue pathway, and (2) reciprocally, in cells lacking DksA, ClpXP is able to rescue non-stop stalled ribosomes and prevent accumulation of wasteful or toxic C-terminally truncated proteins by targeted proteolysis, mitigating otherwise harmful effects onthe cell's physiological state.

In conclusion It makes sense that growth rate control is dependent on DksA when one takes into account that DksA is essential for growth in minimal media and its well-established role in regulating transcription at rRNA operons. I hope this work has provided a broad but accurate explanation for many pleotropic effects previously reported involving DksA.

Future Directions

Exploring genetic interactions identified in the dksA transposon-screen.

It would be also worth testing if DksA is essential outside of *E.coli.* One of the first experiments I would recommend would be to check if *dksA* is essential for viability in minimal media conditions using a similar method to that shown in (Fig 2.1). I would propose these experiments to be performed in *Salmonella enterica* and *Vibrio fischeri* to see if dksA is essential in a wider phylogenetic context.

Killing of dksA cells begins after ~18 hours in Mops minimal media with all cells and complete loss of cellular viability by 48 hours as long as no spontaneous suppressors occur. Seeing if the rate of killing differs in other bacteria species would also be of interest.

I would propose to also test the role of genes identified from the Tn-seq screen and if they play a role in cellular adaptation to starvation, I would propose to perform the nutrient downshift experiments (Fig 2.1) in double deletion strains such as Δ*dksAΔclpP* and *ΔdksAΔclpX* to see if these cells die more rapidly than the single gene deletion *ΔdksA.* This same downshift and killing experiments could be applied to other genes identified from the transposon-screen. A good follow up to the screen would be to perform colony sectoring experiments using plasmid complementation and blue/white sectoring to see if any of the ~40 strongest tn-seq hits are truly synthetically lethal. It has been

shown that *ΔdksA* is synthetically lethal with ppK which was a strong hit in our screen (Gray 2020). Additionally, we see *slmA* being a strong hit which was previously shown to be synthetically lethal with *dksA in a slmA* transposon screen(Bernhardt and De Boer 2005). We would then produce double deletions of genes that are not synthetically lethal to test those strains for viability following nutrient downshift and amino acid starvation, looking to see if the double deletion strains die more rapidly following amino acid starvation. One such gene of interest is Hfq which has recently been shown to physically interact with relA and play a role in the stringent response (McQuail et al. 2020). Given that relA plays a role in ppGpp production and that Hfq came up as a strong hit in our Tn-seq screen with *ΔdksA*, Hfq may play an important role cellular response to starvation. There are three more pathways that would be interesting to follow up including the lipid-polysaccharide biosynthetic pathway which had multiple strong gene hits involving the genes lpxM, rfaH, waaP, waaJ, waaO, galE, waaG, and rfaD. This was the biological pathway with the most transposon insertions observed in a single pathway (Fig2.4A).

Additionally, TolC is of interest since it is a highly expressed protein found in the outer membrane and plays a critical role in drug efflux and multidrug resistance/tolerance. It would be interesting to test if TolC plays a role in efflux of toxic biproducts of anabolic and catabolic pathways and test if TolC plays a physiological role in nutrient stress and not just drug efflux (Reuter et al. 2020).

Rho and DksA

Finally, from the Tn-seq screen we identified rhoL which is the leader peptide found upstream of the Rho coding sequence (Matsumoto et al. 1986). One largely unexplored area of this work is the genetic interaction that seems to exist between DksA and Rho.

Further analysis of the term-seq data is needed to identify what is driving such strong differences in mean transcript lengths between wild-type and dksA following BCM treatment. The most striking difference observed from the term-seq analysis was Δ*dksA* cells showing less deviation in mean transcript length following BCM treatment compared to wild-type cells. (Previous work has shown that dksA is not more sensitive to BCM treatment in a “phageless” background (MDS42) indicating that the sensitivity to BCM in cells lacking dksA in the mg1655 strain is likely due to prophage induction (Zhang et al. 2014). It would be worth checking if *ΔdksA* cells show a higher abundance of Rho dependent or Rho independent transcription termination sites. Further analysis of the Term-seq data could help identify termination sites across *E. coli* with the combination of drugs used in our experiments. Serine hydroxamate (SHX) starves ribosomes and leads to decoupling of transcription/translation. This decoupling may lead to premature transcription termination. We also treated cells with Bicyclomycin which would prevent Rho from causing prematurely terminating transcription (Ray-soni, Bellecourt, and Landick 2016). And a combination of BCM and SHX drug treatments would cause both transcription-translation decoupling and inhibit Rho dependent termination allowing for the identification of most Rho-independent termination sites.

DksA and replication-transcription conflicts

The only successful experiment I performed to look at the role of DksA in preventing replication-transcription conflict was done by examining the DNA replication profile in an asynchronized population of starved Δ*dksA* cells with WGS. In exponentially growing cells one would expect a pyramid-shaped replication profile, with DNA amounts highest at the *oriC*-proximal regions and lowest at the *ter* regions. Comparison with wild-type

cells showed drop offs in chromosomal DNA signals in the profile of Δ*dksA* cells at rRNA operons indicating these as potential positions of replication arrest (*i.e.,* locations where conflicts occur). Based on these observations from the whole genome sequencing experiment of wild-type and dksA cells (Fig S6), replication-transcription conflict in *ΔdksA* cells might happen at highly transcribed genes such as rRNA operons.

In order to map the location of replication-transcription conflicts that result in DNA breaks *in vivo*, I propose two recently published methods that were used to map fragile chromosomal sites in *E.coli* (Mei et al. 2021). One method, known as X-seq uses ChIP of RuvC, a protein involved in resolution of homologous recombination junctions (HJ). This allows one to to identify sites where DNA breaks occur and are repaired. The other method is End-seq and is used to identify DNA ends *in vivo*. It is a NGS sequencing methods which ligates sequencing adaptors to DNA-ends in gently lysed cells trapped within agarose plugs to generate sequencing libraries at DNA breaks(Canela et al. 2016). Both these methods were tested with an inducible I-SCEI site to map breaks at a known location on the chromosome.

In conclusion, coordination of central dogma processes is critical for cellular viability in *E. coli* especially under nutrient limiting conditions. This work expands our understanding of how bacteria coordinate gene expression with cell growth to adapt to stressful conditions. We show that loss of DksA results in over production of ribosome synthesis and slower translation elongation in poor nutrient conditions. This work suggests that growth rate control is dependent on DksA and that nutrient rich media such as LB is able to mask severe phenotypes in Δ*dksA* cells. DksA is essential under in media lacking amino acids. This work highlights the role that DksA plays in regulating

replication, transcription and translation in response to the cell's environment. It should be noted that we do not yet understand how DksA is promoting replication elongation and preventing DNA damage from occurring during amino acid starvation conditions. Further experiments are necessary to identify sites of replication transcription conflicts and how DksA is preventing these conflicts.

Appendix 1: Supplementary Material for Chapter 2 & Tables

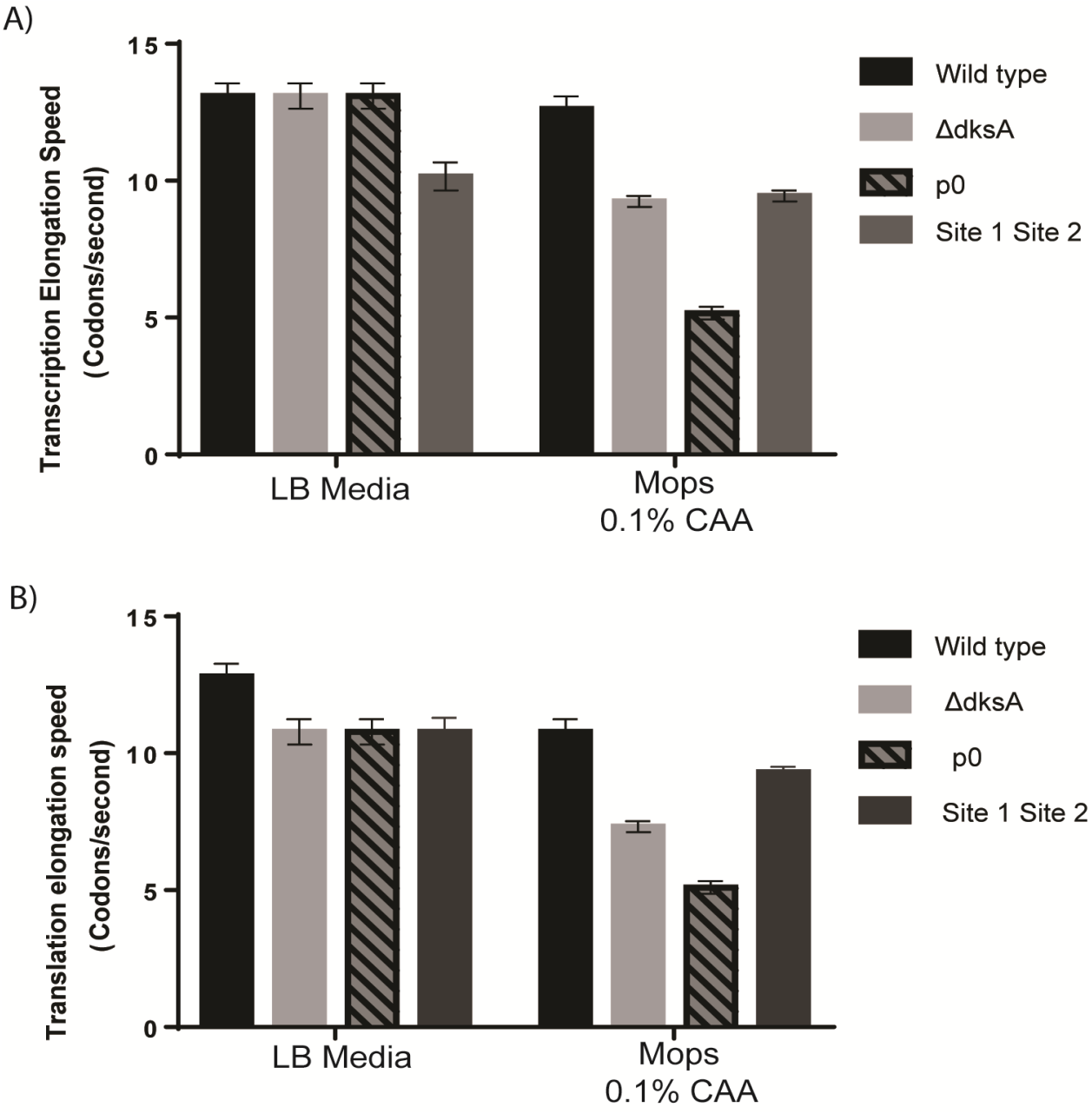

Figure S1: Transcription and translation elongation rates are more severely compromised in P0(*Δ*relA*ΔSpoT*) than in *ΔdksA,* and mildly slower in RNAP mutants unable to bind ppGpp at Site 1 and Site 2.

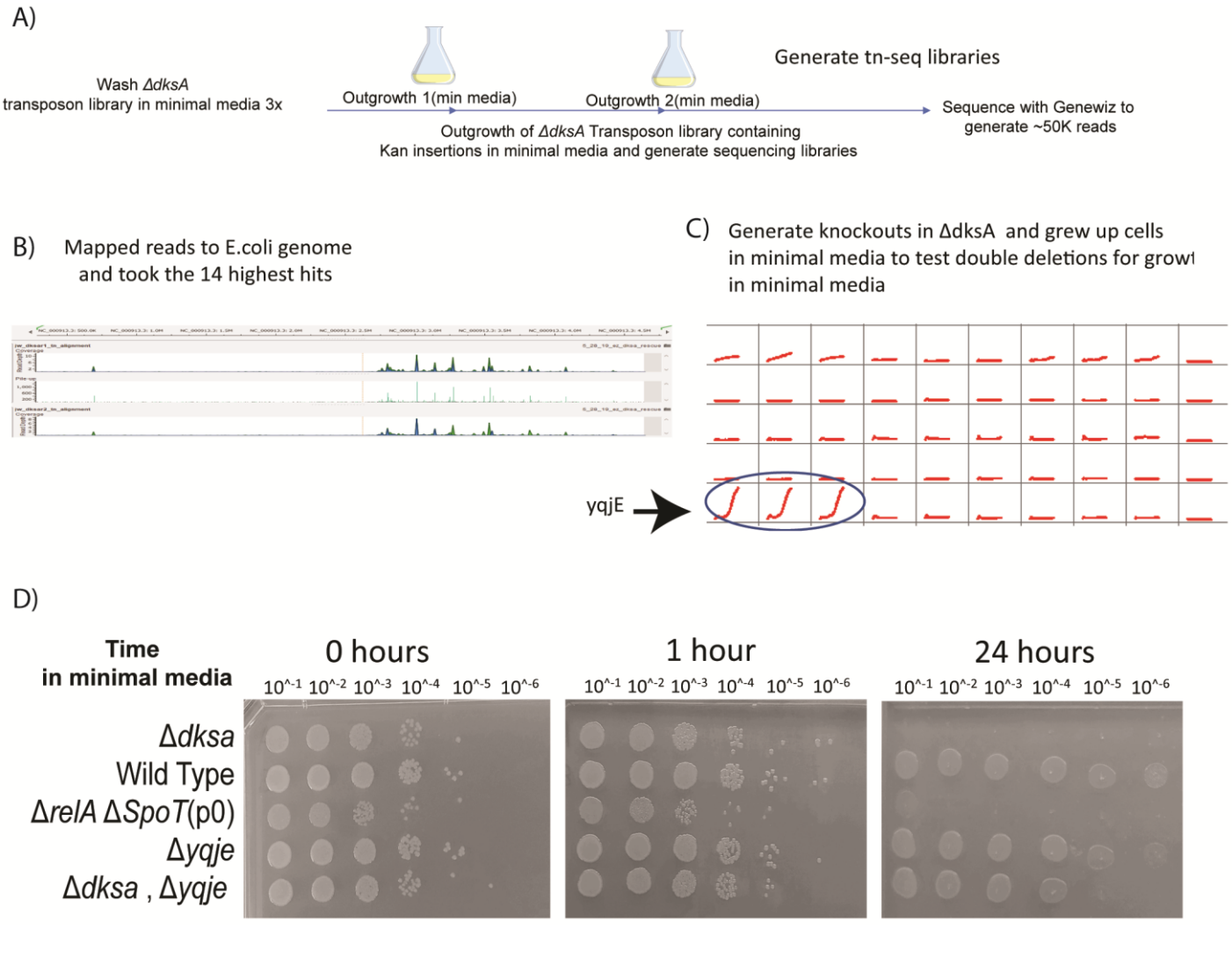

Figure S2: Transposon screen to identify genes that will rescue growth of *ΔdksA* in Mops minimal Media. A) Washed cells in minimal media and outgrew *ΔdksA* cells containing transposon libraries in minimal media twice. **B)** Mapped reads to E.coli genome and identified 14 strongest hits. C) Generate double gene knockouts in *ΔdksA* of identified hits and tried to grow them in Mops Minimal Media overnight in plate reader. D) Tested identified double deletion in minimal media and identified a gene of unknown function (Yqje) whose deletion is able to rescue growth *ΔdksA* in minimal media

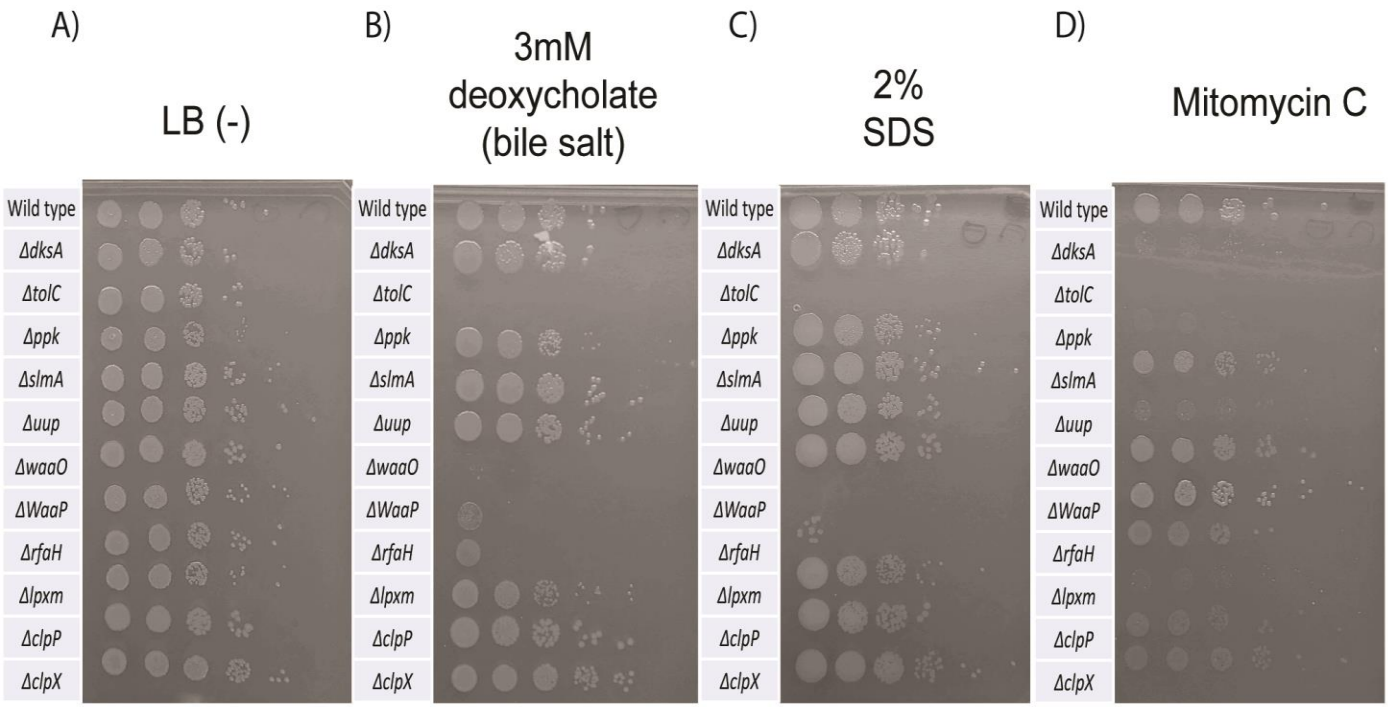

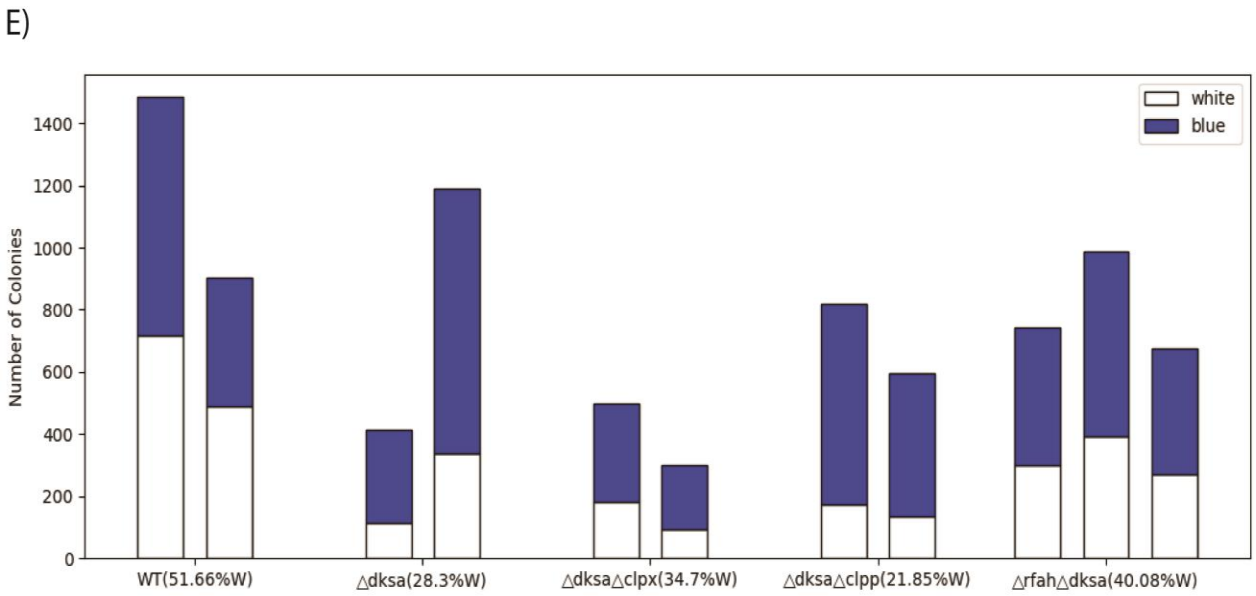

Figure S3: A-D) Spotting assays were performed in LB, 3mM Deoxycholate, 2% SDS and Mitomycin C to test sensitivity of genes identified from the Tn-seq screen done in *ΔdksA* to try and identify parallel genetic interactions*.* E) Colony sectoring was performed using plasmid complementation of dksA and a lacZ reporter with cells played onto X-gal media to identify if cells could lose the plasmid containing dksA. None of the tested genes appeared to be conditional essential since all could lose the plasmid containing dksA

A)

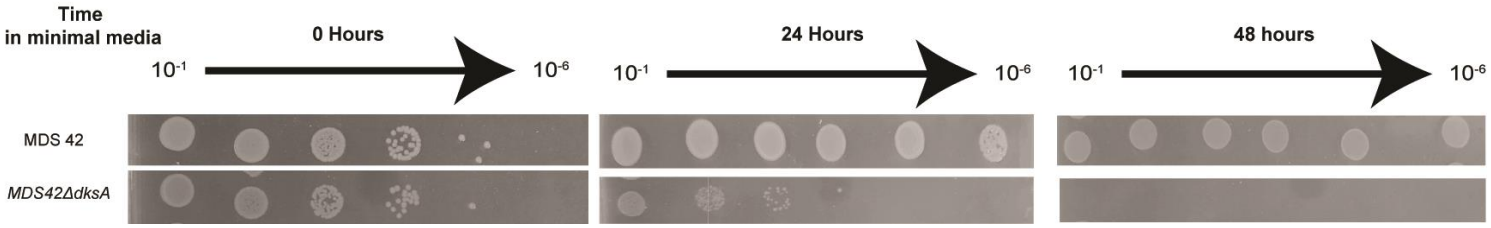

Figure S4 A) Using *the reduced genome E. coli* strain MDS42 does not rescue *ΔdksA* cells from death in minimal medium, suggesting the cell death is not due to prophage activity.

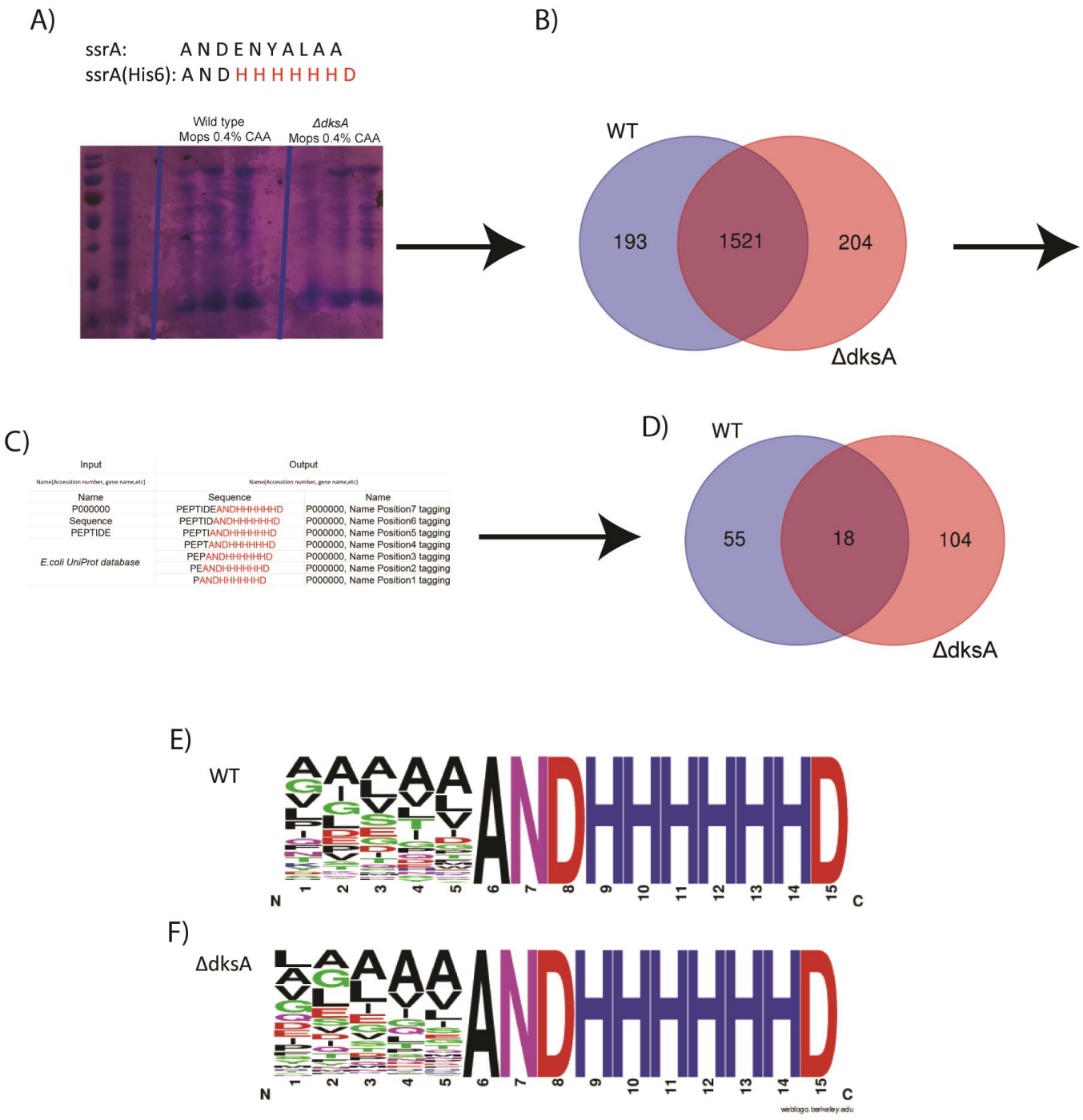

Figure S5) SsrA-his6 purification for proteomic analysis by LC/MS. A) The tmRNA-his6 degradome was purified by nickle column and subjected to proteomic analysis with LC/MS. B-C) 1,918 unique proteins were identified and then aligned with the proteome and tmRNA-his6 tag. D) The remaining 177 proteins which contained mappable polypeptides linked to the tmRNA-his6 tag are listed in Table S2. E-F) Sequence pileup of polypeptides tagged by tmRNA-his6 in wild-type and *ΔdksA* cells.

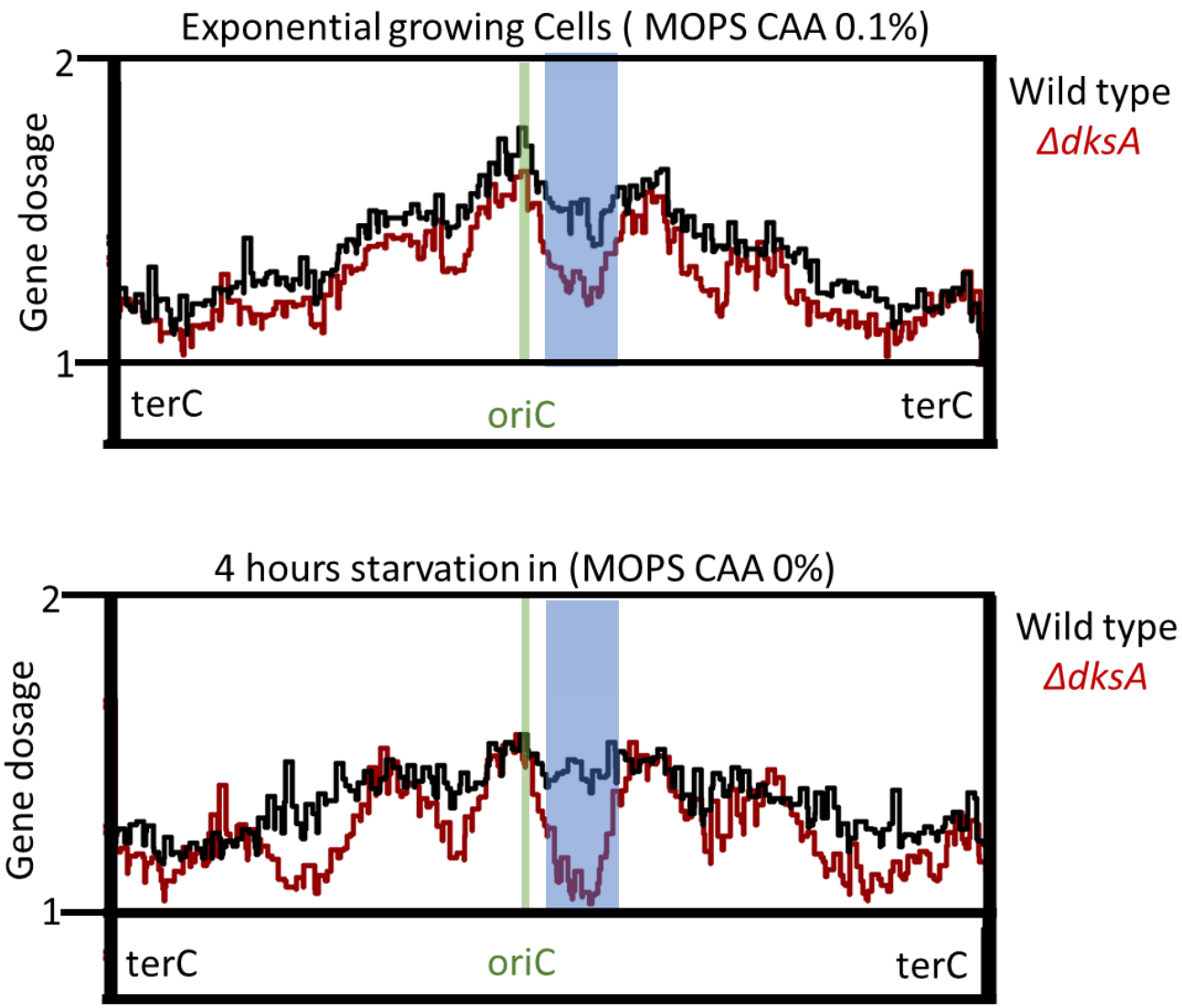

Figure S6) Whole genome sequencing reads of wild-type and *ΔdksA* following nutrient downshift. Green is OriC, Blue is the four rRNA operons found to the right of OriC **Top)** Wild-type cells show a distribution of reads between Ori and Ter commonly seen during rapid growth in exponentially growing cells. *ΔdksA* cells in Mops 0.1% CAA show a slightly lower ori/ter ratio and loss of sequencing coverage around rRNA operons**. Bottom)** The difference in sequencing coverage decreases following nutrient downshift into mops minimal media resulting in less difference in coverage between ori/ter. Starved *ΔdksA* cells see even sharper drops in sequencing coverage around rRNA operons indicating loss of chromosome DNA at these regions or replication occurring around rRNA operons within *ΔdksA* cells.

Tables

Table 1. Strains, plasmids and oligonucleotides used in Chapter 2		
Name of strains/plasmids	**Genotype**	**Origin/reference**
MG1655 "Wild-type" (JDW 401)	***rph+***	**Wild-type *E. coli***
JDW618	**MG1655 Δlac ΔdksA::tet**	**(Blankschien et al., 2009)**
JDW3775	***MG1655 ΔdksA::Kan***	**this work**
JDW1163	***MDS42***	**(Posfai et al., 2006)**
JDW1165	***MDS42 dksA::tet***	**Zhang et al., 2014**
APA752	***WM3064 harboring the pKMW3 mariner transposon vector library (requires DAP)***	**Wetmore et al., 2015**
RLG847	***MG1655 ΔrelA251::kan ΔspoT207::cat "p0"***	**Xiao et al., 1991**
RLG14538	***MG1655-derived strains RNAP(1+2+)***	**Ross et al., 2016**
Keio collection	***BW25113 ΔclpX:Kan***	**Baba et al., 2006**
Keio collection	***BW25113 ΔclpPKan***	**Baba et al., 2006**
Keio collection	***BW25113 Δppk:Kan***	**Baba et al., 2006**
Keio collection	***BW25113 ΔslmA:Kan***	**Baba et al., 2006**
Keio collection	***BW25113 Δuup:Kan***	**Baba et al., 2006**

Keio collection	***BW25113 ΔwaaO:Kan***	**Baba et al., 2006**
Keio collection	***BW25113 ΔwaaP:Kan***	**Baba et al., 2006**
Keio collection	***BW25113 ΔrfaH:Kan***	**Baba et al., 2006**
Keio collection	***BW25113 ΔlpxM:Kan***	**Baba et al., 2006**
Keio collection	***BW25113 ΔtolC:Kan***	**Baba et al., 2006**
JDW4100	**mg1655 ptrc empty vector**	**this work**
JDW4101	**mg1655 ptrc dksa (iptg inducible)**	**this work**
JDW4102	**mg1655 ptrc empty vector clpX:kan**	**this work**
JDW4103	**mg1655 ptrc dksa (iptg inducible) clpX:kan**	**this work**
JDW4104	**mg1655 ptrc empty vector clpP:kan**	**this work**
JDW4105	**mg1655 ptrc dksa (iptg inducible) clpP:kan**	**this work**
JDW4123	***mg1655 ptrc empty vector clpX:kan dksA:tet***	**this work**
JDW4124	***mg1655 ptrc dksa (iptg inducible) clpX:kan dksA:tet***	**this work**
JDW4125	***mg1655 ptrc empty vector clpP:kan dksA:tet***	**this work**
JDW4126	**mg1655 ptrc dksa (iptg inducible)**	**this work**

	clpP:kan dksA:tet	
Plasmids	***GENOTYPE***	**REFERENCE**
pBA169	***pTrc99A ΔncoI, ApR***	**(Walsh et al., 2003)**
pDksA	**pBA169/dksA, ApR**	**(Blankschien et al., 2009)**
p31Cm	**PLtetO None Untagged**	**(Butzin and Mather 2018)**
p31CmNB02	**PLtetO YFP Untagged**	**(Butzin and Mather 2018)**
p31CmNB95	**PLtetO YFP-LAA C 11 aa LAA tag**	**(Butzin and Mather 2018)**
Name	**Usage**	**Sequences are 5'-end to 3'end**
oJW4176	**Reverse transcription primer term-seq**	**TCTACACTCTTTCCCTACACGACGCTCTTC**
oJW4173	**RNA 3' ligation adapter**	**NNCTCTCTATNNNN-AGATCGGAAGAGCGTCGTGT**
oJW4174	**RNA 3' ligation adapter**	**NNTATCCTCTNNNNAGATCGGAAGAGCGTCGTGT**
oJW4175	**RNA 3' ligation adapter**	**NNGTAAGGAGNNNN-AGATCGGAAGAGCGTCGTGT**
oJW4179	**PCR reverse primer**	**CAAGCAGAAGACGGCATACGAGATTCGCCTTAGTGACTGGAGTTCAGAC**
oJW4180	**PCR reverse primer**	**CAAGCAGAAGACGGCATACGAGATCTAGTACGGTGACTGGAGTTCAGAC**
oJW4181	**PCR reverse primer**	**CAAGCAGAAGACGGCATACGAGATTTCTGCCTGTGACTGGAGTTCAGAC**
oJW4182	**PCR reverse primer**	**CAAGCAGAAGACGGCATACGAGATGCTCAGGAGTGACTGGAGTTCAGAC**
oJW4183	**PCR reverse primer**	**CAAGCAGAAGACGGCATACGAGATAGGAGTCCGTGACTGGAGTTCAGAC**
oJW4184	**PCR reverse primer**	**CAAGCAGAAGACGGCATACGAGATCATGCCTAGTGACTGGAGTTCAGAC**
oJW4185	**PCR reverse primer**	**CAAGCAGAAGACGGCATACGAGATGTAGAGAGGTGACTGGAGTTCAGAC**
oJW4186	**PCR reverse primer**	**CAAGCAGAAGACGGCATACGAGATCCTCTCTGGTGACTGGAGTTCAGAC**
oJW4178	**PCR fwd primer term-seq**	**AATGATACGGCGACCACCGAGATCTACACTCTTTCCCTACACG ACGCTCT**

oJW3662	**Tn-seq indexing primers**	**CAA GCA GAA GAC GGC ATA CGA GAT TGG TCA GTG ACT GGA GTT CAG ACG TGT GCT CTT CCG ATC T**
oJW3663	**Tn-seq indexing primers**	**CAA GCA GAA GAC GGC ATA CGA GAT GCC TAA GTG ACT GGA GTT CAG ACG TGT GCT CTT CCG ATC T**
oJW3664	**Tn-seq indexing primers**	**CAA GCA GAA GAC GGC ATA CGA GAT ACA TCG GTG ACT GGA GTT CAG ACG TGT GCT CTT CCG ATC T**
oJW3665	**Tn-seq indexing primers**	**CAA GCA GAA GAC GGC ATA CGA GAT CGT GAT GTG ACT GGA GTT CAG ACG TGT GCT CTT CCG ATC T**
oJW3661	**tn-seq ligation adaptor**	**AAT GAT ACG GCG ACC ACC GAG ATC TAC ACT CTT TCC CTA CAC GAC GCT CTT CCG ATC TNN NNN NCG CCC TGC AGG GAT GTC CAC GAG**
p1578 F	**lacZ transcription kinetics primer**	**GCTGGATCAAATCTGTCGATCC**
p1578R	**lacZ transcription kinetics primer**	**GGAAGGGCTGGTCTTCATCC**
p3105 F	**lacZ transcription kinetics primer**	**GGCACATGGCTGAATATCGACG**
p3105 R	**lacZ transcription kinetics primer**	**GACACCAGACCAACTGGTAATGG**

Table 2. Proteomic identification of SsrA-His$_6$ tagged polypeptides in wild-type and dksA cells

Strain identity	LC/MS Identified Proteins
dksa & WT	metL
dksa & WT	ansB
dksa & WT	ansB
dksa & WT	ampC
dksa & WT	lysA
dksa & WT	metG

Strain identity	LC/MS Identified Proteins
dksA	yjcC
dksA	psuG
dksA	psuG
dksA	yebE
dksA	purT
dksA	yjfC

dksa & WT	glyS		dksA	yehR
dksa & WT	tyrB		dksA	yehX
dksa & WT	gltX		dksA	nikB
dksa & WT	nlpA		dksA	chpB
dksa & WT	kdsB		dksA	napA
dksa & WT	rbsA		dksA	iceT
dksa & WT	recD		dksA	dsbD
dksa & WT	dnaX		dksA	cspB
dksa & WT	aceF		dksA	purU
dksa & WT	fhuB		dksA	ybcF
dksa & WT	hisD		dksA	mdtK
dksa & WT	hisD		dksA	yjjI
dksa & WT	hisD		dksA	zntA
dksa & WT	rsmA		dksA	yhhS
dksa & WT	ompC		dksA	mdtF
dksa & WT	cheA		dksA	bcsE
WT	deoA		dksA	yhjX
WT	cpdB		dksA	yiaD
WT	dnaJ		dksA	waaF
WT	xylB		dksA	rfbA
WT	uhpC		dksA	ydjE
WT	ackA		dksA	ytfF
WT	ackA		dksA	tamB
WT	yeiP		dksA	bdcA
WT	galK		dksA	nanS
WT	murA		dksA	kptA
WT	nusB		dksA	mcrC
WT	pyrI		dksA	yjiY
WT	rpsE		dksA	patA
WT	smg		dksA	hrpA
WT	tnaA		dksA	lpoA
WT	ubiE		dksA	yhbV
WT	yeeN		dksA	proQ

WT	ppsR
WT	trmI
WT	thrS
WT	rpoC
WT	rpoC
WT	rpoC
WT	fbaB
WT	glnA
WT	yeiL
WT	metR
WT	aceA
WT	slyD
WT	qmcA
WT	codB
WT	codB
WT	ybhL
WT	cadB
WT	artP
WT	napG
WT	ybjN
WT	pntB
WT	pntB
WT	accB
WT	cdsA
WT	mrdB
WT	dcuB
WT	tolQ
WT	flgB
WT	flgC
WT	fliQ
WT	folP
WT	waaA
WT	wcaF
WT	glpG
WT	lpxP
WT	yigM
WT	yigM
WT	araE
WT	astA
WT	mazF

dksA	ybgF
dksA	yhdP
dksA	rnlA
dksA	rnlA
dksA	yfjT
dksA	hslJ
dksA	rsmH
dksA	can
dksA	ybcW
dksA	yebV
dksA	yeiS
dksA	fieF
dksA	hda
dksA	ybhI
dksA	ltaE
dksA	hcr
dksA	ycaN
dksA	ycaP
dksA	ycdX
dksA	ycgV
dksA	puuP
dksA	ydaU
dksA	ynbA
dksA	lsrR
dksA	sad
dksA	ydfR
dksA	yeaH
dksA	yedP
dksA	zinT
dksA	zinT
dksA	zinT
dksA	lpxT
dksA	atoA
dksA	atoB
dksA	yfaP
dksA	yfcP
dksA	yffO
dksA	eutQ
dksA	maeB
dksA	hldE

WT	cpxA
WT	arcB
WT	dam
WT	dsbA
WT	emrB
WT	envZ
WT	galU
WT	gss
WT	gudD
WT	hdeA
WT	nagC
WT	yjbB
WT	nuoM
WT	nuoM
WT	pbpG
WT	pbpG
WT	yjdM
WT	ydiK
dksA	mepM
dksA	glrR
dksA	yhiD
dksA	sbmA
dksA	sspB
dksA	rho
dksA	ssb
dksA	ssb
dksA	sapB
dksA	tufB
dksA	rlpA
dksA	iap
dksA	glpD
dksA	sbcC
dksA	fecB
dksA	purH
dksA	cysM
dksA	rhsC
dksA	parE
dksA	recJ
dksA	asnB
dksA	prc

dksA	hldE
dksA	dsbG
dksA	ybbY
dksA	mscK
dksA	abgA
dksA	djlB
dksA	ompG
dksA	ybbP
dksA	citA
dksA	prpB
dksA	fryC
dksA	yagF
dksA	yagF
dksA	rsxC
dksA	ydcN
dksA	puuA
dksA	feaB
dksA	yqeA
dksA	ygfK
dksA	ygbL
dksA	ygbN
dksA	ispD
dksA	ygcU
dksA	dinB
dksA	dinB
dksA	yfiP
dksA	araJ
dksA	acrF
dksA	codA
dksA	gabD
dksA	cbdB
dksA	wecC
dksA	tatD
dksA	metQ
dksA	leuB
dksA	thiF
dksA	yaaJ
dksA	basS
dksA	ydeJ
dksA	setC

dksA	fepG
dksA	panC
dksA	yciK
dksA	yihS
dksA	ubiC

dksA	yidK
dksA	yidK
dksA	lptD
dksA	hchA

References (Chapter 1)

1 K. Potrykus and M. Cashel, *Annu. Rev. Microbiol*., 2008, **62**, 35.

2 B. Field, *J. Exp. Bot*., 2018, **69**, 2797.

3 W.C. Nierman and M.J. Chamberlin, *J. Biol. Chem*., 1980**, 254(16)**, 7921.

4 L. Krásny and R.L. Gourse, *EMBO J.,* 2004, **23(22)**, 4473.

5 H.D. Murray, D.A. Schneider and R.L. Gourse, *Mol. Cell*, 2003, **12(1)**, 125.

6 L. Sojka, T. Kouba, I. Barvíkš, H. Šanderová, Z. Maderová, J. Jonák and L. Krásný, *Nucl. Acids Res.* 2011, **39(11)**, 4598.

7 T. Gaal, M.S. Bartlett, W. Ross, C.L. Turnbough and R.L. Gourse, *Science*, 1997, **278(5346)**, 2092.

8 C.M. Lew and J.D. Gralla, *Biochemistry*, 2004, *J. Biol. Chem*. **279(19):**19481.

9 M.M. Barker and R.L. Gourse, *J. Bacteriol.* 2001, **183(21),** 6315.

10 N.V. Vo, L.M. Hsu, C.M. Kane and M.J. Chamberlin, *Biochemistry*, 2003, **42(13)**, 3798.

11 G.A. Belogurov and I. Artsimovitch, *J. Mol. Biol.*, 2019, **431(20)**, 3975.

12 M.H. Larson, R.A. Mooney, J.M. Peters, T. Windgassen, D. Nayak, C.A. Gross, S.M. Block, W.J. Greenleaf, R. Landick and J.S. Weissman, *Science*, 2014, **344(6187)**, 1042.

13 I.O. Vvedenskaya, H. Vahedian-Movahed, J.G. Bird, J.G. Knoblauch, S.R. Goldman, Y. Zhang, R.H. Ebright and B.E. Nickels, *Science*, 2014, **344(6189)**, 1285.

14 J.T. *Winkelman*, C. Pukhrambam, I.O. Vvedenskaya, Y. Zhang, D.M. Taylor, P. Shah, R.H. Ebright and B.E. Nickels, *Mol. Cell,* 2020, **79(5)**, 797.

15 C. L. Turnbough and R. L. Switzer, *Micro. Mol. Biol.Rev.,* 2008**, 72(2),** 266*.*

16 F. Qi and C.L. Turnbough, *J. Mol. Biol.*, 1995, **254(4)**, 552.

17 C. Liu, L.S. Heath and C.L. Turnbough, *Genes Dev.*, 1994, **8(23),** 2904.

18 Y. Cheng, S.M. Dylla and C.L. Turnbough, *J. Bacteriol*., 2001, **183(1)**, 221.

19 E. Lerner, S. Chung, B. L. Allen, S. Wang, J. Lee, S. W. Lu, L. W. Grimaud, A. Ingargiola, X. Michalet, Y. Alhadid, S. Borukhov, T. R. Strick, D. J. Taatjes and S. Weiss*, Proc. Natl. Acad. Sci. USA*, 2016, **113(43)**, E6562-E6571.

20 J.T. Winkelman, P. Chandrangsu, W. Ross and R.L. Gourse, *Proc. Natl. Acad. Sci. USA,* 2016, **113(13)**, E1787–E1795.

21 M. Cashel and J. Gallant, *Nature*, 1969, **221(5183)**, 838.

22 N. Fiil, K. von Meyenburg and J.D. Friesen, *J. Mol. Biol*., 1972, **71(3)**, 769.

23 M. Cashel, D. Gentry, V.J. Hernandez and D. Vinella. *In Escherichia coli and Salmonella: Cellular and Molecular Biology,* 1996. ed. F.C. Neidhardt, Washington, DC: ASM Press. **1**, 1458.

24 V. Hauryliuk, G.C. Atkinson, K.S. Murakami, T. Tenson and K. Gerdes, *Nature Rev. Microbiol.*, 2015, **13(5)**, 298.

25 A. Srivatsan, Y. Han, J. Peng, A. K. Tehranchi, R. Gibbs, J.D. Wang and R. Chen, *PLoS Genet.*, 2008, **4(8)**, e1000139.

26 D. Lee, G. Feng and R. Landick, *J. Biol. Chem.*,1994, **269(35)**, 22295.

27 S. Iyer, D. Le, B. R. Park and M. Kim, *Nat. Microbiol.* 2018, **3(6)**, 741.

28 A. Battesti and E. Bouveret, *Molecular Microbiology*, 2006, **62(4)**, 1048.

29 M. Nomura, R. Gourse and G. Baughman, *Annu. Rev. Biochem.*, 1984, **53**, 75.

30 M. Schaechter, O. Maaloe and N.O. Kjeldgaard, *J. Gen. Microbiol.*, 1958, **19(3)**, 592.

31 J. Ryals, R. Little and H. Bremer, *J. Bacteriol.*, 1982, **151(3)**, 1261.

32 J.M. Lopez, A. Dromerick and E. Freese, *J. Bacteriol.*, 1981, **146(2)**, 605.

33 K. Ochi, J. Kandala and E. Freese, *J Bacteriol*., 1982, **151(2)**, 1062

34 K. Liu, A.R. Myers, J.L. Keck, J.D. Wang, K. Liu, A.R. Myers, T. Pisithkul, K.R. Claas, K. A. Satyshur and D. Amador-Noguez, *Mol. Cell*, 2015, **57(4)**, 735.

35 A. Kriel, A.N. Bittner, S.H. Kim, K. Liu, A.K. Tehranchi, W.Y. Zou, S. Rendon, R. Chen, B.P. Tu and J.D. Wang, *Mol Cell*, 2012, **48(2)**, 231.

36 B.W. Anderson, A. Hao, K.A. Satyshur, J.L. Keck and J.D. Wang, *J. Mol. Biol.* 2020, **432(14)**, 4108.

37 B.W. Anderson, K. Liu, C. Wolak, K. Dubiel, F. She, K.A. Satyshur, J.L. Keck and J.D. Wang, *eLife*, 2019, **8**, e47534.

38 B. Wang, R.A. Grant, M.T. Laub, B. Wang, R.A. Grant and M.T. Laub, *Mol. Cell*, 2020, **80(1)**, 29.

39 B. Wang, P. Dai, D. Ding, A. del Rosario, R.A. Grant, B.L. Pentelute and M. T. Laub, *Nat. Chem. Biol.*, 2019, **15(2)**, 141.

40 Y. Zhang, E. Zborníková, D. Rejman and K. Gerdes, *mBio*, 2018, **9**, e02188-17.

41 W. Ross, P. Sanchez-Vazquez, A.Y. Chen, J.H. Lee, H.L. Burgos and R.L. Gourse, *Mol. Cell*, 2016, **62**, 811.

42 P. Sanchez-Vazquez, C.N. Dewey, N. Kitten, W. Ross and R.L. Gourse, *Proc. Natl. Acad. Sci. USA,* 2019, **116(17)**, 8310.

43 A. Kriel, S.R. Brinsmade, J.L. Tse, A.K. Tehranchi, A.N. Bittner, A.L. Sonenshein and J.D. Wang, *J. Bacteriol.*, 2014, **196(1)**, 189.

44 V.M. Levdikov, E. Blagova, P. Joseph, A.L. Sonenshein and A.J. Wilkinson, *J. Biol. Chem.*, 2006, **281(16)**, 11366.

45 S.R. Brinsmade and A.L. Sonenshein, *J. Bacteriol.*, 2011, **193(20)**, 5637.

46 L. Krásný, H. Tišerová, J. Jonák, D. Rejman and H. Šanderová, *Mol. Microbiol.,* 2008, **69(1)**, 42.

47 S. Tojo, T. Satomura, K. Kumamoto, K. Hirooka and Y. Fujita, *J. Bacteriol.,* 2008, **190(18)***,* 6134.

48 V. Molle, Y. Nakaura, R.P. Shivers, H. Yamaguchi, R. Losick, Y. Fujita and A.L. Sonenshein, *J. Bacteriol.*, 2003, **185(6)**, 1911.

49 B.W. Anderson, M.A. Schumacher, J. Yang, A. Turdiev, H. Turdiev, Q. He, V.T. Lee, R.G. Brennan and J.D. Wang, **doi:** https://doi.org/10.1101/2020.12.02.409011.

50 B.J. Paul, M.M. Barker, W. Ross, D.A. Schneider, C. Webb, J.W. Foster and R.L. Gourse, *Cell*, 2004, **118(3)**, 311.

51 P.J. Kang and E. A. Craig, *J. Bacteriol.*, 1990, **172**, 2055–2064.

52 A. Perederina, V. Svetlov, M.N. Vassylyeva, T.H. Tahirov, S. Yokoyama, I. Artsimovitch and D.G. Vassylyev, *Cell*, 2004, **118**, 297.

53 P. Chandrangsu, L. Wang, S.H. Choi and R.L. Gourse, *J. Bacteriol.*, 2012, **194(6)**, 1437.

54 S. Borukhov, V. Sagitov and A. Goldfarb, *Cell*, 1993, **72(3)**, 459.

55 N. Opalka, M. Chlenov, P. Chacon, W.J. Rice, W. Wriggers and S.A. Darst, *Cell*, 2003, **114(3)**, 335.

56 J.H. Lee, C.W. Lennon, W. Ross and R.L. Gourse, *J. Mol. Biol.*, 2012, **416(4)**, 503.

57 G.H. Feng, D.N. Lee, D. Wang, C.L. Chan and R. Landick, *J. Biol. Chem*., 1994, **269(35)**, 22282.

58 B.J. Paul, M.B. Berkmen and R. L. Gourse, *Proc. Natl, Acad, Sci. USA*, 2015, **102(22)**, 7823.

59 S.T. Rutherford, J.J. Lemke, C.E. Vrentas, T. Gaal, W. Ross and R.L. Gourse, *J. Mol. Biol.*, 2007, **366(4)**, 1243.

60 C.E. Vrentas, T. Gaal, W. Ross, R. H. Ebright and R. L. Gourse, *Genes Dev.*, 2005, **19(19)**, 2378.

61 H. Murphy and M. Cashel, *Meth. Enzymol*, 2003, **371**, 596.

62 S.T. Rutherford, C.L. Villers, J.H. Lee, W. Ross and R.L. Gourse, *Genes Dev.,* 2009, **23(2)**, 236.

63 I. Artsimovitch, V. Patlan, S. Sekine, M.N. Vassylyeva, T. Hosaka, K. Ochi, S. Yokoyama and D.G. Vassylyev, *Cell*, 2004, **117(3)**, 299.

64 C.E. Vrentas, T. Gaal, M.B. Berkmen, S.T. Rutherford, S.P. Haugen, D.G. Vassylyev, W. Ross and R.L. Gourse, *J. Mol. Biol.*, 2008, **377(2)**, 551.

65 K. Kasai, T. Nishizawa, K. Takahashi, T. Hosaka, H. Aoki and K. Ochi, *J. Bacteriol.*, 2006, **188(20)**, 7111.

66 K.D. Westover, D.A. Bushnell and R.D. Kornberg, *Cell*, 2004, **119(4)**, 481.

67 W. Ross, C.E. Vrentas, P. Sanchez-Vazquez, T. Gaal and R.L. Gourse, *Mol. Cell*, 2013, **50(3)**, 420.

68 Y. Zuo, Y. Wang and T.A. Steitz, *Mol. Cell*, 2013, **50(3)**, 430.

69 U. Mechold, K. Potrykus, H. Murphy, K.S. Murakami and M. Cashel, *Nucl. Acids Res.*, 2013, **41(12)**, 6175.

70 K.G. Roelofs, J. Wang, H.O. Sintim and V.T. Lee, *Proc. Natl. Acad. Sci.USA*, 2011, **108(37)**, 15528.

71 V. Molodtsov, E. Sineva, L. Zhang, X. Huang, M. Cashel, S.E. Ades and K.S. Murakami, *Mol Cell*, 2018, **69(5)**, 828.

72 A.Y. Chen, A. Feklistov, J. Chen, S. Gopalkrishnan, Z. Zhang, C.S. Potter, B. Carragher, R.L. Gourse, S.A. Darst and W. Ross, unpublished.

73 A.R. Myers, D. P. Thistle, W. Ross and R. L. Gourse, *Front. Microbiol*., 2020, **11**, 587098.

74 T. Durfee, A.M. Hansen, H. Zhi, F.R. Blattner and J.J. Ding, *J. Bacteriol.*, 2008, **190(3)**, 1084.

75 M.F. Traxler, V.M. Zacharia, S. Marquardt, S.M. Summers, H.T. Nguyen, S.E. Stark and T. Conway, *Mol. Microbiol.*, 2011, **79(4)**, 830.

76 M.F. Traxler, S.M. Summers, H.T. Nguyen, V.M. Zacharia, G.A. Hightower, J.T. Smith and T. Conway, *Mol. Microbiol.*, 2008, **68(5)**, 1128.

77 A. Åberg, J. Fernández-Vázquez, J.D. Cabrer-Panes, A. Sánchez and C. Balsalobre, *J. Bacteriol.*, 2009, **191(10)**, 3226.

78 S.P. Haugen, W. Ross and R.L. Gourse, *Nat. Rev. Microbiol.*, 2008, **6**, 507.

79 R.M. Saecker, M.T. Record Jr., P.L. Dehaseth. *J. Mol. Biol*., 2011. **412(5)**, 754.

80 M.D. Blankschien, K. Potrykus, E. Grace, A. Choudhary, D. Vinella, M. Cashel and C. Herman, *PLoS Genet.*, 2009, **5(1)**, e1000345.

81 S. Gopalkrishnan, W. Ross, A.Y. Chen and R.L. Gourse, *Proc. Natl. Acad. Sci. USA*, 2017, **114(28)**, E5539.

82 J. Chen, H. Boyaci and E.A. Campbell, *Nat. Rev. Microbiol.,* 2021, **19**, 95.

83 J. Chen, C. Chiu, S. Gopalkrishnan, A.Y. Chen, P.D.B. Olinares, R.M. Saecker, J.T. Winkelman, M.F. Maloney, B.T. Chait, W. Ross, R.L. Gourse, E.A. Campbell and S.A. Darst, *Mol. Cell*, 2020, **78**, 275.

84 M.M. Barker, T. Gaal, C.A. Josaitis and R.L. Gourse, *J. Mol. Biol.*, 2001, **305**, 673.

85 L. Rao, W. Ross, J. Appleman, T. Gaal, S. Leirmo, P.J. Schlax , M.T. Record, R.L. Gourse, *J. Mol. Biol*., 1994, **235**, 1421.

86 A.A. Travers, *J. Bacteriol.*, 1980, **141**, 973.

87 S.P. Haugen, M. B. Berkmen, W. Ross, T. Gaal, C. Ward and R. L. Gourse, *Cell*, 2006, **125**, 1069.

88 A. Feklistov and S.A. Darst, *Cell*, 2011, **147**, 1257.

89 M.L. Gleghorn, E.K. Davydova, R. Basu, L.B. Rothman-Denes and K.S. Murakami, *Proc. Natl. Acad. Sci. USA*, 2011, **108**, 3566.

90 X.J. da Costa and S.W. Artz, *J. Bacteriol.* 1997, **179**, 5211.

91 D.L. Riggs, R.D. Mueller, H.S. Kwan and S.W. Artz, *Proc. Natl. Acad. Sci. USA*, 1986, **83**, 9333.

92 J. Chen, S. Gopalkrishnan, C. Chiu, A.Y. Chen, E.A. Campbell, R.L. Gourse, W. Ross and S.A. Darst, *eLife*, 2019, **8**, e49375.

93 R.L. Gourse, A.Y. Chen, S. Gopalkrishnan, P. Sanchez-Vazquez, A. Myers and W. Ross, *Annu. Rev. Microbiol.*, 2018, **72**, 163.

94 E. A. Galburt, *Proc. Natl. Acad. Sci. USA*, 2018, **115(50)**, E11604.

95 B. Gummesson, M. Lovmar and T. Nyström, *J. Biol. Chem.*, 2013, **288(29)**, 21055.

96 V. Mekler, L. Minakhin, S. Borukhov, A. Mustaev and K. Severinov, *J. Mol. Biol.*, 2014, **426**, 3973.

97 S.K. Stumper, H. Ravi, L.J. Friedman, R.A. Mooney, I.R. Corrêa, A. Gershenson, R. Landick and J. Gelles. 2019. *eLife*, **8**, e40576.

98 C.W. Lennon, T. Gaal, W. Ross and R.L. Gourse, *J. Bacteriol.*, 2009, **191**, 5854.

99 J. Saba, X.Y. Chua, T.V. Mishanina, D. Nayak, T.A. Windgassen, R.A. Mooney and R. Landick, *eLife*, 2019, **8**, e40981.

100 R.E. Kingston, W.C. Nierman and M.J. Chamberlin, *J. Biol. Chem.*, 1981, **256**, 2787.

101 V. Kamarthapu, V. Epshtein, B. Benjamin, S. Proshkin, A. Mironov, M. Cashel and E. Nudler, *Science*, 2016, **352(6288)**, 993.

102 R.E. Kingston and M.J. Chamberlin, *Cell*, 1981, **27**, 523.

103 R. Furman, A. Sevostyanova and I. Artsimovitch, *Nucl. Acids Res.*, 2012, **40(8)**, 3392.

104 U. Vogel and K. F. Jensen, *J. Biol. Chem.*, 1994, **269**, 16236.

105 U. Vogel, K. F. Jensen, *J. Biol. Chem.*, 1995, **270(31)**,18335.

106 M.S. Bartlett, T. Gaal, W. Ross and R.L. Gourse, J. Mol. Biol., 1998, **279(2)**, 331.

107. P. McGlynn and R.G. Lloyd, *Cell*, 2000, **101(1)**, 35.

108 B.W. Trautinger and R.G. Lloyd, *EMBO J.* 2002, **21**, 6944.

109 B.W. Trautinger, R.P. Jaktaji, E. Rusakova and R.G. Lloyd, *Mol. Cell*, 2005, **19(2)**, 247–258.

110 Y. Zhang, R. Mooney, J. Grass, P. Sivaramakrishnan, C. Herman, R. Landick and J. Wang, *Mol. Cell*, 2014, **53(5)**, 766.

111 C.C. Traverse and H. Ochman, *Proc. Natl. Acad. Sci. USA*, 2016, **113**, 3311.

112 M. Imashimizu, T. Oshima, L. Lubkowska and M. Kashlev, *Nucl. Acids Res.*, 2013, **41**, 9090.

113 M. Roghanian, N. Zenkin and Y. Yuzenkova, *Nucl. Acids Res.*, 2015, **43**, 1529.

114 D. Satory, A.J. Gordon, M. Wang, J.A. Halliday, I. Golding, C. Herman, *Nucl. Acids Res*. 2015, **43(21)**:10190.

115 C.C. Traverse and H. Ochman, *G3,* 2018, **8(7)**, 2257.

116 A.K. Tehranchi, M.D. Blankschien, Y. Zhang, J.A. Halliday, A. Srivatsan, J. Peng, C. Herman and J.D. Wang, *Cell*, 2010, **141(4)**:595.

117 A. Serganov and E. Nudler, *Cell*, 2013, **152**, 17.

118 W. Winkler, A. Nahvi and R.R. Breaker, *Nature*, 2002, **419**, 952.

119 M.E. Sherlock, N. Sudarsan and R.R. Breaker, *Proc. Natl. Acad. Sci.* **115**, 6052.

120 J.W. Nelson, R.M. Atilho, M.E. Sherlock, R.B. Stockbridge and R.R. Breaker, *Mol. Cell*, 2017, **65**, 220.

121 M.E. Sherlock, N. Sudarsan, S. Stav and R.R. Breaker, *eLife*, 2018, **7**, e33908.

122 A.J. Knappenberger, C.W. Reiss and S.A. Strobel, *eLife*, 2018, **7**, e36381.

References: Chapter 2 & 3

Azriel, Shalhevet, Alina Goren, Galia Rahav, and Ohad Gal-mor. 2016. “The Stringent Response Regulator DksA Is Required for Salmonella Enterica Serovar Typhimurium Growth in Minimal Medium , Motility , Biofilm Formation , and Intestinal Colonization” 84 (1): 375–84. https://doi.org/10.1128/IAI.01135-15.Editor.

Basta, David W., Megan Bergkessel, and Dianne K. Newman. 2017. “Identification of Fitness Determinants during Energy-Limited Growth Arrest in Pseudomonas Aeruginosa.” *MBio* 8 (6). https://doi.org/10.1128/mBio.01170-17.

Bernhardt, Thomas G., and Piet A.J. De Boer. 2005. “SlmA, a Nucleoid-Associated, FtsZ Binding Protein Required for Blocking Septal Ring Assembly over Chromosomes in E. Coli.” *Molecular Cell* 18 (5): 555–64. https://doi.org/10.1016/j.molcel.2005.04.012.

Bittner, Lisa Marie, Jan Arends, and Franz Narberhaus. 2016. “Mini Review: ATP-Dependent Proteases in Bacteria.” *Biopolymers* 105 (8): 505–17. https://doi.org/10.1002/bip.22831.

Boyle, William K., Crystal L. Richards, Daniel P. Dulebohn, Amanda K. Zalud, Jeff A. Shaw, Sándor Lovas, Frank C. Gherardini, and Travis J. Bourret. 2021. “DksA-Dependent Regulation of RpoS Contributes to Borrelia Burgdorferi Tick-Borne Transmission and Mammalian Infectivity.” *PLoS Pathogens* 17 (2): 1–29. https://doi.org/10.1371/JOURNAL.PPAT.1009072.

Brooks, John F, Mattias C Gyllborg, David C Cronin, Sarah J Quillin, Celeste A Mallama, Randi Foxall, Cheryl Whistler, Andrew L Goodman, and Mark J Mandel. 2014. “Global Discovery of Colonization Determinants in the Squid Symbiont Vibrio Fischeri.” *Proceedings of the National Academy of*

Sciences of the United States of America 111 (48): 17284–89. https://doi.org/10.1073/pnas.1415957111.

Brown, Larissa, Daniel Gentry, Thomas Elliott, and Michael Cashel. 2002. “DksA Affects PpGpp Induction of RpoS at a Translational Level.” *Journal of Bacteriology* 184 (16): 4455–65. https://doi.org/10.1128/JB.184.16.4455-4465.2002.

Buskirk, Allen R., and Rachel Green. 2017. “Ribosome Pausing, Arrest and Rescue in Bacteria and Eukaryotes.” *Philosophical Transactions of the Royal Society B: Biological Sciences* 372 (1716). https://doi.org/10.1098/rstb.2016.0183.

Butzin, Nicholas C., and William H. Mather. 2018. “Crosstalk between Diverse Synthetic Protein Degradation Tags in Escherichia Coli.” *ACS Synthetic Biology* 7 (1): 54–62. https://doi.org/10.1021/acssynbio.7b00122.

Canela, Andres, Sriram Sridharan, Nicholas Sciascia, Anthony Tubbs, Paul Meltzer, Barry P. Sleckman, and André Nussenzweig. 2016. “DNA Breaks and End Resection Measured Genome-Wide by End Sequencing.” *Molecular Cell* 63 (5): 898–911. https://doi.org/10.1016/j.molcel.2016.06.034.

Chadani, Yuhei, Katsuhiko Ono, Shin Ichiro Ozawa, Yuichiro Takahashi, Kazuyuki Takai, Hideaki Nanamiya, Yuzuru Tozawa, Kazuhiro Kutsukake, and Tatsuhiko Abo. 2010. “Ribosome Rescue by Escherichia Coli ArfA (YhdL) in the Absence of Trans-Translation System.” *Molecular Microbiology* 78 (4): 796–808. https://doi.org/10.1111/j.1365-2958.2010.07375.x.

Chou, Wen Kang, and Mark P. Brynildsen. 2019. “Loss of DksA Leads to Multi-Faceted Impairment of Nitric Oxide Detoxification by Escherichia Coli.” *Free Radical Biology and Medicine* 130 (October 2018): 288–96. https://doi.org/10.1016/j.freeradbiomed.2018.10.435.

Condon, C., S. French, C. Squires, and C. L. Squires. 1993. “Depletion of Functional Ribosomal RNA Operons in Escherichia Coli Causes Increased Expression of the Remaining Intact Copies.” *EMBO Journal* 12 (11): 4305–15. https://doi.org/10.1002/j.1460-2075.1993.tb06115.x.

Dai, Xiongfeng, Manlu Zhu, Mya Warren, Rohan Balakrishnan, Vadim Patsalo, Hiroyuki Okano, James R Williamson, Kurt Fredrick, Yi-ping Wang, and Terence Hwa. 2017. “Reduction of Translating Ribosomes Enables Escherichia Coli to Maintain Elongation Rates during Slow Growth” 16231 (December 2016). https://doi.org/10.1038/nmicrobiol.2016.231.

Dar, Daniel, Maya Shamir, J R Mellin, Mikael Koutero, Noam Stern-ginossar, Pascale Cossart, and Rotem Sorek. 2016. “Resistance in Bacteria” 352 (6282). https://doi.org/10.1126/science.aad9822.

Fei, Xue, Tristan A. Bell, Sarah R. Barkow, Tania A. Baker, and Robert T. Sauer. 2020. “Structural Basis of Clpxp Recognition and Unfolding of Ssra-Tagged Substrates.” *ELife* 9: 1–39. https://doi.org/10.7554/eLife.61496.

Flynn, Julia M., Saskia B. Neher, Yong In Kim, Robert T. Sauer, and Tania A. Baker. 2003. “Proteomic Discovery of Cellular Substrates of the ClpXP Protease Reveals Five Classes of ClpX-Recognition Signals.” *Molecular Cell* 11 (3): 671–83. https://doi.org/10.1016/S1097-2765(03)00060-1.

Garza-Sánchez, Fernando, Ryan E. Schaub, Brian D. Janssen, and Christopher S. Hayes. 2011. “TmRNA Regulates Synthesis of the ArfA Ribosome Rescue Factor.” *Molecular Microbiology* 80 (5): 1204–19. https://doi.org/10.1111/j.1365-2958.2011.07638.x.

Gourse, Richard L., Albert Y. Chen, Saumya Gopalkrishnan, Patricia Sanchez-Vazquez, Angela Myers, and Wilma Ross. 2018. “Transcriptional Responses to PpGpp and DksA.” *Annual Review of Microbiology* 72 (1): 163–84. https://doi.org/10.1146/annurev-micro-090817-062444.

Gray, Michael J. 2020. “Interactions between DksA and Stress-Responsive Alternative Sigma Factors Control Inorganic Polyphosphate Accumulation in Escherichia Coli.” *Journal of Bacteriology* 202 (14). https://doi.org/10.1128/JB.00133-20.

Henard, Calvin A., and Andrés Vázquez-Torres. 2012. “Dksa-Dependent Resistance of Salmonella Enterica Serovar Typhimurium against the Antimicrobial Activity of Inducible Nitric Oxide Synthase.” *Infection and Immunity* 80 (4): 1373–80. https://doi.org/10.1128/IAI.06316-11.

Hong, Sue Jean, Faith H. Lessner, Elisabeth M. Mahen, and Kenneth C. Keiler. 2007. “Proteomic Identification of TmRNA Substrates.” *Proceedings of the National Academy of Sciences of the United States of America* 104 (43): 17128–33. https://doi.org/10.1073/pnas.0707671104.

Hui, Sheng, Josh M Silverman, Stephen S Chen, David W Erickson, Markus Basan, Jilong Wang, Terence Hwa, and James R Williamson. 2015. “Quantitative Proteomic Analysis Reveals a Simple Strategy of Global Resource Allocation in Bacteria.” *Molecular Systems Biology* 11 (2): 784. https://doi.org/10.15252/msb.20145697.

Ii, John F.Brooks, Mattias C. Gyllborg, David C. Cronin, Sarah J. Quillin, Celeste A. Mallama, Ri Foxall, Cheryl Whistler, Andrew L. Goodman, and Mark J. Mel. 2014. “Global Discovery of Colonization Determinants in the Squid Symbiont Vibrio Fischeri.” *Proceedings of the National Academy of Sciences of the United States of America* 111 (48): 17284–89. https://doi.org/10.1073/pnas.1415957111.

Imholz, Nicole C.E., Marek J. Noga, Niels J.F. van den Broek, and Gregory Bokinsky. 2020. “Calibrating the Bacterial Growth Rate Speedometer: A Re-Evaluation of the Relationship Between Basal PpGpp, Growth, and RNA Synthesis in Escherichia Coli.” *Frontiers in Microbiology* 11 (September): 1–9. https://doi.org/10.3389/fmicb.2020.574872.

Iyer, Sukanya, Dai Le, Bo Ryoung Park, and Minsu Kim. 2018. “Distinct Mechanisms Coordinate Transcription and Translation under Carbon and Nitrogen Starvation in Escherichia Coli.” *Nature Microbiology* 3 (6): 741–48. https://doi.org/10.1038/s41564-018-0161-3.

Ju, Xiangwu, Dayi Li, and Shixin Liu. 2019. “Full-Length RNA Profiling Reveals Pervasive Bidirectional Transcription Terminators in Bacteria.” *Nature Microbiology* 4 (11): 1907–18. https://doi.org/10.1038/s41564-019-0500-z.

Keiler, Kenneth C. 2008. “Biology of Trans-Translation.” *Annual Review of Microbiology* 62: 133–51. https://doi.org/10.1146/annurev.micro.62.081307.162948.

Klumpp, Stefan, Matthew Scott, Steen Pedersen, and Terence Hwa. 2013. “Molecular Crowding Limits Translation and Cell Growth.” https://doi.org/10.1073/pnas.1310377110/-/DCSupplemental.www.pnas.org/cgi/doi/10.1073/pnas.1310377110.

Krasich, Rachel, Sunny Yang Wu, H. Kenny Kuo, and Kenneth N. Kreuzer. 2015a. “Functions That Protect Escherichia Coli from DNA-Protein Crosslinks.” *DNA Repair* 28: 48–59. https://doi.org/10.1016/j.dnarep.2015.01.016.

———. 2015b. “Functions That Protect Escherichia Coli from DNA-Protein Crosslinks.” *DNA Repair* 28: 48–59. https://doi.org/10.1016/j.dnarep.2015.01.016.

Maharjan, Ram, Geraldine Sulivan, Felise Adams, Natasha Delgado, Lucie Semenec, Hue Dinh, Liping Li, Francesca Short, Julian Parkhill, and Ian Paulsen. 2021. “DksA Is a Central Regulatory Switch for Stress Protection and Virulence in Acinetobacter Baumannii.”

Matsumoto, Y, K Shigesada, M Hirano, and M Imai. 1986. “Autogenous Regulation of the Gene for Transcription Termination Factor Rho in Escherichia Coli: Localization and Function of Its Attenuators.” *Journal of Bacteriology* 166 (3): 945–58. https://doi.org/10.1128/jb.166.3.945-958.1986.

McQuail, Josh, Amy Switzer, Lynn Burchell, and Sivaramesh Wigneshweraraj. 2020. “The RNA-Binding Protein Hfq Assembles into Foci-like Structures in Nitrogen Starved Escherichia Coli.” *Journal of Biological Chemistry* 295 (35): 12355–67. https://doi.org/10.1074/jbc.RA120.014107.

Mei, Qian, Devon M. Fitzgerald, Jingjing Liu, Jun Xia, John P. Pribis, Yin Zhai, Ralf B. Nehring, et al.

2021. “Two Mechanisms of Chromosome Fragility at Replication-Termination Sites in Bacteria.” *Science Advances* 7 (25): eabe2846. https://doi.org/10.1126/sciadv.abe2846.

Miller, Mickey R., and Allen R. Buskirk. 2014. “The SmpB C-Terminal Tail Helps TmRNA to Recognize and: Enter Stalled Ribosomes.” *Frontiers in Microbiology* 5 (SEP): 1–7. https://doi.org/10.3389/fmicb.2014.00462.

Miyoshi, Toshio, Norimasa Miyairi, Hatsuo Aoki, Masanobu Kohsaka, Hei ichi Sakai, and Hiroshi Imanaka. 1972. “Bicyclomycin, a New Antibiotic: Taxonomy, Isolation and Characterization.” *Journal of Antibiotics* 25 (10): 569–75. https://doi.org/10.7164/antibiotics.25.569.

Murphy, Helen, and Michael Cashel. 2003. “Isolation of RNA Polymerase Suppressors of a (p)PpGpp Deficiency.” *Methods in Enzymology* 371 (1993): 596–601. https://doi.org/10.1016/S0076-6879(03)71044-1.

Myers, Angela R., Danielle P. Thistle, Wilma Ross, and Richard L. Gourse. 2020. “Guanosine Tetraphosphate Has a Similar Affinity for Each of Its Two Binding Sites on Escherichia Coli RNA Polymerase.” *Frontiers in Microbiology* 11 (November). https://doi.org/10.3389/fmicb.2020.587098.

Neher, Saskia B., Judit Villén, Elizabeth C. Oakes, Corey E. Bakalarski, Robert T. Sauer, Steven P. Gygi, and Tania A. Baker. 2006. “Proteomic Profiling of ClpXP Substrates after DNA Damage Reveals Extensive Instability within SOS Regulon.” *Molecular Cell* 22 (2): 193–204. https://doi.org/10.1016/j.molcel.2006.03.007.

Paul, B. J., M. B. Berkmen, and R. L. Gourse. 2005. “DksA Potentiates Direct Activation of Amino Acid Promoters by PpGpp.” *Proceedings of the National Academy of Sciences* 102 (22): 7823–28. https://doi.org/10.1073/pnas.0501170102.

Paul, Brian J., Melanie M. Barker, Wilma Ross, David A. Schneider, Cathy Webb, John W. Foster, and Richard L. Gourse. 2004. “DksA: A Critical Component of the Transcription Initiation Machinery That Potentiates the Regulation of RRNA Promoters by PpGpp and the Initiating NTP.” *Cell* 118 (3): 311–22. https://doi.org/10.1016/j.cell.2004.07.009.

Paul, Brian J, Melanie M Barker, Wilma Ross, David A Schneider, Cathy Webb, John W Foster, Richard L Gourse, and Henry Mall. 2004. “DksA : A Critical Component of the Transcription Initiation Machinery That Potentiates the Regulation of RRNA Promoters by PpGpp and the Initiating NTP” 118: 311–22.

Ray-soni, Ananya, Michael J Bellecourt, and Robert Landick. 2016. “Mechanisms of Bacterial Transcription Termination : All Good Things Must End,” no. March: 1–29. https://doi.org/10.1146/annurev-biochem-060815-014844.

Reuter, Audrey, Chloé Virolle, Kelly Goldlust, Annick Berne-Dedieu, Sophie Nolivos, and Christian Lesterlin. 2020. “Direct Visualisation of Drug-Efflux in Live Escherichia Coli Cells.” *FEMS Microbiology Reviews* 44 (6): 782–92. https://doi.org/10.1093/femsre/fuaa031.

Robinson, Jonathan L., and Mark P. Brynildsen. 2015. “An Ensemble-Guided Approach Identifies ClpP as a Major Regulator of Transcript Levels in Nitric Oxide-Stressed Escherichia Coli.” *Metabolic Engineering* 31: 22–34. https://doi.org/10.1016/j.ymben.2015.06.005.

Roche, Eric D., and Robert T. Sauer. 2001. “Identification of Endogenous SsrA-Tagged Proteins Reveals Tagging at Positions Corresponding to Stop Codons.” *Journal of Biological Chemistry* 276 (30): 28509–15. https://doi.org/10.1074/jbc.M103864200.

Ross, Wilma, Patricia Sanchez-Vazquez, Albert Y. Chen, Jeong Hyun Lee, Hector L. Burgos, and Richard L. Gourse. 2016. “PpGpp Binding to a Site at the RNAP-DksA Interface Accounts for Its Dramatic Effects on Transcription Initiation during the Stringent Response.” *Molecular Cell* 62 (6): 811–23. https://doi.org/10.1016/j.molcel.2016.04.029.

Ross, Wilma, Patricia Sanchez-vazquez, Albert Y Chen, Jeong-hyun Lee, Hector L Burgos, Richard L

Gourse, Wilma Ross, et al. 2016. “PpGpp Binding to a Site at the RNAP-DksA Interface Accounts for Its Dramatic Effects on Transcription Initiation during the Stringent Response Article PpGpp Binding to a Site at the RNAP-DksA Interface Accounts for Its Dramatic Effects on Transcription In.” *Molecular Cell* 62 (6): 811–23. https://doi.org/10.1016/j.molcel.2016.04.029.

Ross, Wilma, Catherine E. Vrentas, Patricia Sanchez-Vazquez, Tamas Gaal, and Richard L. Gourse. 2013. “The Magic Spot: A PpGpp Binding Site on E. Coli RNA Polymerase Responsible for Regulation of Transcription Initiation.” *Molecular Cell* 50 (3): 420–29. https://doi.org/10.1016/j.molcel.2013.03.021.

Sanchez-vazquez, Patricia, Colin N Dewey, Nicole Kitten, Wilma Ross, and Richard L Gourse. n.d. “Genome-Wide Effects on Escherichia Coli Transcription Polymerase” l (1).

Scott, Matthew, Stefan Klumpp, Eduard M Mateescu, and Terence Hwa. 2014. “Emergence of Robust Growth Laws from Optimal Regulation of Ribosome Synthesis.” *Molecular Systems Biology* 10 (8): 747. https://doi.org/10.15252/msb.20145379.

Tehranchi, Ashley K, Matthew D Blankschien, Yan Zhang, Jennifer A Halliday, Anjana Srivatsan, Jia Peng, Christophe Herman, and Jue D Wang. 2010. “The Transcription Factor DksA Prevents Conflicts between DNA Replication and Transcription Machinery.” *Cell* 141 (4): 595–605. https://doi.org/10.1016/j.cell.2010.03.036.

Turner, Arthur K., Margaret A. Lovell, Scott D. Hulme, Li Zhang-Barber, and Paul A. Barrow. 1998. “Identification of Salmonella Typhimurium Genes Required for Colonization of the Chicken Alimentary Tract and for Virulence in Newly Hatched Chicks.” *Infection and Immunity* 66 (5): 2099–2106. https://doi.org/10.1128/iai.66.5.2099-2106.1998.

Wetmore, Kelly M., Morgan N. Price, Robert J. Waters, Jacob S. Lamson, Jennifer He, Cindi A. Hoover, Matthew J. Blow, et al. 2015. “Rapid Quantification of Mutant Fitness in Diverse Bacteria by Sequencing Randomly Bar-Coded Transposons.” *MBio* 6 (3): 1–15. https://doi.org/10.1128/mBio.00306-15.

Zhang, Yan, Rachel A Mooney, Jeffrey A Grass, Priya Sivaramakrishnan, Christophe Herman, and Robert Landick. 2014. “Article DksA Guards Elongating RNA Polymerase against Ribosome-Stalling-Induced Arrest.” *Molecular Cell* 53 (5): 766–78. https://doi.org/10.1016/j.molcel.2014.02.005.

Zhu, Manlu, and Xiongfeng Dai. 2019. “Growth Suppression by Altered (p)PpGpp Levels Results from Non-Optimal Resource Allocation in Escherichia Coli.” *Nucleic Acids Research* 47 (9): 4684–93. https://doi.org/10.1093/nar/gkz211.

Zhu, Manlu, Matteo Mori, Terence Hwa, and Xiongfeng Dai. 2019. “Disruption of Transcription–Translation Coordination in Escherichia Coli Leads to Premature Transcriptional Termination.” *Nature Microbiology* 4 (12): 2347–56. https://doi.org/10.1038/s41564-019-0543-1.